Angewandte Chemie
Eine Zeitschrift der Gesellschaft Deutscher Chemiker

Supporting Information

Interconversion of Phosphinyl Radical and Phosphinidene Complexes by Proton Coupled Electron Transfer

Josh Abbenseth, Daniel Delony, Marc C. Neben, Christian Würtele, Bas de Bruin, and Sven Schneider**

ange_201901470_sm_miscellaneous_information.pdf

Supporting Information

Author Contributions

J.A.: Synthesis: Lead; Formal Analysis: Lead; Investigation: Lead; Writing-original draft: Equal
D.D: ITC: Lead
M.N: Synthesis and Investigation: Supporting
C.W.: Crystallography: Lead
B.B.: EPR and BDE computations: Lead; Writing-original draft: Equal
S.S.: Conceptualization: Lead; Funding acquisition: Lead; Methodology: Lead; Supervision: Lead, Writing-original draft: Equal

Table of content

Experimental Details and Spectroscopy 1
Materials and Methods 1
Syntheses 2
[OsHCl(PHMes*)(PNP)] (4) 2
[OsH(PHMes*)(PNP)] (5) 2
[OsH(PMes*)(PNP)] (6) 2
[Os(5,7-di-*tert*-butyl-3,3-dimethyl-2,3-dihydro-1H-phosphindole)H(PNP)] (7) 2
[Os(PHMes*)(PNP)(CO)] (8) 3
[OsH(PHMes*)(PNP)][Al(OR)$_4$] (9) 3
Spectroscopic characterization of 4 4
Spectroscopic characterization of 5 6
Spectroscopic characterization of 6 10
Spectroscopic characterization of 7 11
Spectroscopic characterization of 8 12
Spectroscopic characterization of 9 14
Titration Calorimetry 16
Crystallographic Details 19
X-ray Single-Crystal Structure Analysis of 4 20
X-ray Single-Crystal Structure Analysis of 5 25
X-ray Single-Crystal Structure Analysis of 8 29
X-ray Single-Crystal Structure Analysis of 9 34
Computational Details 40
BDE calculations 41
EPR Property calculations 41

Experimental Details and Spectroscopy

Materials and Methods

All experiments were carried out using Schlenk (argon atmosphere) and glovebox (argon atmosphere) techniques. All solvents were dried by passing through columns packed with activated alumina. Deuterated solvents were obtained from Euriso-Top GmbH, dried over Na/K (THF, Toluene, Benzene), distilled by trap-to-trap transfer *in vacuo*, and degassed by three freeze–pump–thaw cycles, respectively. Silica gel 60 silanized was purchased from Merck KGaA and heated at 120°C *in vacuo* for 5 days prior to use. $Ag[Al(OR)_4]$ (R = $C(CF_3)_3$, Iolitec), $CoCp_2$ (abcr), KO*t*Bu (Sigma-Aldrich), NBu_4PF_6 (Sigma-Aldrich), PH_2Mes^* (Sigma-Aldrich) were used as purchased. CO (Linde) was cooled to -80°C in metal tubings for 2h prior to use. TEMPO (Sigma-Aldrich) was sublimed prior to use. **3** and 2,4,6-tri-tert-butylphenoxylradical (Mes*O) were prepared according to literature procedures.[1] IR spectra were recorded with a Thermo Scientific Nicolet iZ10 FT/IR spectrometer at room temperature. Elemental analyses were obtained from the analytical laboratories at the University of Göttingen with an Elementar Vario EL 3 analyzer. NMR Spectra were recorded with a Bruker Avance III HD 500 NMR spectrometer and were calibrated to the residual solvent proton resonance (C_6D_6 δ_H = 7.16 ppm, THF-d_8 δ_H = 3.58 ppm). Magnetic moments in solution (C_6D_6) were determined at room temperature by Evans' method as modified by Sur and corrected for diamagnetic contribution.[2] LIFDI mass spectrometry was performed using a Joel AccuTOF spectrometer under inert conditions. Cyclic voltammograms were recorded with a Metrohm Autolab PGSTAT101 using Ag/Ag^+ reference, glassy-carbon working and Pt-wire counter electrodes. Experimental X-band EPR spectra were recorded with a Bruker ELEXSYS-II E500 CW-EPR spectrometer. The spectra were simulated by iteration of the anisotropic g-values, (super)hyperfine coupling constants, and line widths using the EPR-simulation program W95EPR.[3] Experimental details for the isothermal titration calorimetry are presented in the respective chapter.

Syntheses

[OsCl(PHMes*)H(PNP)] (4)

$[OsCl_2(PNP)]$ (42.5 mg, 68.8 µmol, 1.0 eq.) and $CoCp_2$ (13.1 mg, 69.3 µmol, 1.0 eq.) are dissolved in Et_2O (5 mL) and stirred for 1 min at room temperature. PH_2Mes^* (19.2 mg, 68.8 µmol, 1.0 eq) is added and stirring is continued for 2h. After filtration the solvent is evaporated and the crude product is extracted with pentane (10 x 3 mL). The solution is concentrated and stored at -40°C for 3 days. The solvent is decanted off and the solid is washed with cold pentane. After extraction with benzene (3 x 5 mL), lyophilization yields **4** as a blue powder (42.8 mg, 49.7 µmol, 72%).
Anal. Calcd for $C_{38}H_{71}ClNOsP_3$ (860.58): C, 53.04; H, 8.32; N, 1.63 Found: C, 53.54; H, 7.82; N, 1.45. NMR (THF-d_8, -30°C): ^{1}H (500 MHz): δ = 18.5 (d, $^1J_{HP}$ = 337.2 Hz, 1H, P*H*Mes*), 7.34 (d, $^4J_{HH}$ = 1.93 Hz, 1H, $C_{meta}H$, Mes*), 7.26 (d, $^4J_{HH}$ = 1.93 Hz, 1H, $C_{meta}H$, Mes*), 6.82 – 6.70 (m, 2 H, NC*H*CHP), 4.35 (m, $^3J_{HH}$ = 6.0 Hz, 1H, NCHC*H*P), 4.14 (m, $^3J_{HH}$ = 6.0 Hz, 1H, NCHC*H*P), 1.64 (d, $^3J_{HP}$ = 10.5 Hz, 9H, PC(CH_3)$_3$), 1.45 (d, $^3J_{HP}$ = 9.8 Hz, 9H, PC(CH_3)$_3$), 1.36 (s, 9H, C_{ortho}C(CH_3)$_3$, Mes*), 1.34 (s, 9H, C_{ortho}C(CH_3)$_3$, Mes*), 1.30 (s, 9H, C_{para}C(CH_3)$_3$, Mes*), 1.17 (d, $^3J_{HP}$ = 10.7 Hz, 9H, PC(CH_3)$_3$), 1.00 (d, $^3J_{HP}$ = 9.7 Hz, 9H, PC(CH_3)$_3$), -5.37 (m, 1H, Os*H*). ^{13}C{^{1}H} (125.76 MHz): δ = 162.8 (dd, $^2J_{CP}$ = 11.5Hz, $^3J_{CP}$ = 4.7Hz, 1C, N*C*HCHP), 162.1 (dd, $^2J_{CP}$ = 10.4Hz, $^3J_{CP}$ = 3.8Hz 1C, N*C*HCHP), 153.9 (s, 1C, C_{ortho}, Mes*), 152.6 (s, 1C, C_{ortho}, Mes*), 148.9 (s, 1C, C_{para}, Mes*), 146.4 (br, 1C, C_{ipso}, Mes*), 125.5 (s, 1C, C_{meta}, Mes*), 123.1 (s, 1C, C_{meta}, Mes*), 93.9 (m, $^1J_{CP}$ = 31.5Hz, $^3J_{CP}$ = 7.3Hz, 1C, NCH*C*HP), 92.6 (m, $^1J_{CP}$ = 34.5Hz, $^3J_{CP}$ = 4.9Hz, 1C, NCH*C*HP), 42.8 (dd, $^1J_{CP}$ = 14.3Hz, $^3J_{CP}$ = 7.7Hz 1C, P*C*(CH_3)$_3$), 40.7 (s, 1C, $C_{para}C(CH_3)_3$, Mes*) 40.0 (s, 1C, $C_{ortho}C(CH_3)_3$, Mes*), 39.6 (dd, $^1J_{CP}$ = 13.6Hz, $^3J_{CP}$ = 6.5Hz 1C, P*C*(CH_3)$_3$), 38.8 (dd, $^1J_{CP}$ = 21.4Hz, $^3J_{CP}$ = 6.1Hz 1C, P*C*(CH_3)$_3$), 35.9 (dd, $^1J_{CP}$ = 19.0Hz, $^3J_{CP}$ = 6.0Hz 1C, P*C*(CH_3)$_3$), 35.6 (s, 1C, $C_{ortho}C(CH_3)_3$, Mes*), 33.7 (br, 3C, PC(*C*H_3)$_3$), 33.5 (br, 3C, PC(*C*H_3)$_3$), 33.2 (s, 3C, C_{ortho}C(*C*H_3)$_3$), 32.8 (s, 3C, $C_{para}C(CH_3)_3$), 31.6 (s, 3C C_{ortho}C(*C*H_3)$_3$), 31.5-30.8 (br, 6C, PC(*C*H_3)$_3$). ^{31}P{^{1}H} (161.25 MHz): δ = 103.9 (m, 1P, *P*HMes*), 31.6 (dd, $^2J_{PP}$ = 259.8Hz, $^2J_{PP}$ = 20.1Hz, 1P, *P*C(CH_3)$_3$), 30.0 (dd, $^2J_{PP}$ = 259.8Hz, $^2J_{PP}$ = 18.3Hz, 1P, *P*C(CH_3)$_3$). IR (Nujol, cm^{-1}): 2349 (ν_{P-H}). LIFDI-MS (toluene, m/z): 861.5 (39%, $[M]^+$), 825.5 (100%, $[M\text{-}HCl]^+$).

[Os(PHMes*)H(PNP)] (5)

Route A: **4** (30 mg, 34.9 µmol, 1.0 eq) and $CoCp_2$ (6.6 mg, 34.9 µmol, 1.0 eq) are dissolved in pentane (3 mL) and stirred for 5 minutes at room temperature. After filtration and extraction of the residue with pentane (3 x 1 ml) the solvent is evaporated. After column chromatography (silanized silica, pentane), the solvent is evaporated. **5** is obtained after lyophilization as a dark green powder (23 mg, 27.9 µmol, 80%).
Anal. Calcd for $C_{38}H_{71}NOsP_3$ (825.1): C, 55.1; H, 8.53; N, 1.68 Found: C, 54.9; H, 8.65; N, 1.65. IR (Nujol, cm^{-1}): 2345 (ν_{P-H}), 2180 (ν_{Os-H}). LIFDI-MS (toluene, m/z): 826.4 (100%, $[M]^+$).

Route B: $[OsCl_2(PNP)]$ (35 mg, 56.7 µmol, 1.0 eq) and $CoCp_2$ (21.4 mg, 113.3 µmol, 2.0 eq) are dissolved in C_6H_6 (3 mL) and stirred for 2 minutes at room temperature. PH_2Mes^* (15.8 mg, 56.7 µmol, 1.0 eq) is added and stirring is continued for additional 4 hours. The solvent is removed and the crude product is extracted with pentane (5 x 1 mL) and the solvent is evaporated. After column chromatography (silanized silica, pentane), the solvent is evaporated. Lyophilization yields **5** as a dark green powder (41.8 mg, 50.7 µmol, 89%)
Anal. Calcd for $C_{38}H_{71}NOsP_3$ (825.1): C, 55.3; H, 8.67; N, 1.70 Found: C, 54.9; H, 8.65; N, 1.65. IR (Nujol, cm^{-1}): 2345 (ν_{P-H}), 2180 (ν_{Os-H}). LIFDI-MS (toluene, m/z): 826.4 (100%, $[M]^+$). μ_{eff}^{298K} = 1.51 μ_B

[Os(PMes*)H(PNP)] (6)

Route A: **5** (10.0 mg, 12.1 µmol, 1.0 eq) and TEMPO (5.7 mg, 38.4 µmol, 3.0 eq) are dissolved in pentane and stirred for 10 minutes at room temperature. After column chromatography (silanized silica, pentane) and removal of the solvent, **7** is obtained as a violet powder (9.0 mg, 10.9 µmol, 90%).
NMR (THF-d_8, -30°C): ^{1}H (500 MHz): δ =7.36 (d, $^4J_{HH}$ = 1.8 Hz, 1H, $C_{meta}H$), 7.23 (m, $^3J_{HH}$ = 6.1 Hz, 2H, NC*H*), 7.03 (d, $^4J_{HH}$ = 1.8 Hz, 1H, $C_{meta}H$), 4.63 (m ,$^3J_{HH}$ = 5.0 Hz, 2H, PC*H*), 1.55 (s, 9H, $C_{ortho}C(CH_3)_3$), 1.35 (s, 9H, $C_{ortho}C(CH_3)_3$), 1.34 (s, 9H, $C_{para}C(CH_3)_3$), 1.22 (br, 18H, PC(CH_3)$_3$), 1.20 (br, 18H, PC(CH_3)$_3$), -15.91 (t, $^2J_{HP}$ = 14.5 Hz, 1H, Os*H*). ^{31}P{^{1}H} (161.25 MHz): δ = 825.1 (t, $^2J_{PP}$ = 36.6 Hz, 1P, *P*H), 43.2 (d, $^2J_{PP}$ = 36.6 Hz, 2P, *P*C(CH_3)$_3$). LIFDI-MS (toluene, m/z): 825.5 (100%, $[M]^+$).

Route B: **5** (10 mg, 12.1 µmol, 1.0 eq) is dissolved in THF (1 mL) and cooled to -80°C. Ag[Al(O-^{t}Bu-F_9)$_4$] (13 mg, 12.1 µmol, 1.0 eq) is added and the solution is stirred for 30 seconds. KOtBu (1.4 mg, 1.0 µmol, 1.0 eq) is added and stirring is continued for three minutes. After evaporation of the solvent the crude product is extracted with pentane and purified by chromatography (silanized silica, pentane). NMR spectra (-30°C) were identical with spectra of the product obtained by route A.

[Os(5,7-di-*tert*-butyl-3,3-dimethyl-2,3-dihydro-1H-phosphindole)H(PNP)] (7)

Complex **6** prepared by route A is dissolved in benzene-d_6 (0.5 mL), transferred to a J-Young NMR tube and stirred at room temperature until complete conversion of **6** is detected by NMR. Lyophilization yields a brown powder as a mixture of the two diastereomers of **7** in a ratio about 60 (**A**) : 40 (**B**) according to NMR spectroscopy.
Anal. Calcd for $C_{39}H_{70}NOOsP_3$ (825.1):C, 55.4; H, 8.56; N, 1.70 Found: C, 55.5; H, 8.63, N, 1.68. LIFDI-MS (toluene, m/z): 825.5 (100%, $[M]^+$). NMR (**A**, C_6D_6, RT): ^{1}H (500 MHz): δ = 8.34 (m,$^1J_{HP}$ = 308.7 Hz, $^3J_{HP}$ = 9.14, $^3J_{HP}$ = 4.67, P*H*), 7.55 -7.40 (m, 3H, NC*H*, $C_{meta}H$), 7.18-7.15 (m, 1H, $C_{meta}H$), 4.52-4.44 (m, 2H, PC*H*), 2.92-2.85 (m, 1H, PCH_2C(CH_3)$_2$), 2.69-2.63 (m, 1H, PCH_2C(CH_3)$_2$), 1.71 (s, 9H, $C_{ortho}C(CH_3)_3$), 1.64 (m, 3H, PCH_2C(CH_3)$_2$), 1.49 (d, $^2J_{HP}$ = 12.4 Hz, 9H, PC(CH_3)$_3$), 1.32 (s, 9H, $C_{para}C(CH_3)_3$), 1.25 (d, $^2J_{HP}$ = 12.1 Hz, 9H, PC(CH_3)$_3$), 1.14 (m, 3H, PCH_2C(CH_3)$_2$), 0.96 (d, $^2J_{HP}$ = 12.7 Hz, 9H, PC(CH_3)$_3$), 0.93 (d, $^2J_{HP}$ = 11.0 Hz, 9H, PC(CH_3)$_3$), -44.7 (ddd, $^2J_{HP}$ = 18.4 Hz, $^2J_{HP}$ = 13.1 Hz, $^2J_{HP}$ = 13.0 Hz, Os*H*). ^{31}P{^{1}H} (161.25 MHz): δ = 64.9 (dd, $^2J_{PP}$ = 234.4 Hz, $^2J_{PP}$ = 11.5 Hz), 53.0 (dd, $^2J_{PP}$ = 234.4 Hz, $^2J_{PP}$ = 10.9 Hz), -54.6 (dd, $^2J_{PP}$ = 11.5 Hz, $^2J_{PP}$ = 10.9 Hz). NMR (**B**, C_6D_6, RT): ^{1}H (500 MHz): δ = 8.43 (m,$^1J_{HP}$ = 300.7 Hz, $^3J_{HP}$ =

8.7, $^{3}J_{HP}$ = 4.8, P*H*), 7.55 -7.40 (m, 3H, NC*H*, C_{meta}*H*), 7.18-7.15 (m, 1H, C_{meta}*H*), 4.57-4.52 (m, 2H, PC*H*), 2.53-2.41 (m, 2H, PCH_2C(CH_3)$_2$), 1.51(s, 9H, C_{ortho}C(CH_3)$_3$), 1.50 (m, 3H, PCH_2C(CH_3)$_2$), 1.43 (d, $^{2}J_{HP}$ = 11.4 Hz, 9H, PC(CH_3)$_3$), 1.41 (d, $^{2}J_{HP}$ = 12.43 Hz, 9H, PC(CH_3)$_3$), 1.33 (s, 9H, C_{para}C(CH_3)$_3$), 1.11 (d, $^{2}J_{HP}$ = 12.6 Hz, 9H, PC(CH_3)$_3$), 1.11 (m, 3H, PCH_2C(CH_3)$_2$), 0.91 (d, $^{2}J_{HP}$ = 12.5 Hz, 9H, PC(CH_3)$_3$), -45.7 (ddd, $^{2}J_{HP}$ = 21.4 Hz, $^{2}J_{HP}$ = 14.4 Hz, $^{2}J_{HP}$ = 14.4 Hz, Os*H*). ^{31}P{^{1}H} (161.25 MHz): δ = 68.0 (dd, $^{2}J_{PP}$ = 234.8 Hz, $^{2}J_{PP}$ = 10.5 Hz), 58.0 (dd, $^{2}J_{PP}$ = 234.8 Hz, $^{2}J_{PP}$ = 10.8 Hz), -55.4 (dd, $^{2}J_{PP}$ = 10.8 Hz, $^{2}J_{PP}$ = 10.5 Hz).

[Os(PHMes*)(PNP)(CO)] (8)

5 (20 mg, 24.2 µmol, 1.0 eq) and TEMPO (11.4 mg, 72.7 µmol, 3.0 eq) are dissolved in pentane and stirred for 10 min at room temperature. The solution is degassed by three freeze-pump-thaw cycles and one atmosphere of CO is added. The solution is stirred at -80°C for 5 minutes and the solvent is removed *i. vac*. The crude product is purified *via* column chromatography (silanized silica, pentane) and crystalized at -80°C to give **8** (16.5 mg, 19.36 µmol, 80 %) as dark red crystals.

Anal. Calcd for $C_{39}H_{70}NOOsP_3$ (825.1): C, 54.9; H, 8.28; N, 1.64 Found: C, 54.6; H, 8.34; N, 1.55. NMR (THF-d_8): ^{1}H (500 MHz): δ = 9.79 (ddd, $^{1}J_{PH}$ = 308.9 Hz, $^{3}J_{PH}$ = 13.3 Hz, $^{3}J_{PH}$ = 4.9 Hz, 1H, P*H*Mes*), 7.44 (ddd, $^{3}J_{PH}$ = 36.6 Hz, $^{3}J_{HH}$ = 6.0 Hz, $^{4}J_{PH}$ = 1.4 Hz, 1H, NC*H*), 7.33 (ddd, $^{3}J_{PH}$ = 34.6 Hz, $^{3}J_{HH}$ = 5.9 Hz, $^{4}J_{PH}$ = 2.2 Hz, 1H, NC*H*), 7.24 (m, 2H, C_{meta}*H*), 4.44 (m, $^{2}J_{PH}$ = 5.1 Hz, $^{3}J_{HH}$ = 6.0 Hz, $^{4}J_{PH}$ = 1.7 Hz, 1H, PC*H*), 4.33 (m, $^{2}J_{PH}$ = 5.0 Hz, $^{3}J_{HH}$ = 5.8 Hz, $^{4}J_{PH}$ = 1.8 Hz, 1H, PC*H*), 1.62 (s, 9H, C_{ortho}(CH_3)$_3$)), 1.61 (s, 9H, C_{ortho}(CH_3)$_3$)), 1.51 (d, $^{3}J_{PH}$ = 13.5 Hz, 9H, PC(CH_3)$_3$)), 1.31 (d, $^{3}J_{PH}$ = 13.0 Hz, 9H, PC(CH_3)$_3$)) ,1.31 (s, 9H, C_{para}(CH_3)$_3$)), 1.03 (d, $^{3}J_{PH}$ = 13.8 Hz, 9H, PC(CH_3)$_3$)), 0.81 (d, $^{3}J_{PH}$ = 13.4 Hz, 9H, PC(CH_3)$_3$)). ^{13}C{^{1}H} (125.76 MHz): δ = 181.7 (ddd, $^{2}J_{CP}$ = 48.3 Hz, $^{2}J_{CP}$ = 6.0, $^{2}J_{CP}$ = 5.6, 1C, Os-*C*O), 164.9 (d, $^{2}J_{CP}$ = 12.0 Hz, 1C, N*C*H), 163.7 (d, $^{2}J_{CP}$ = 11.0 Hz, 1C, N*C*H), 155.7 (br, 1C, C_{ortho}), 155.6 (d, $^{2}J_{CP}$ = 4.1 Hz, 1C, C_{ortho}), 148.8 (d, $^{4}J_{CP}$ = 2.2 Hz, 1C, C_{para}), 140.2 (d, $^{1}J_{CP}$ = 6.1 Hz, 1C, C_{ipso}), 123.0 (d, $^{3}J_{CP}$ = 5.1 Hz, 1C, C_{meta}), 122.2 (d, $^{3}J_{CP}$ = 10.2 Hz, 1C, C_{meta}), 88.4 (dd, $^{1}J_{CP}$ = 45.5 Hz, $^{3}J_{CP}$ = 3.7 Hz, 1C, P*C*H), 86.7 (dd, $^{1}J_{CP}$ = 46.8 Hz, $^{3}J_{CP}$ = 5.0 Hz, 1C, P*C*H), 41.9 (ddd, $^{1}J_{CP}$ = 22.0 Hz, $^{3}J_{CP}$ = 7.4, $^{3}J_{CP}$ = 3.1 Hz, 1C, P*C*(CH_3)$_3$), 40.8 (ddd, $^{1}J_{CP}$ = 21.1 Hz, $^{3}J_{CP}$ = 7.5, $^{3}J_{CP}$ = 2.9 Hz, 1C, P*C*(CH_3)$_3$), 40.7 (s, 1C, C_{ortho}*C*(CH_3)$_3$), 40.0 (s, 1C, C_{ortho}*C*(CH_3)$_3$), 39.9 (dd, $^{1}J_{CP}$ = 23.5 Hz, $^{3}J_{CP}$ = 2.2, 1C, P*C*(CH_3)$_3$), 37.5 (dd, $^{1}J_{CP}$ = 24.2 Hz, $^{3}J_{CP}$ = 2.0, 1C, P*C*(CH_3)$_3$), 35.3 (s, 1C, C_{para}*C*(CH_3)$_3$), 35.1 (s, 3C, C_{ortho}C(*C*H_3)$_3$), 33.6 (s, 3C, C_{ortho}C(*C*H_3)$_3$), 31.9 (s, 3C, C_{para}C(*C*H_3)$_3$), 31.4 (d, $^{2}J_{CP}$ = 4.9 Hz, 3C, PC(*C*H_3)$_3$), 31.3 (d, $^{2}J_{CP}$ = 3.8 Hz, 3C, PC(*C*H_3)$_3$), 30.5 (br, 3C, PC(*C*H_3)$_3$), 30.2 (br, 3C, PC(*C*H_3)$_3$). ^{31}P{^{1}H} (161.25 MHz): δ = 66.9 (dd, $^{2}J_{PP}$ = 197,1 Hz, $^{2}J_{PP}$ = 35.4, 1P, *P*C(CH_3)$_3$), 53.5 (dd, $^{2}J_{PP}$ = 197,1 Hz, $^{2}J_{PP}$ = 35.3, 1P, *P*C(CH_3)$_3$), 17.7 (dd, $^{2}J_{PP}$ = 35.4 Hz, $^{2}J_{PP}$ = 35.3, 1P, *P*HMes*). IR (KBr, cm^{-1}): 2333 (ν_{P-H}), 1888 (ν_{CO}). LIFDI-MS (toluene, m/z): 853.4 (100%, [M]$^{+}$).

[Os(PHMes*)H(PNP)][Al(OR)$_4$] (9)

5 (10 mg, 12.1 µmol, 1.0 eq) is dissolved in Et_2O (1 mL) and cooled to -35°C. Ag[Al(O-^{t}Bu-F_9)$_4$] (13 mg, 12.1 µmol, 1.0 eq) is added and the solution is stirred for 30 seconds. After filtration the solvent is removed and the residue is extracted with Et_2O (5 x 0.5 mL) at -35°C. After concentration *i. vac.* the solution is layered with pentane (5 mL) and stored at -85°C for 24 h. The solution is decanted off and the solid is washed with pentane at -30°C (5 x 1 mL). After drying *in* vacuo at -30°C, **9** is obtained as a blue solid (18 mg, 10 µmol, 83%). NMR spectroscopic characterization shows minor decomposition products and some residual solvent (Et_2O/pentane). Elemental analysis did not give reproducible data due to low thermal stability.

NMR (THF-d_8, -30°C): ^{1}H (500 MHz): δ = 18.3 (d, $^{1}J_{HP}$ = 345.5 Hz, 1H, P*H*Mes*), 7.86 – 7.68 (m, 2 H, NC*H*CHP), 7.50 (d, $^{4}J_{HH}$ = 1.83 Hz, 1H, C_{meta}*H*, Mes*), 7.42 (d, $^{4}J_{HH}$ = 1.893 Hz, 1H, C_{meta}*H*, Mes*), 5.79 (m, 1H, NCHC*H*P), 5.55 (m, 1H, NCHC*H*P), 1.58 (d, $^{3}J_{HP}$ = 14.0 Hz, 9H, PC(CH_3)$_3$), 1.52 (d, $^{3}J_{HP}$ = 13.9 Hz, 9H, PC(CH_3)$_3$), 1.46 (s, 9H, C_{ortho}C(CH_3)$_3$, Mes*), 1.40 (s, 9H, C_{ortho}C(CH_3)$_3$, Mes*), 1.36 (s, 9H, C_{para}C(CH_3)$_3$, Mes*), 1.10-1.00 (m, 18H, PC(CH_3)$_3$), -21.7 (m, 1H, Os*H*). ^{13}C{^{1}H} (125.76 MHz): δ = 168.2 (m, 1C, N*C*HCHP), 167.4 (m, 1C, N*C*HCHP), 154.5 (s, 1C, C_{para}, Mes*), 151.6 (s, 1C, C_{ortho}, Mes*), 151.9 (s, 1C, C_{ortho}, Mes*), 143.7 (br, 1C, C_{ipso}, Mes*), 125.16 (br, 2C, C_{meta}, Mes*), 122.3 (q, $^{1}J_{CF}$ = 291.8 Hz, 12C, *C*F_3), 110.0-108.9 (m, 2C, NCH*C*HP), 79.9 (br, 4C, *C*CF_3), 40.8 (s, 1C, C_{ortho}*C*(CH_3)$_3$), 40.3 (d, $^{1}J_{CP}$ = 21.6 Hz, 1C, P*C*(CH_3)$_3$), 40.1 (s, 1C, C_{ortho}*C*(CH_3)$_3$), 38.2 (d, $^{1}J_{CP}$ = 21.3 Hz, 1C, P*C*(CH_3)$_3$), 37.73 (d, $^{1}J_{CP}$ = 22.7 Hz, 1C, P*C*(CH_3)$_3$), 35.8 (s, 1C, C_{para}*C*(CH_3)$_3$), 34.7 (d, $^{1}J_{CP}$ = 22.4 Hz, 1C, P*C*(CH_3)$_3$), 33.8 (s, 3C, C_{ortho}C(*C*H_3)$_3$), 33.6 (s, 3C, C_{ortho}C(*C*H_3)$_3$), 31.4 (s, 3C, C_{para}C(*C*H_3)$_3$), 30.9 (br, 3C, PC(*C*H_3)$_3$), 30.7 (br, 3C, PC(*C*H_3)$_3$), 30.0 (br, 3C, PC(*C*H_3)$_3$), 29.3 (br, 3C, PC(*C*H_3)$_3$). ^{31}P{^{1}H} (161.25 MHz): δ = 169.2 (m, 1P, *P*HMes*), 61.5 (dd, $^{2}J_{PP}$ = 224.0Hz, $^{2}J_{PP}$ = 18.0Hz, 1P, *P*C(CH_3)$_3$), 52.28 (dd, $^{2}J_{PP}$ = 224.0Hz, $^{2}J_{PP}$ = 14.2Hz, 1P, *P*C(CH_3)$_3$). IR (Nujol, cm^{-1}): 2350 (ν_{P-H}). LIFDI-MS (THF, m/z): 826.4 (100%, [M]$^{+}$).

Spectroscopic characterization of 4

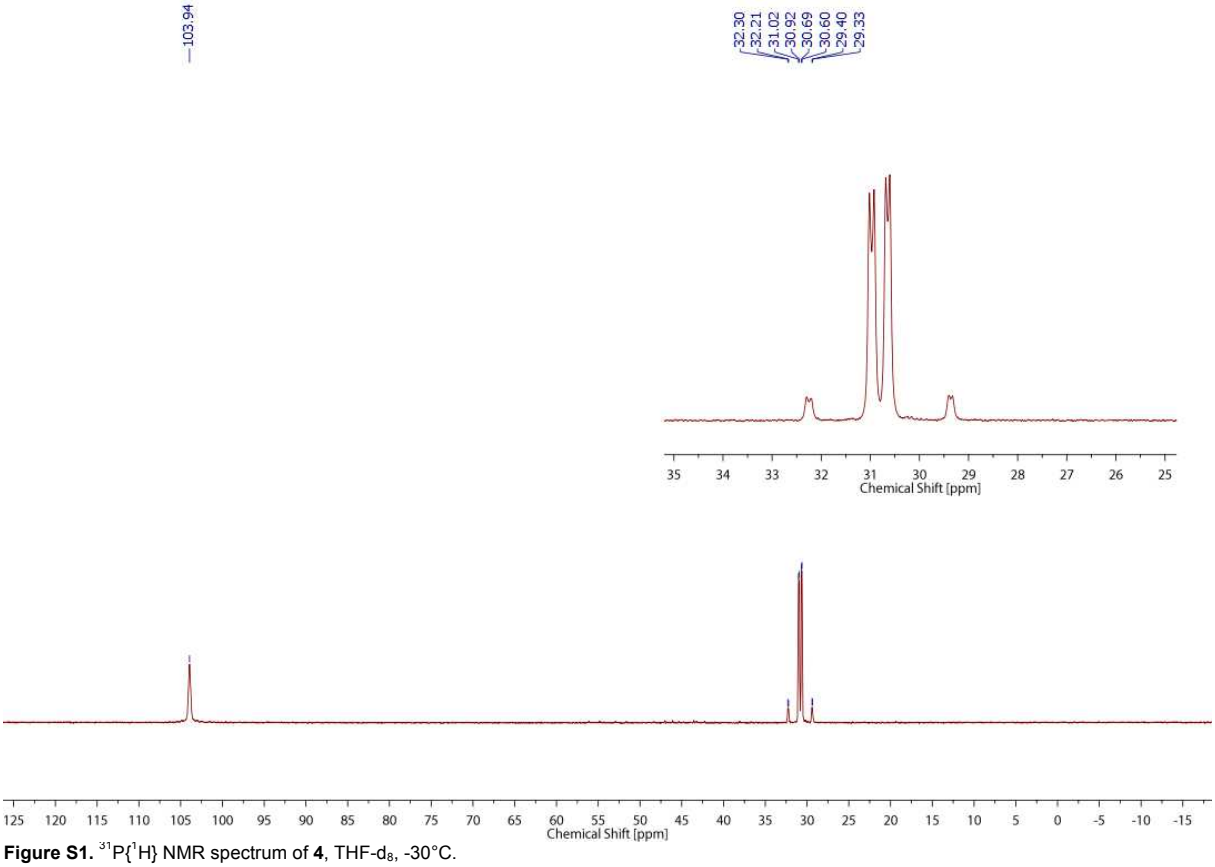

Figure S1. $^{31}P\{^{1}H\}$ NMR spectrum of **4**, THF-d_8, -30°C.

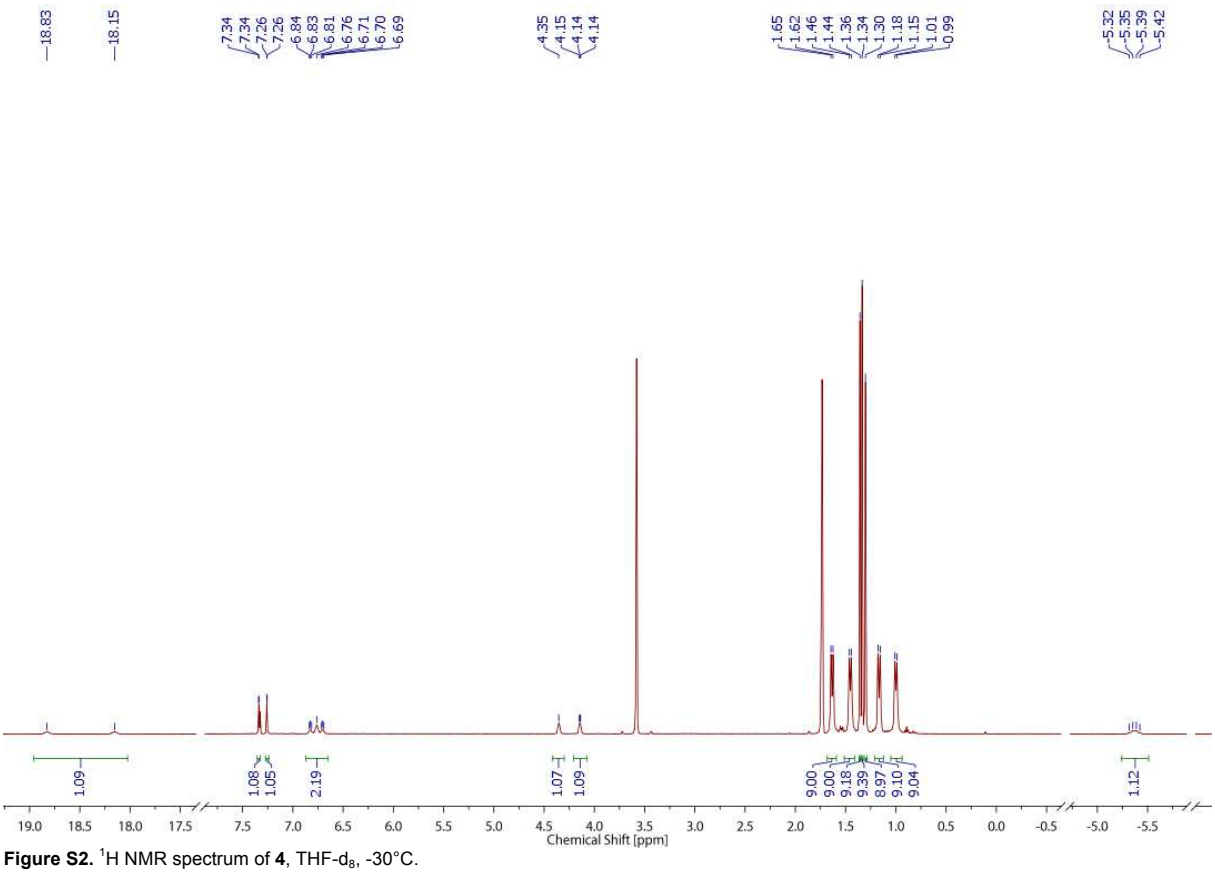

Figure S2. ^{1}H NMR spectrum of **4**, THF-d_8, -30°C.

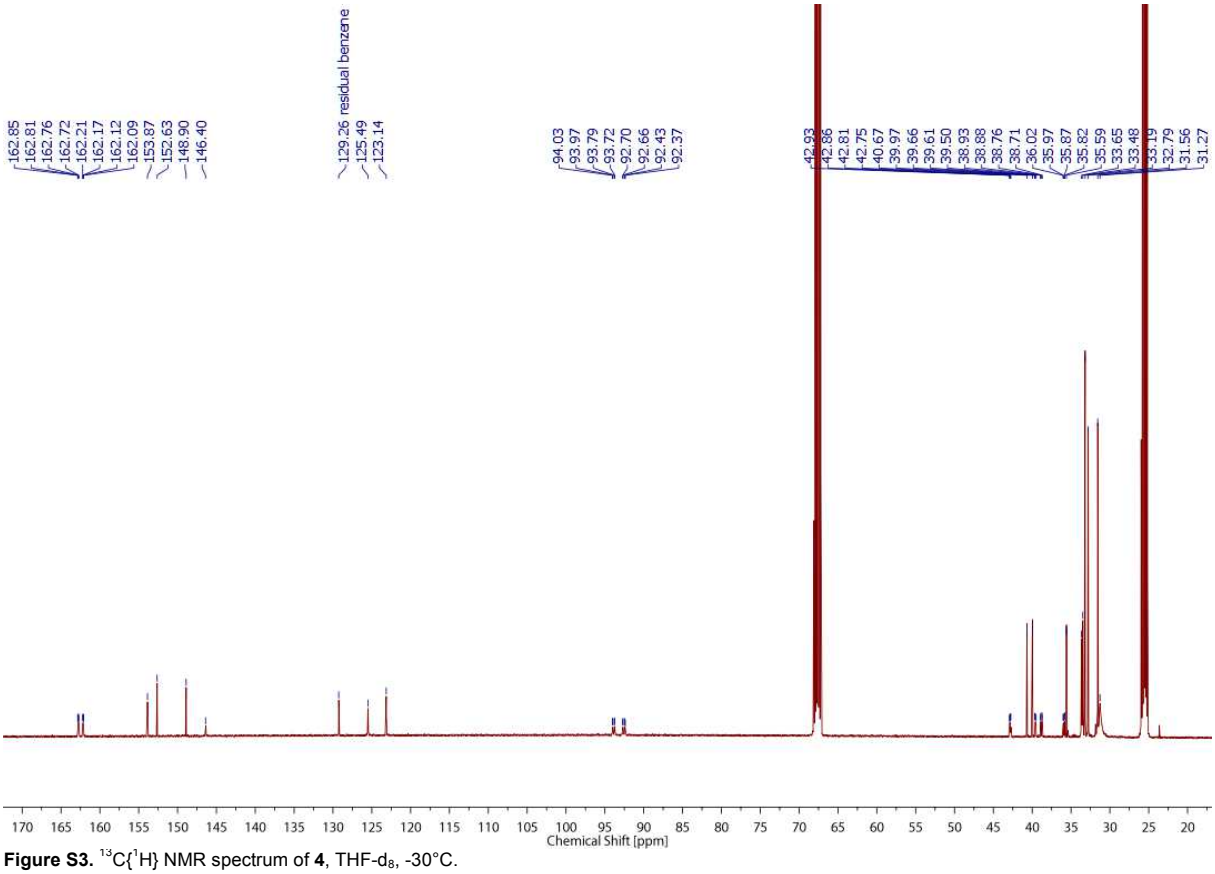

Figure S3. $^{13}C\{^{1}H\}$ NMR spectrum of **4**, THF-d_8, -30°C.

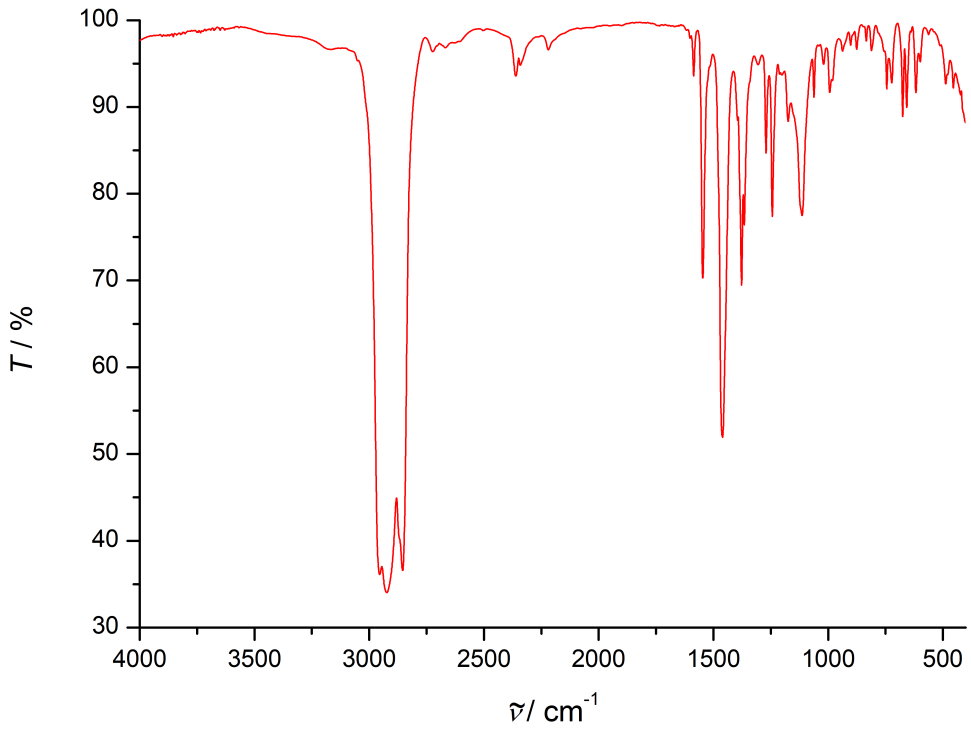

Figure S4. IR spectrum of **4**, Nujol, RT.

Spectroscopic characterization of 5

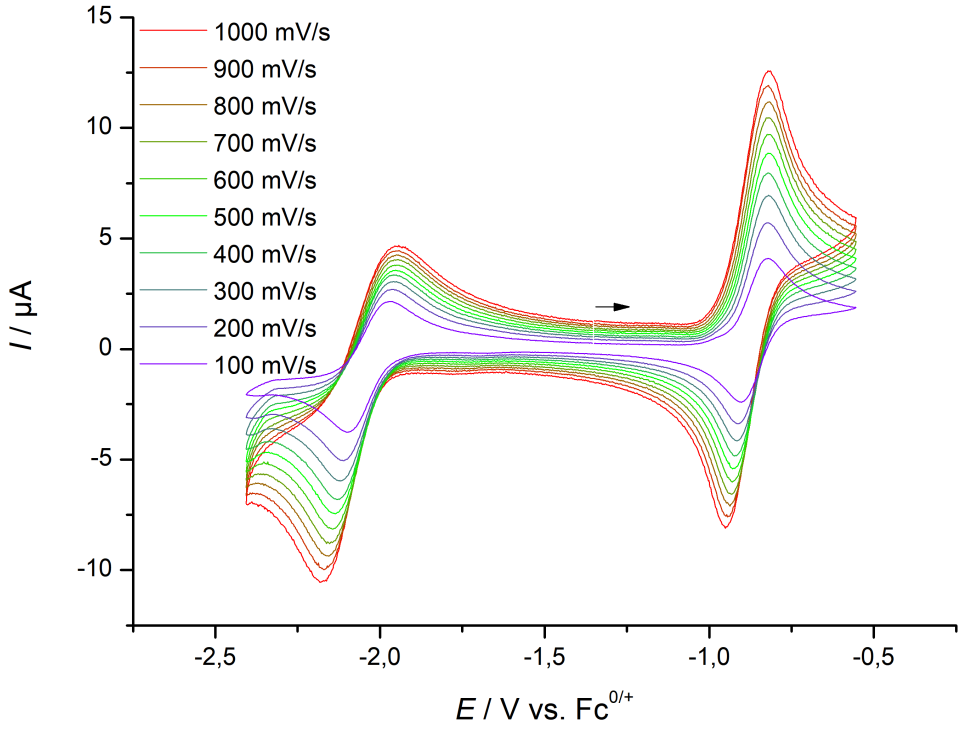

Figure S5. Cyclic voltammogram of **5**, 2nd scan, 1 mM, 0.1 M NBu_4PF_6, THF, RT.

The EPR spectrum of complex **5** is shown in Figure S6. The spectrum reveals fully resolved ^{31}P hyperfine interactions (HFI) and partially resolved ^{189}Os (16% natural abundance) HFI satellites. Simulation of the spectrum assuming coaxial g- and ^{31}P hyperfine A-tensors (W95EPR) yields ^{31}P hyperfine values (Figure S6) that deviate largely from the DFT calculated ones (Table S1).

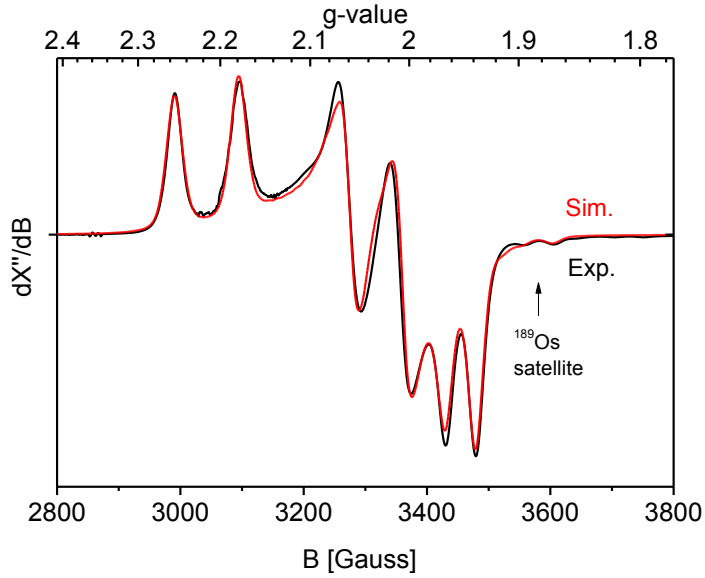

Figure S6. EPR spectrum of **5** (red), toluene, 148 K, 9.436620 GHz, simulation **assuming coaxial g- and ^{31}P A-tensors** (blue): g_{11} = 2.215, g_{22} = 2.032, g_{33} = 1.951, $A_{11}(^{31}P)$ = 322 MHz, $A_{22}(^{31}P)$ = 243 MHz, $A_{33}(^{31}P)$ = 136 MHz, $A_{11}(^{189}Os)$ = 230 MHz, $A_{22}(^{189}Os)$ and $A_{33}(^{189}Os)$ not resolved.

However, closer inspection of the DFT calculated EPR parameters reveals that the g-tensor of complex **5** is strongly tilted with respect to the molecular symmetry axes (Figure S7). This is most likely caused by predominant spin orbit coupling involving the SOMO and HOMO of **5** along these g-tensor axes.

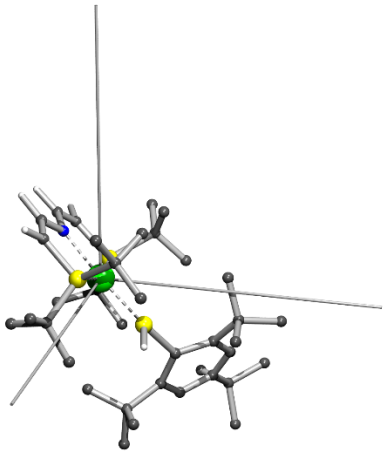

Figure S7. The electronic g-tensor directions of complex 5 are strongly tilted w.r.t. the molecular symmetry axes of the molecule.

In contrast, the ^{31}P hyperfine A-tensor is closely aligned with the molecular symmetry axes (Figure S8). In combination with the abovementioned strongly tilted g-tensor directions w.r.t. the molecular symmetry axes, the g- and A-tensors of complex **5** are not coaxial (Figure S9), with large DFT computed Euler angles of α = –74.3°, β = +142.7° and γ = –7.5°.

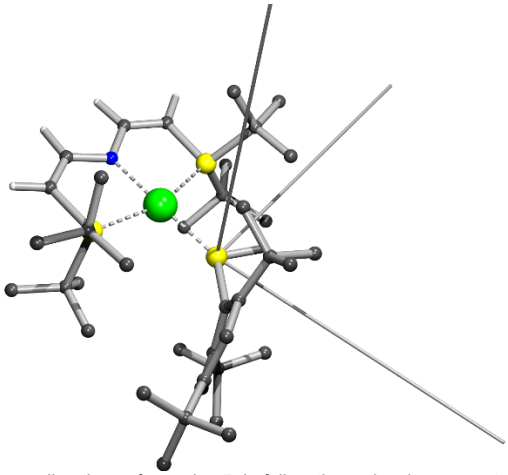

Figure S8. The phosphorus hyperfine A-tensor directions of complex **5** do follow the molecular symmetry axes of the molecule.

.

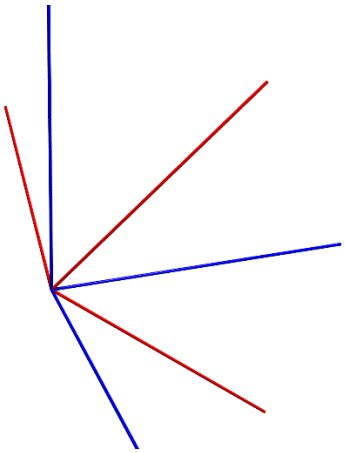

Computed tensor directions:

g =

-0.2268	0.7015	0.6756
0.4804	0.6840	-0.5489
0.8472	-0.2001	0.4922

A =

0.1790	-0.0050	-0.9838
0.6619	0.7405	0.1167
-0.7279	0.6721	-0.1359

Figure S9. The g-tensor (blue) and A-tensor (red) of complex 5 are not coaxial, with DFT computed Euler angles of α = –74.3°, β = +142.7° and γ = –7.5°.

Similarly, the ^{189}Os hyperfine interaction (HFI) tensor (16% natural abundance; HFI tensor roughly aligned along the symmetry axes of the molecule) is rotated with respect to the electronic g-tensor, with computed Euler angles of α = +90.5°, β = +51.7° and γ = +106.5°.

It is therefore clear that the experimental spectrum needs to be simulated using non-coaxial g- and A-tensors, the thus obtained simulation provides an excellent fit with g- and A-tensor values and Euler angles that closely match the DFT calculated EPR parameters (Figure S10, Table S1).

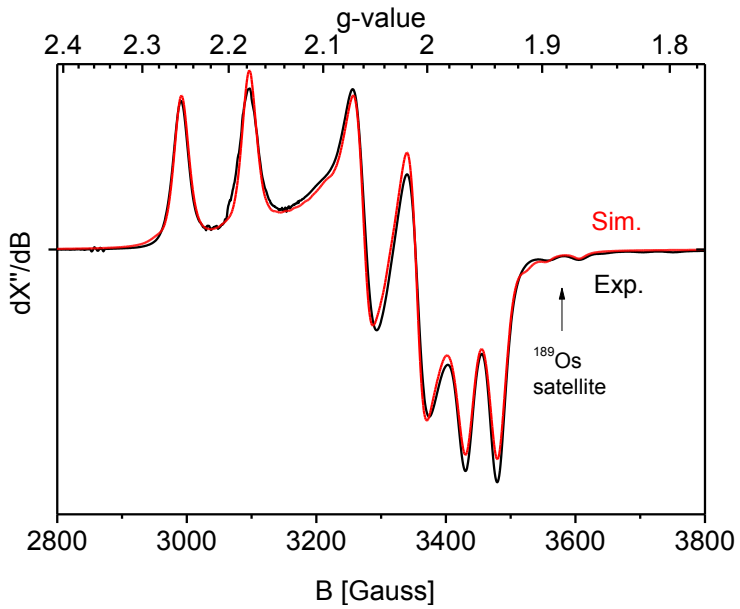

Figure S10. EPR spectrum of **5** (black), toluene, 148K, 9.436620 GHz, simulation **using non-coaxial g- and ^{31}P A-tensors** (red) using parameters shown in Table S1.

Table S1. Experimental[a] and DFT calculated[b] EPR parameters of **5**.

	Exp.[a]	***DFT [b]***
Electronic g-tensor		
g_{11}	1.9515	*1.9510*
g_{22}	2.0340	*2.0240*
g_{33}	2.2140	*2.2300*
^{31}P HFI tensor		
A^{31P}_{11}	+57 MHz [d]	*+57.5 MHz*
A^{31P}_{22}	+107 MHz	*+94.8 MHz*
A^{31P}_{33}	+440 MHz	*+440.8 MHz*
α^{31P} [c]	−72	*−74.3*
β^{31P} [c]	+137	*+142.7*
γ^{31P} [c]	−7.5	*−7.5*
^{189}Os HFI tensor		
A^{189Os}_{11}	−240 MHz	*−277.0 MHz*
A^{189Os}_{22}	NR [e]	*−36.9 MHz*
A^{189Os}_{33}	NR [e]	*+16.0 MHz*
α^{189Os} [c]	+90	*+90.5*
β^{189Os} [c]	+45	*+51.7*
γ^{189Os} [c]	+107	*+106.5*

[a] Derived from spectral simulation.
[b] ADF, B3LYP, all electron ZORA/QZ4P, unrestricted, collinear, spinorbit.
[c] Euler angles.
[d] A^{31P}_{11} is poorly resolved with these Euler angles (varying ± 50 MHz still gives a decent fit).
[e] NR = not resolved.

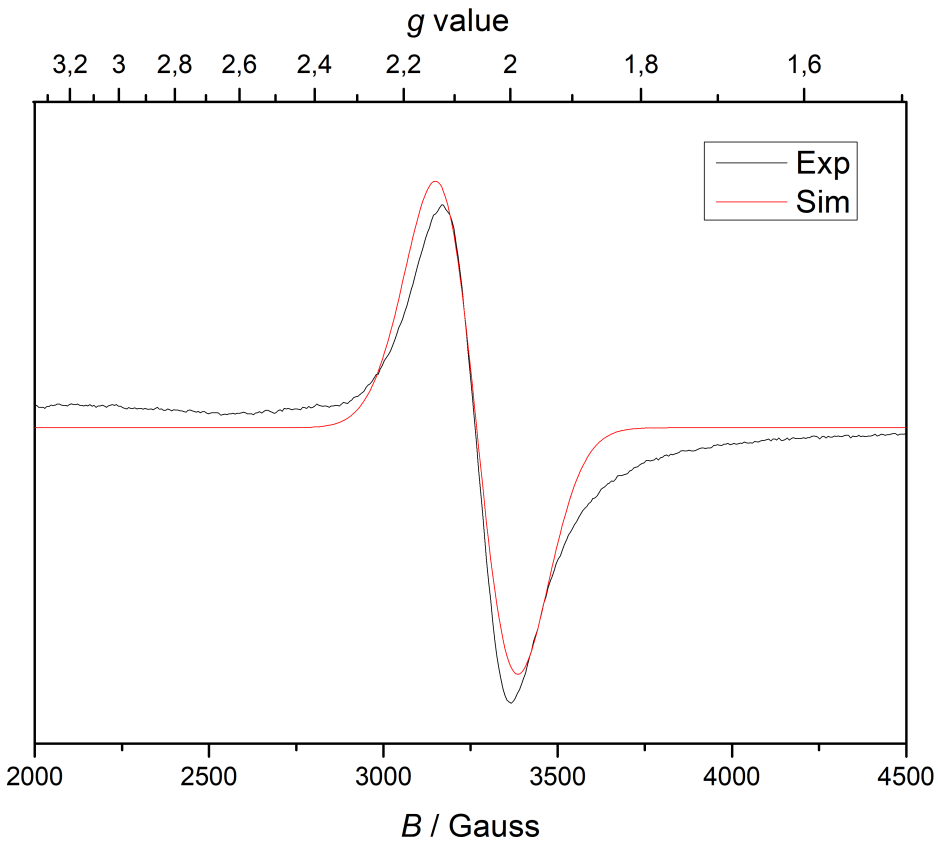

Figure S11. EPR spectrum of **5** (black), toluene, 293 K, 9.4262 GHz, simulation (red), g_{iso} = 2.0611.

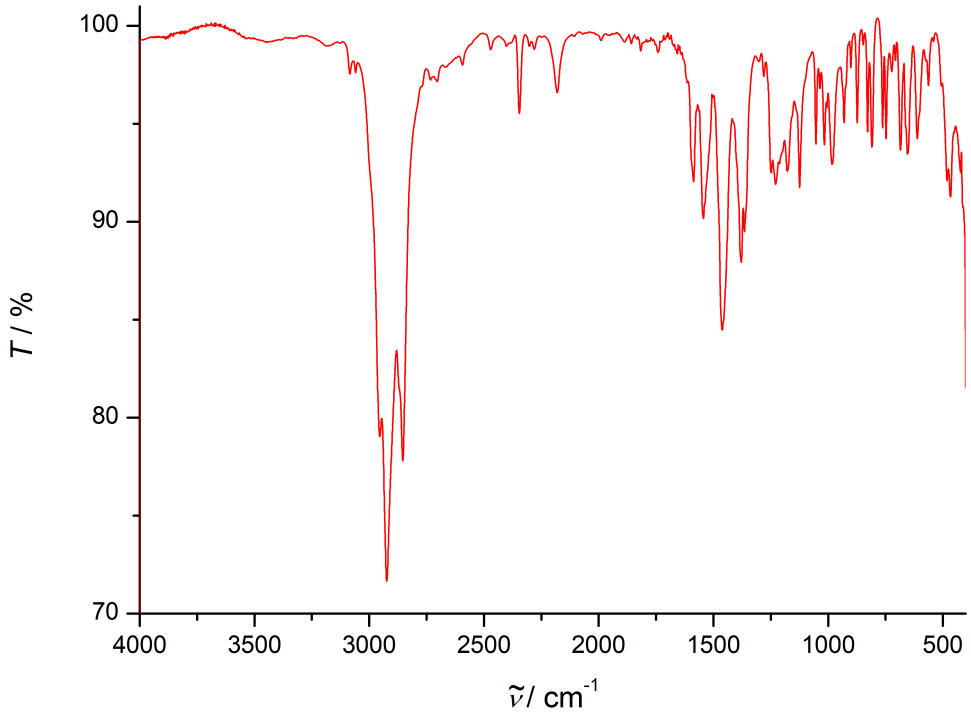

Figure S12. IR spectrum of **5**, Nujol, RT.

Spectroscopic characterization of 6

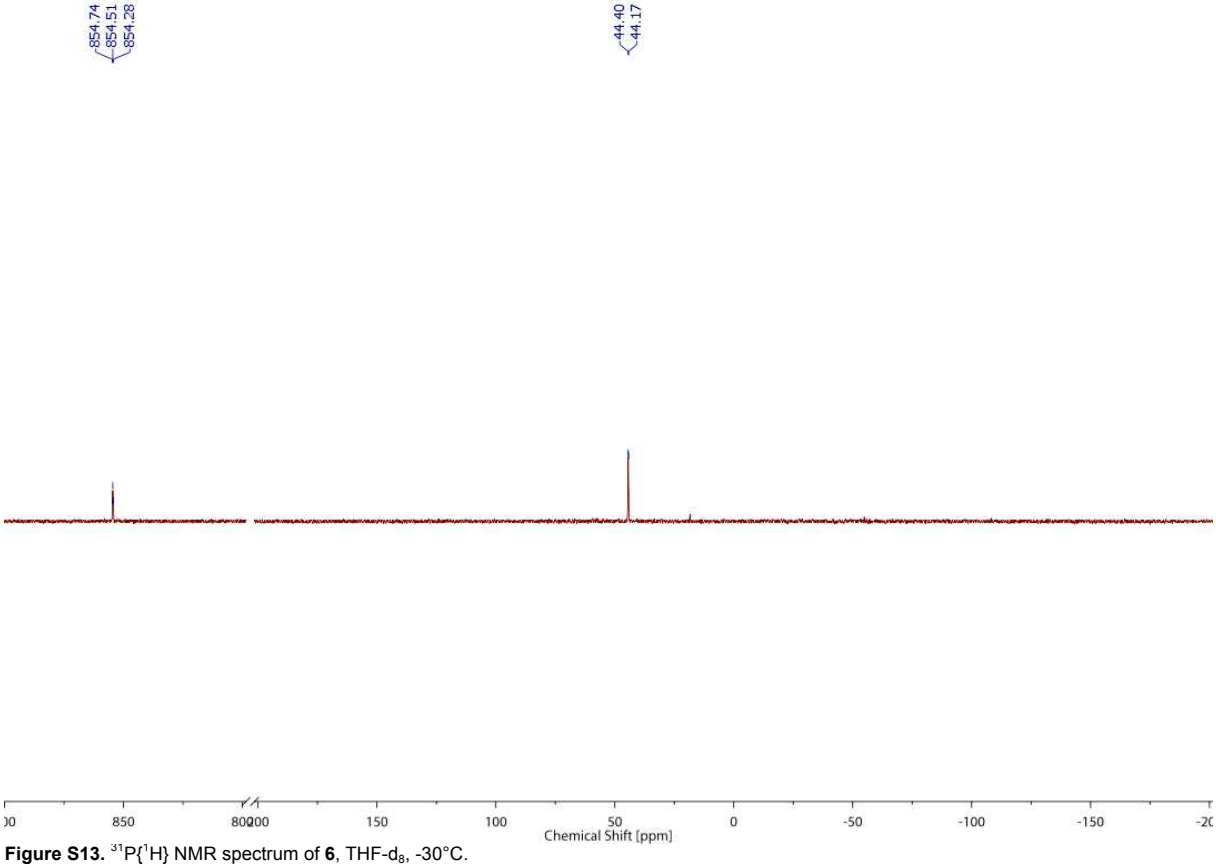

Figure S13. $^{31}P\{^{1}H\}$ NMR spectrum of **6**, THF-d_8, -30°C.

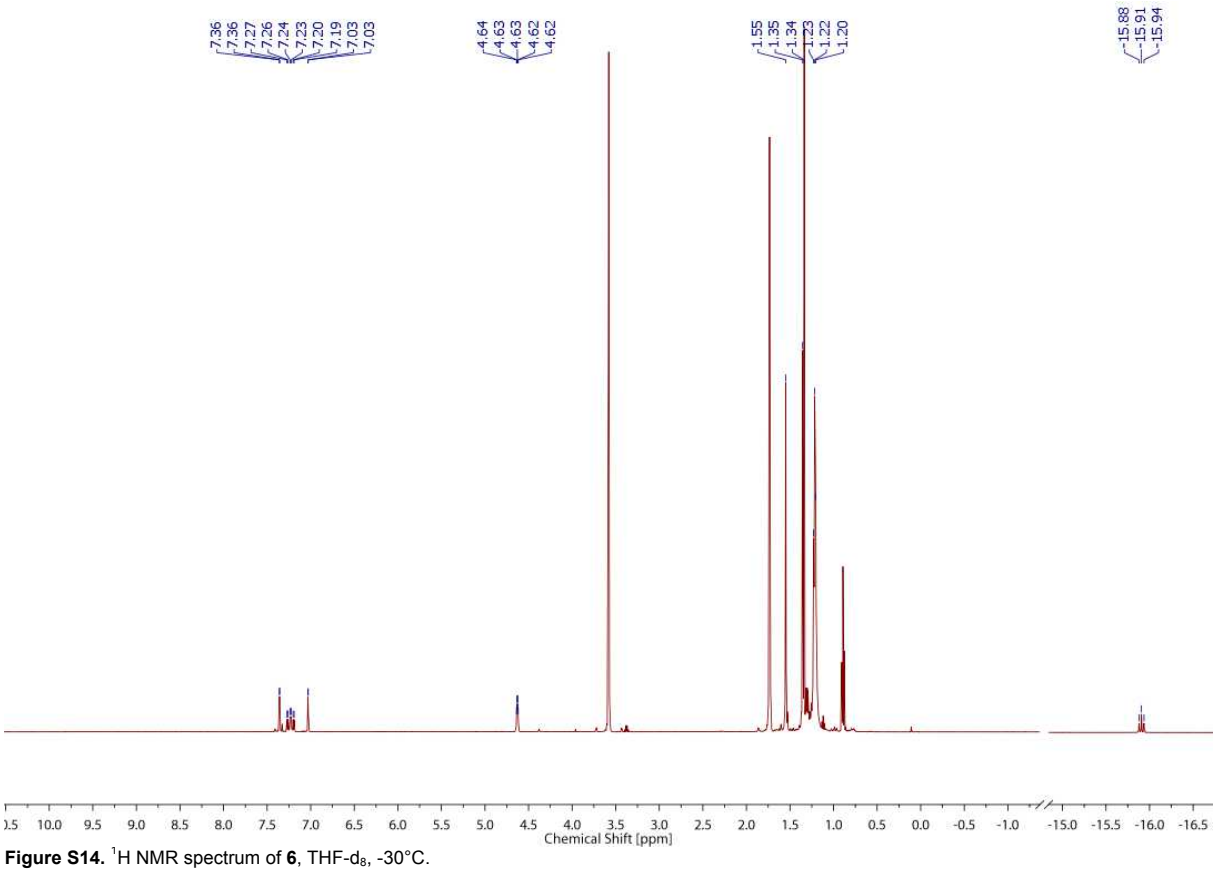

Figure S14. ^{1}H NMR spectrum of **6**, THF-d_8, -30°C.

Spectroscopic characterization of 7

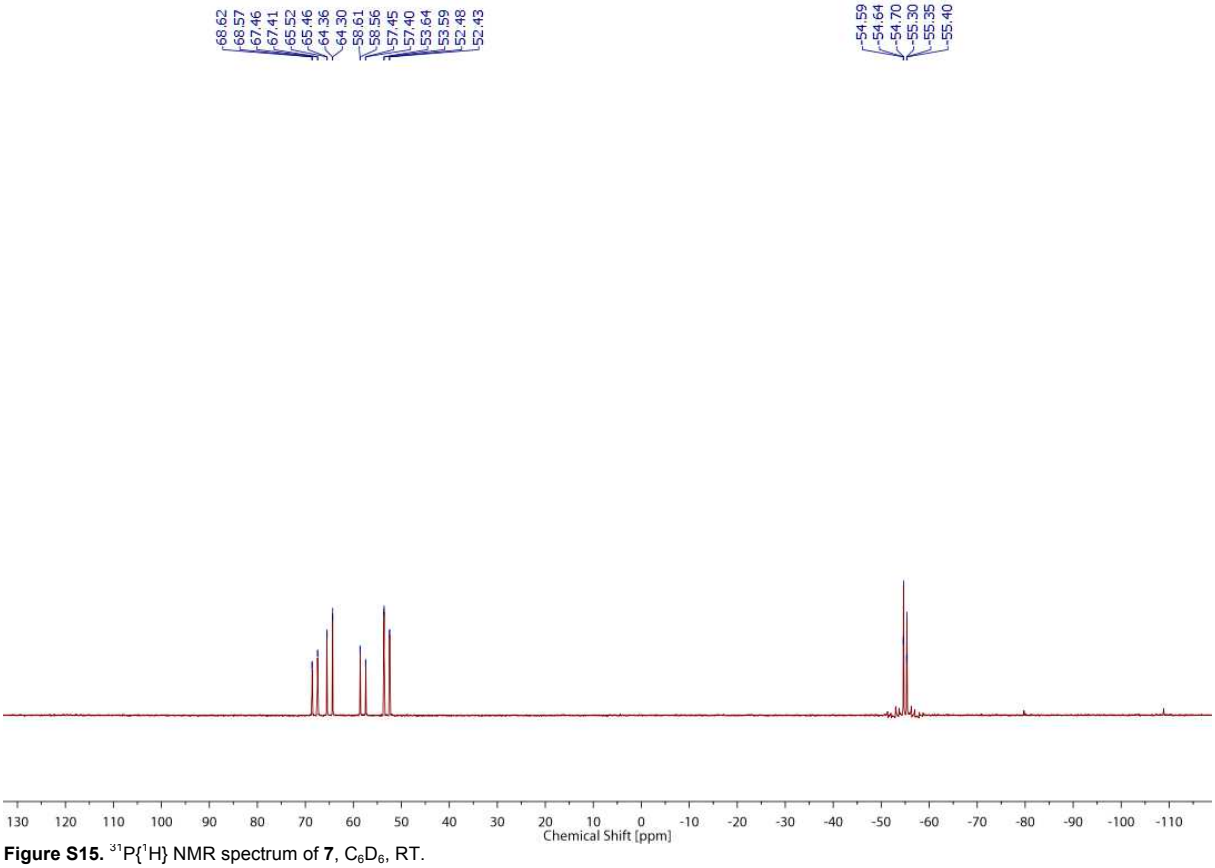

Figure S15. $^{31}P\{^{1}H\}$ NMR spectrum of **7**, C_6D_6, RT.

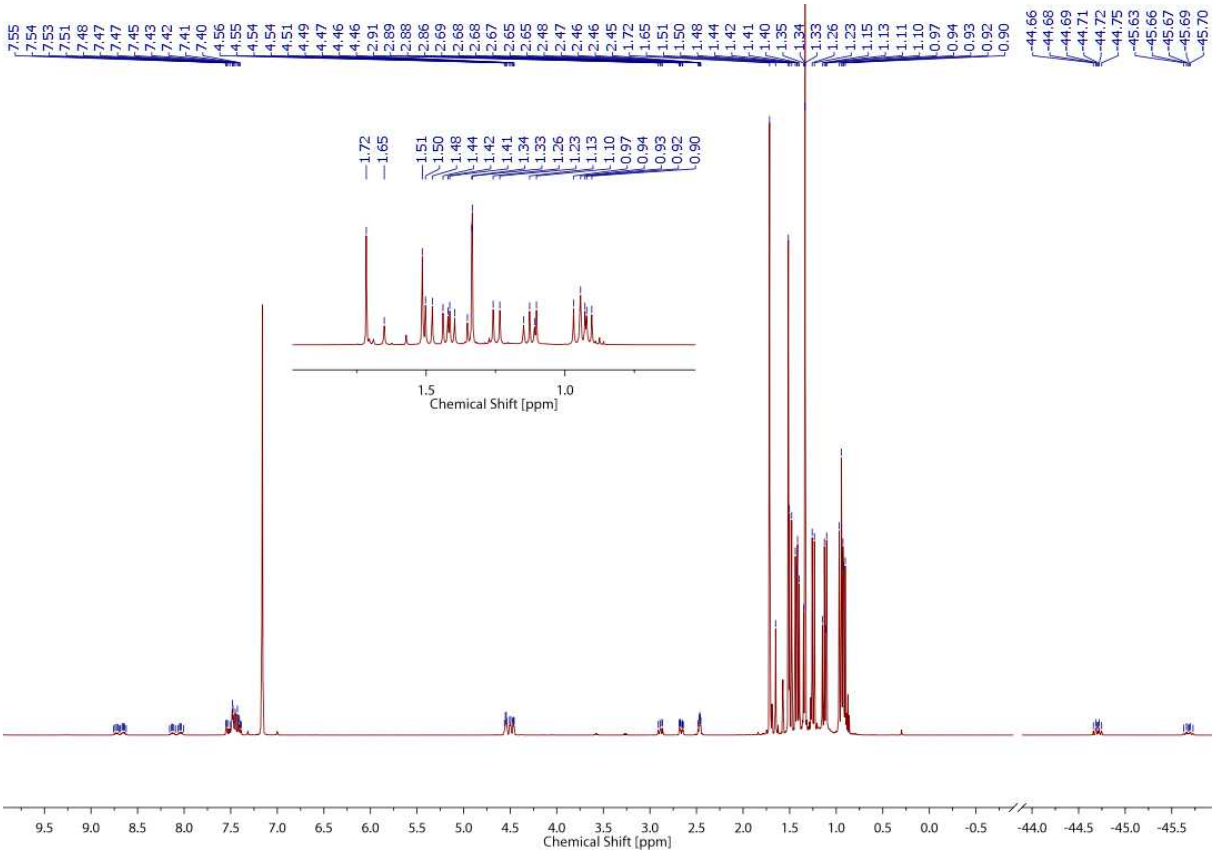

Figure S16. ^{1}H NMR spectrum of **7**, C_6D_6, RT.

Spectroscopic characterization of 8

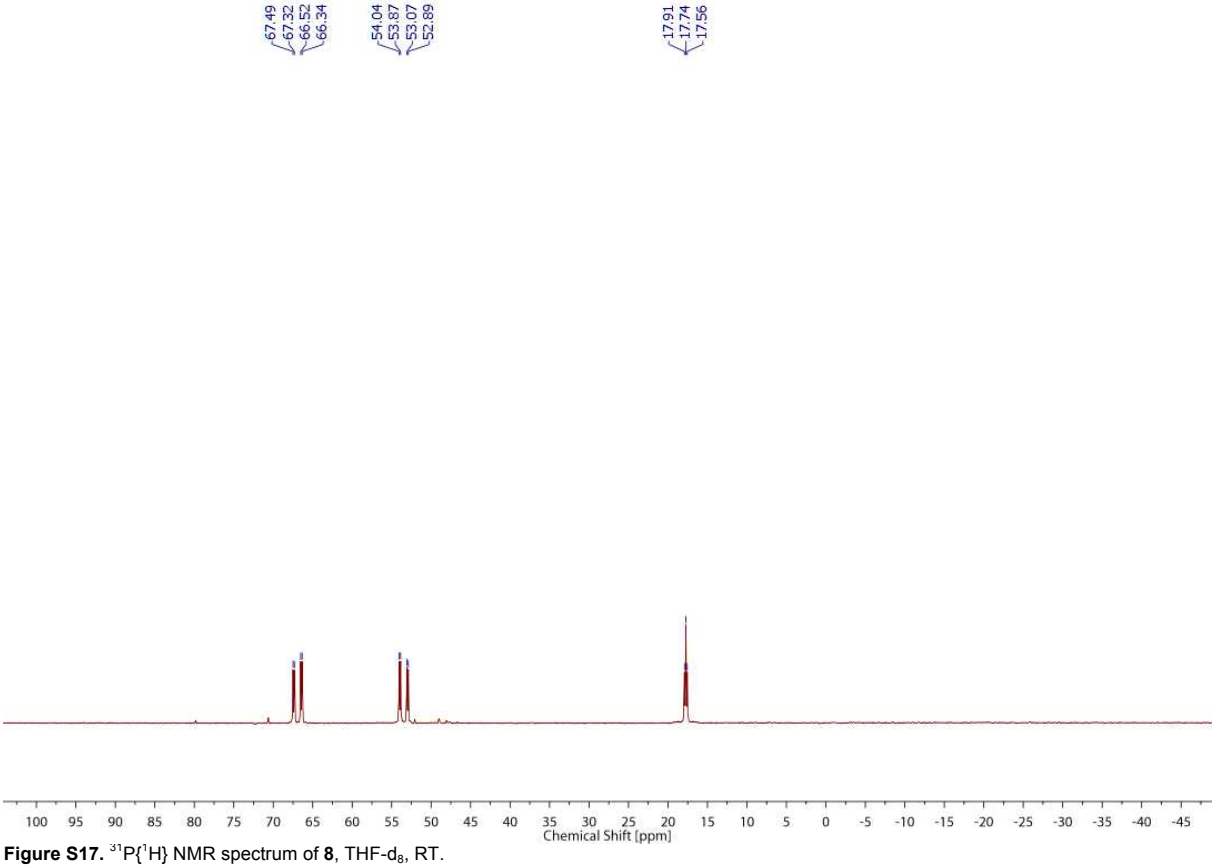

Figure S17. $^{31}P\{^{1}H\}$ NMR spectrum of **8**, THF-d_8, RT.

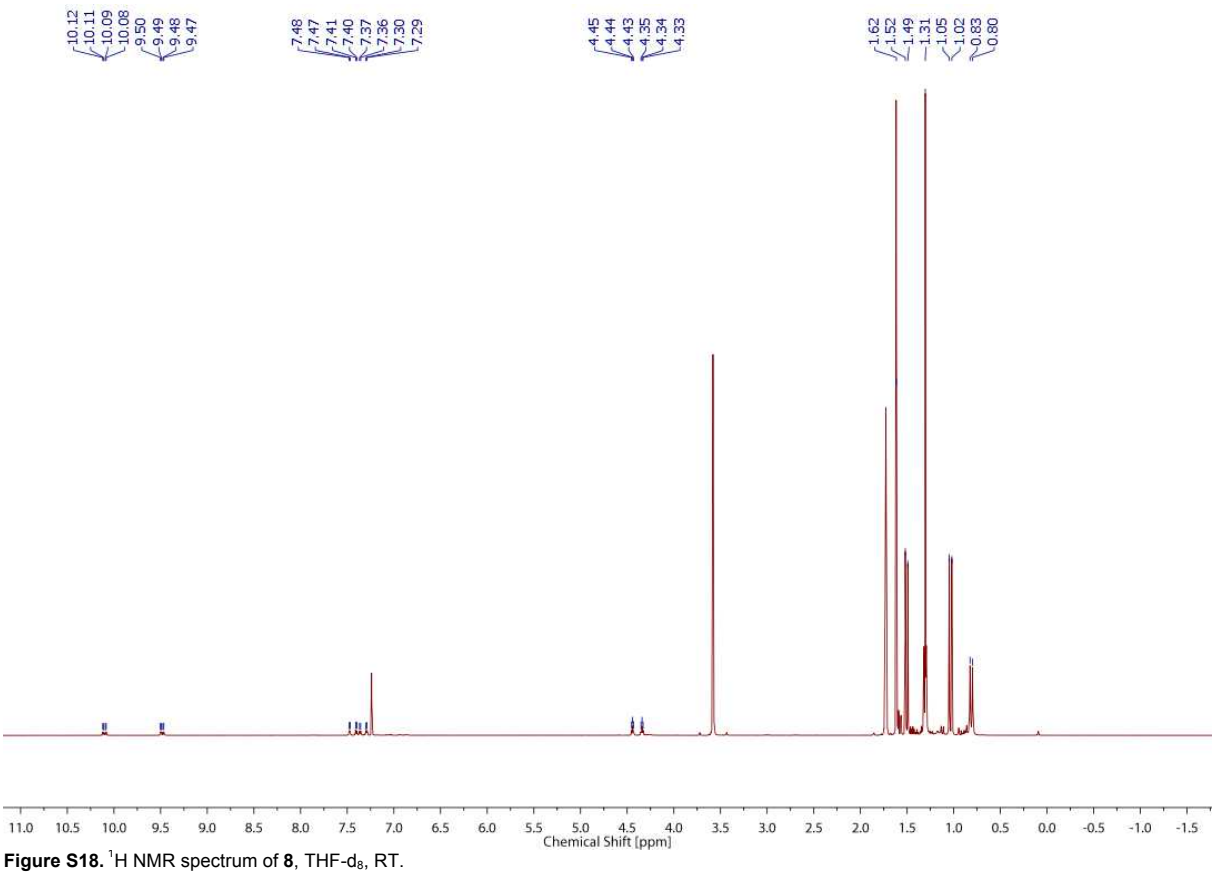

Figure S18. ^{1}H NMR spectrum of **8**, THF-d_8, RT.

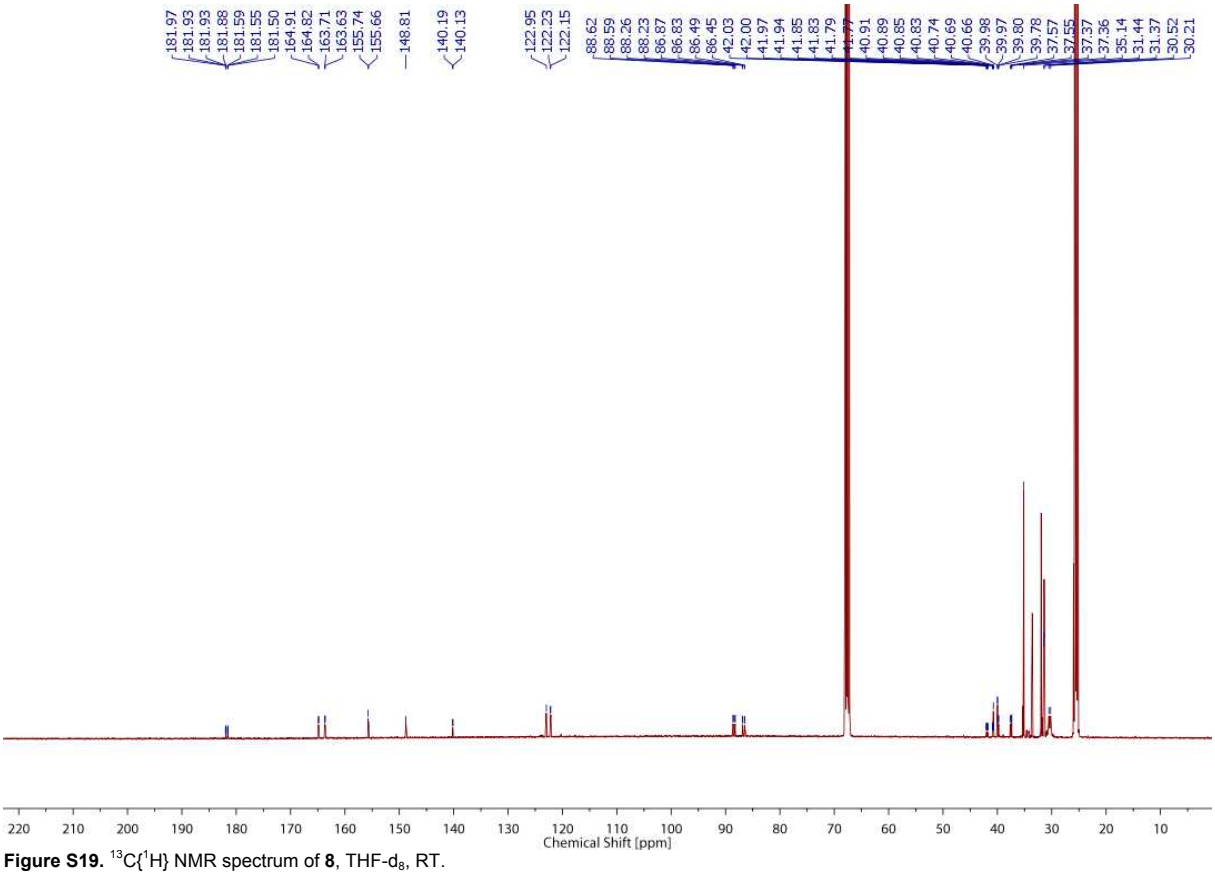

Figure S19. $^{13}C\{^{1}H\}$ NMR spectrum of **8**, THF-d_8, RT.

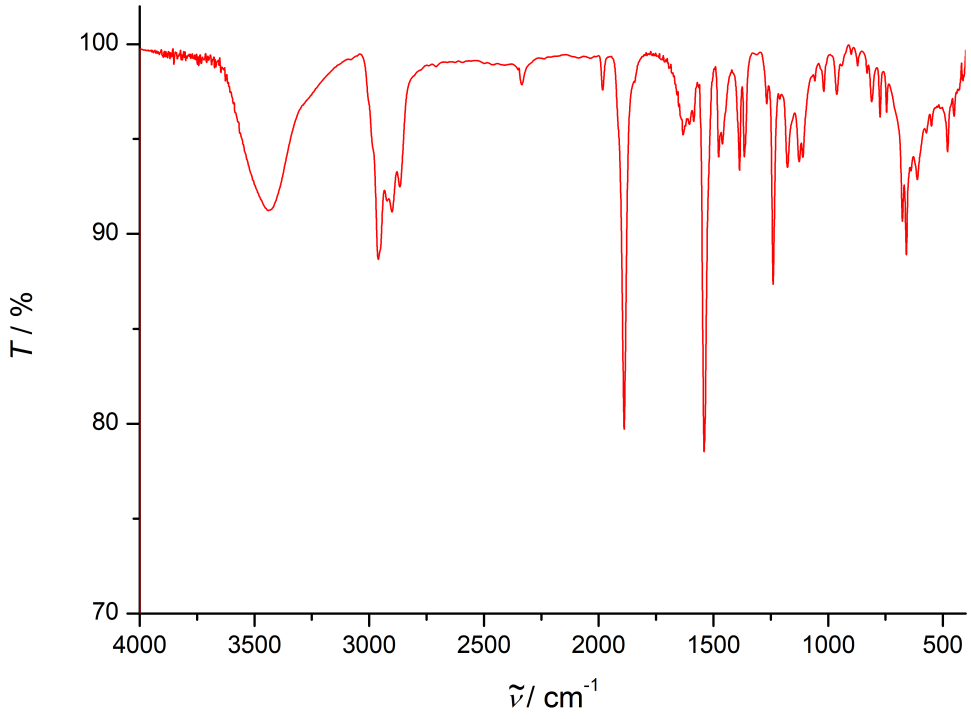

Figure S20. IR spectrum of **8**, KBr, RT.

Spectroscopic characterization of 9

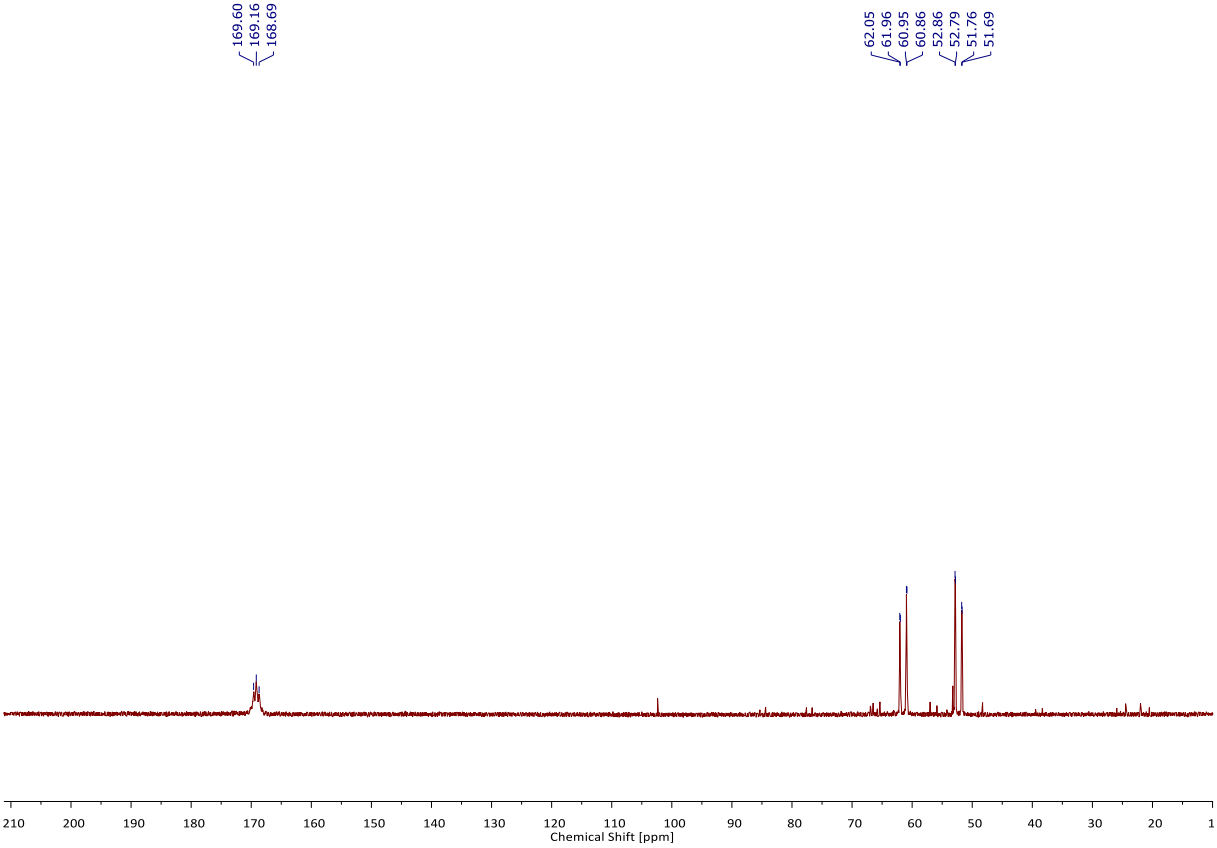

Figure S21. $^{31}P\{^{1}H\}$ NMR spectrum of **9**, THF-d_8, -30°C.

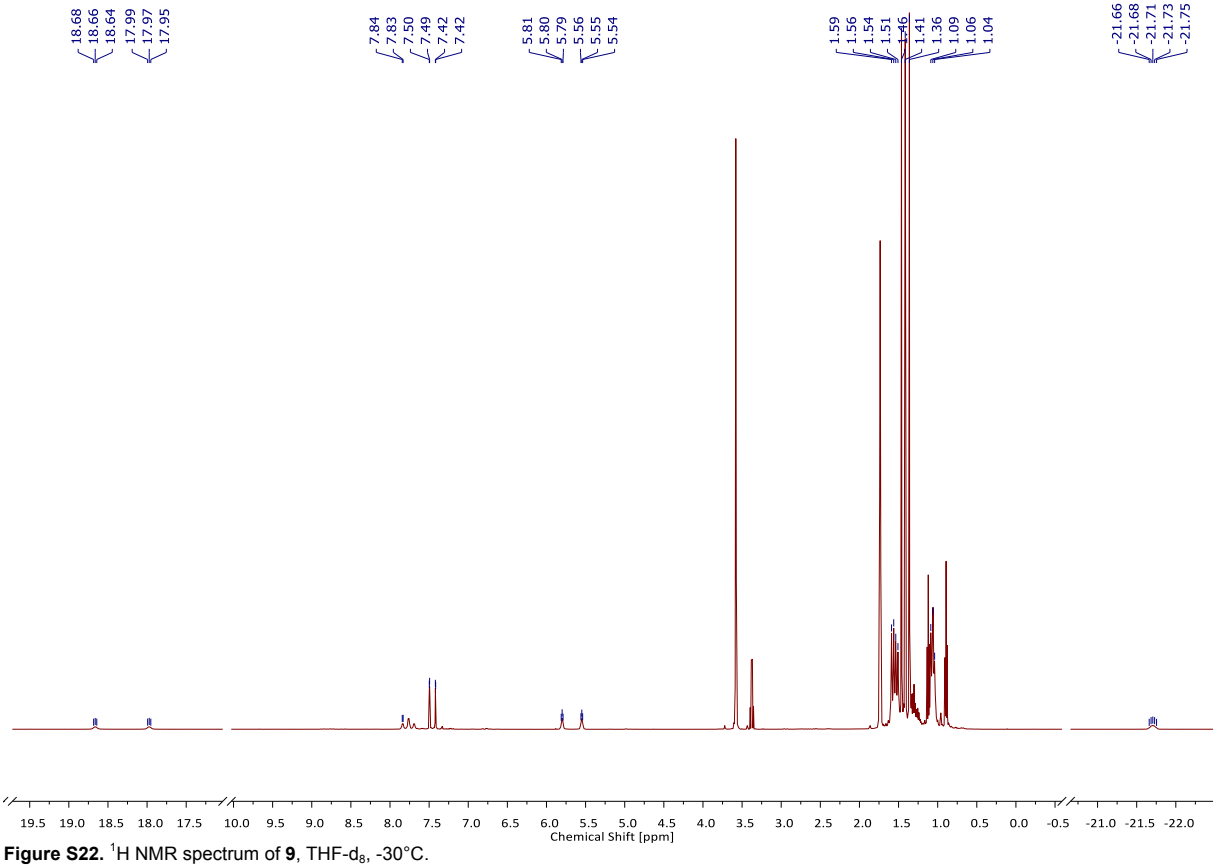

Figure S22. ^{1}H NMR spectrum of **9**, THF-d_8, -30°C.

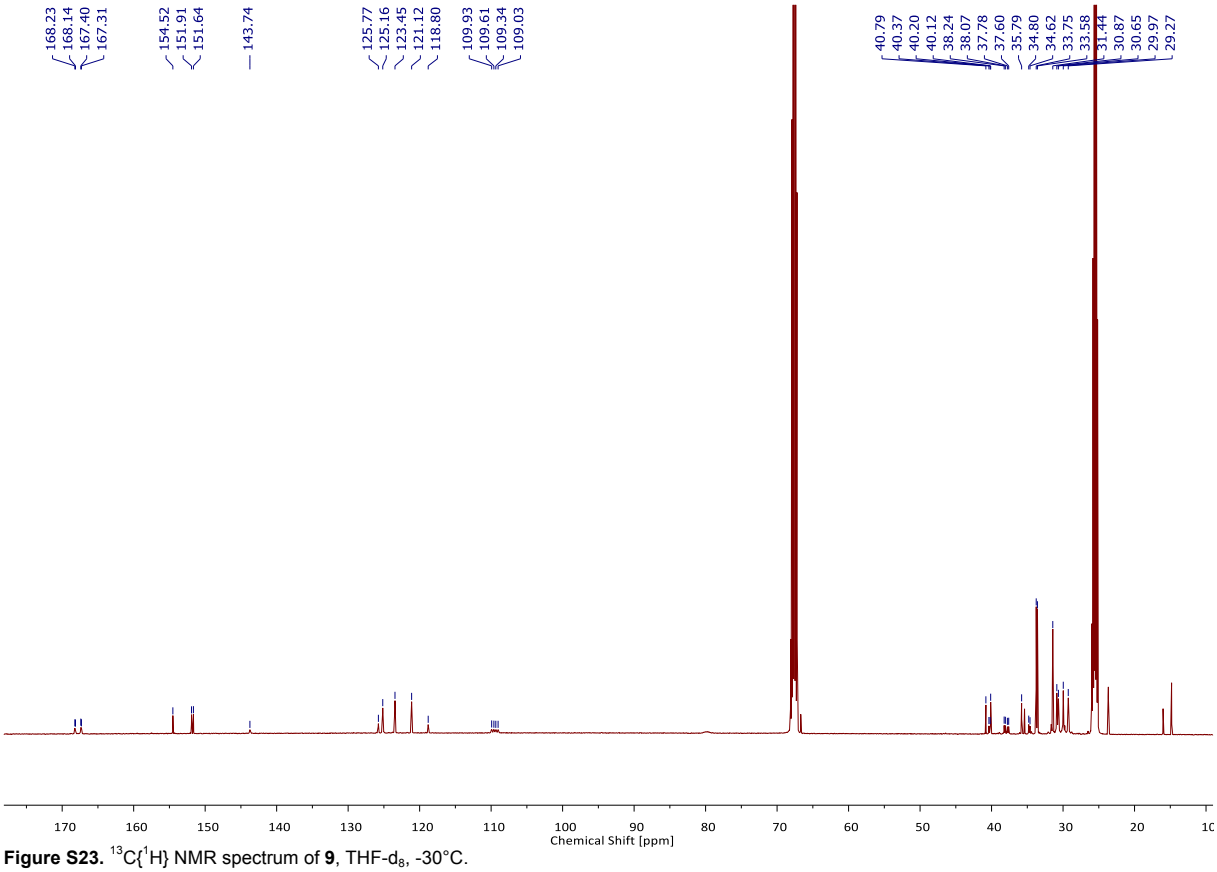

Figure S23. $^{13}C\{^{1}H\}$ NMR spectrum of **9**, THF-d_8, -30°C.

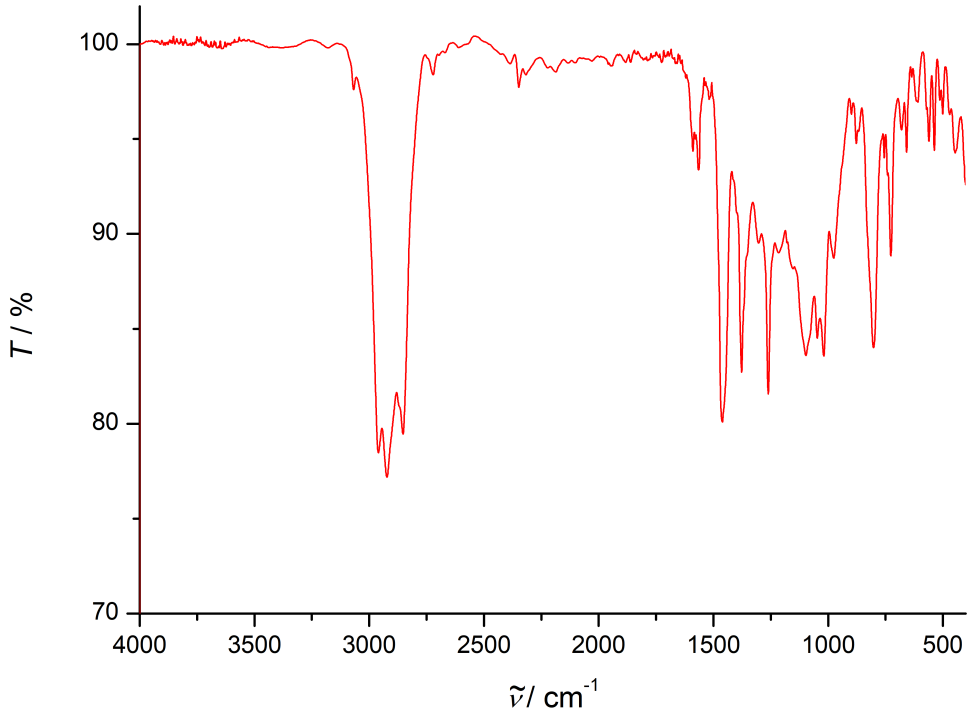

Figure S24. IR spectrum of **9**, Nujol, RT.

Titration Calorimetry

ITC in benzene

The Bond Dissociation Energy (BDE) of **5** was determined by Isothermal Titration Calorimetry using a TA INSTRUMENTS NanoITC equipped with a 24K gold cell (1 mL sample volume) and a 250 µL titration syringe operated in overfill mode. The instrument was run under an inert atmosphere inside an argon filled glove box. The syringe concentration was chosen to be 6.4 times higher than the cell concentration to have a titration range from 0 to 2 eq. 2,4,6-Tris-*tert*-butyl-phenoxyradical (Mes*O; BDE(O–H) = 81.6 kcal/mol)[4] was used as titrant. Both reactant solutions were prepared with Na/K dried benzene with a sample mass of more than 10.0 mg for sufficient accuracy. Titrations were carried out at 10 °C to suppress decay of **6** to **7** and corrected vs. addition of Mes*O to pure benzene in the sample cell (18 µJ p. addition). Further experimental conditions are detailed in Table S1. The data was evaluated using the implemented NanoAnalyze software.[5]

Table S2. Experimental details of Isothermal Titration Calorimetry in benzene.

Concentration and volume of **5**	1.02 mM/950 µL
Concentration and volume of TBP	9.18 mM/250 µL
Injection Steps/Injected Volume	33@7.5µL
Waiting time between two additions	350-650 s*
Stirring rate	350 rpm
Equilibration Time befor experiment start	1514 s

* The peaks for the BDE determination had a waiting time of 350 s.

A representative thermogram is shown in Figure S25. The first two peaks of each titration were generally neglected due to diffusion of reactant solution into the cell during equilibration of the instrument. Around the addition of one equivalent of Mes*O, the peaks show increased tailing, which is tentatively attributed to follow-up reactivity of **6**. The P–H BDE was therefore determined at an early titration stage from the average of injections 3-6 (Tables 2 and 3) while reliable BDFE determination was not possible. A cumulative error of 5 % for stock solution concentrations was estimated from the fitted n-value (0.95) which gives rise to an error in ΔH of 0.8 kcal/mol.

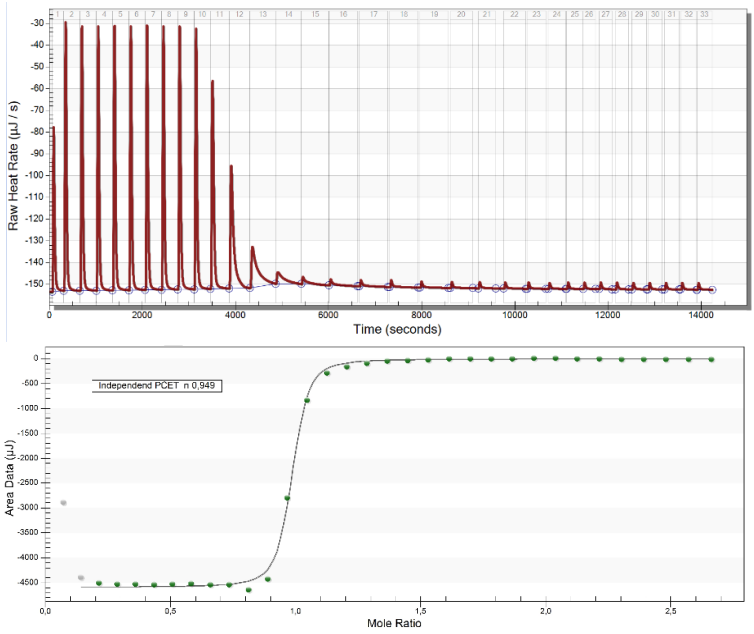

Figure S25. Representative thermogram (top) and integrated titration curve (bottom) of calorimetric titration of **5** with Mes*O in benzene.

Table S3. Integrated heats of the injections 3-6 for the BDE determination of **5** in benzene.

Injection	Heats [µJ] 1st run	Heats [µJ] 2nd run	Added moles
3	4682	4678	6.82E-8
4	4708	4678	6.82E-8
5	4703	4709	6.82E-8
6	4716	4711	6.82E-8
Mean	4702.25	4694	

Table S4. Results of the calorimetric BDE determination in benzene.

	ΔH (kJ/mol)	ΔH (kcal/mol)
Mean 1st run	-68.9	-16.5
Mean 2nd run	-68.8	-16.4
Mean	-68.9	-16.5
Mes*O[5]		81.6
BDE [Os]-PHAr		65.1±0.8

ITC in THF

The BDE measurement was also performed in THF to calculate a pK_A value of **5** via the Bordwell equation:

BDE = 23.06E^0 + 1.37pK_A + C_H. Where C_H(THF) = 66 kcal/mol.[6]

Otherwise, the experimental procedure was carried out as described above using the parameters listed in Table S5.

Table S5. Experimental details of Isothermal Titration Calorimetry in THF.

Concentration and volume of **5**	1.4 mM/950 µL
Concentration and volume of TBP	11.7 mM/250 µL
Injection Steps/Injected Volume	49@5µL
Waiting time between two additions	300 s
Stirring rate	350 rpm
Equilibration Time befor experiment start	1671 s

The P–H BDE of **5** was calculated from the mean heat evolved at the peaks 2-5 (Figure S26). The O-H BDE of Mes*OH in THF was determined by a square scheme using the oxidation potential of the Mes*-O/Mes*-O$^-$ redox couple (E^0 = -0.955 V vs. Fc/Fc$^+$; Figure S27). The pK_a value of Mes*OH was calculated from the reported value in DMSO according to Ding *et al.* (pK_a^{THF}(Mes*OH) = 1.03·17.8+11.3 = 29.6).[7,8] This results in a BDE of 84.5 kcal/mol for Mes*O/Mes*OH.

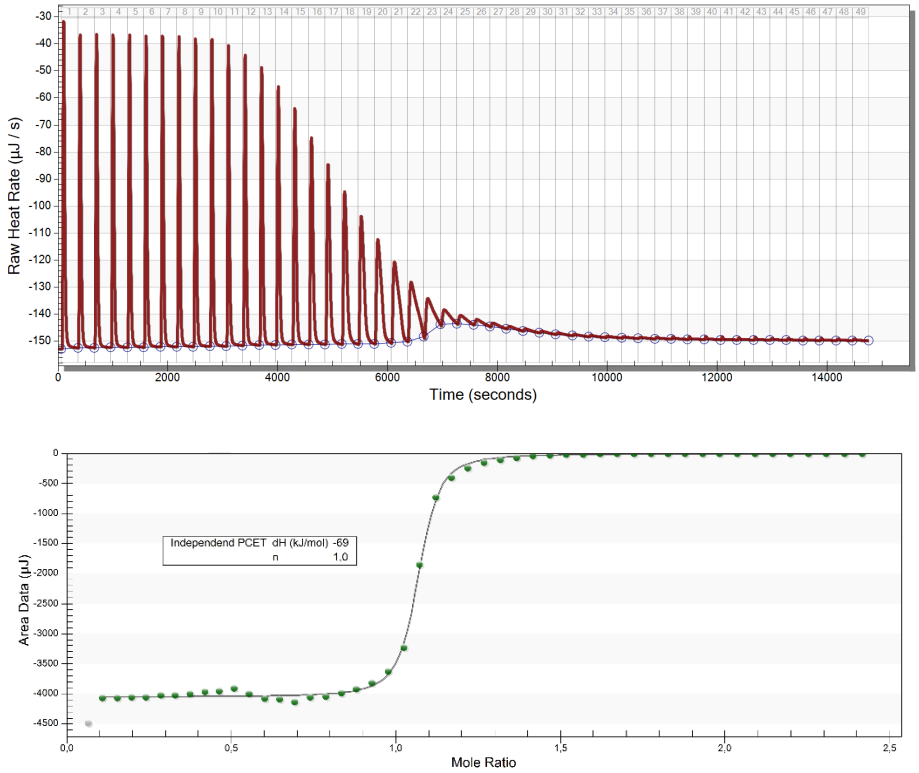

Figure S26. Representative thermogram (top) and integrated titration curve (bottom) of calorimetric titration of **5** with Mes*O in THF.

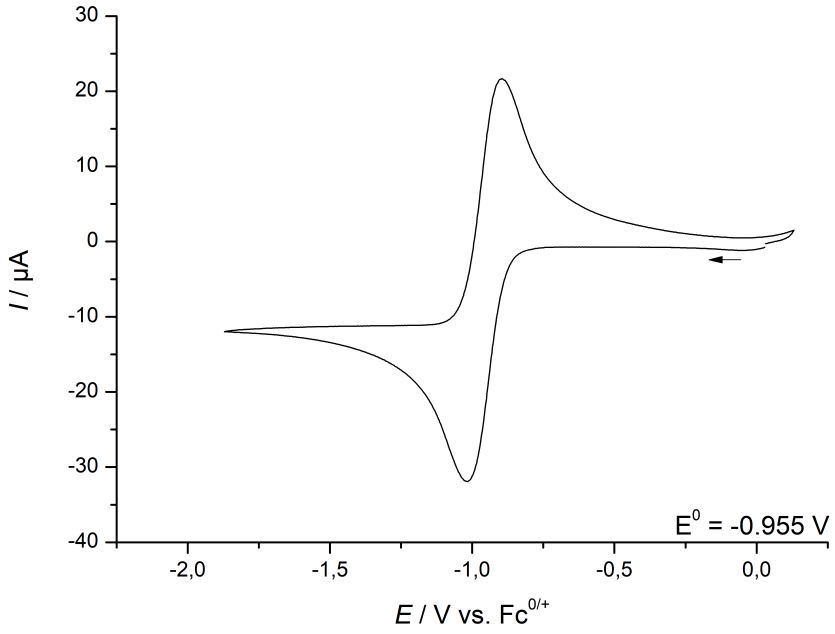

Figure S27. Cyclic voltammogram of Mes*O, 100 mV/s, 1 mM, 0.1 M NBu_4PF_6, THF, RT.

Table S6. Integrated heats of the injections 2-5 for the BDE determination of **5** in THF.

Injection*	Heats [µJ]	Added moles
2	4069	5.69E-8
3	4066	5.69E-8
4	4050	5.69E-8
5	4049	5.69E-8
Mean	4059	

Table S7. BDE determination in THF.

	ΔH (kJ/mol)	ΔH (kcal/mol)
Mean heat peaks 2-5	-71	-17
Mes*O(THF)		84.5
BDE [Os]-PHAr		67±1

The pK_A value of **9** was calculated using E^0(**5**) = -0.88 V and $BDE_{P–H}$(**5**) = 67 kcal mol^{-1}:

$$\mathrm{p}K_a = \frac{BDE - 23.06E^0 - C_H}{1.37} = 16$$

Crystallographic Details

CCDC-1894136 **(4)**, CCDC-1894134 **(5)**, CCDC-1894133 **(8)** and CCDC-1894135 **(9)** contain the supplementary crystallographic data for this paper. This data can be obtained free of charge via http://www.ccdc.cam.ac.uk/products/csd/request/ (or from Cambridge Crystallographic Data Centre, 12 Union Road, Cambridge, CB2 1EZ, UK. Fax: +44-1223- 336-033; e-mail: deposit@ccdc.cam.ac.uk).

Suitable single crystals for X-ray structure determination were selected from the mother liquor under an inert gas atmosphere and transferred in protective perfluoro polyether oil on a microscope slide. The selected and mounted crystals were transferred to the cold gas stream on the diffractometer. The diffraction data were obtained at 100 K on a Bruker D8 three-circle diffractometer, equipped with a PHOTON 100 CMOS detector and an INCOATEC microfocus source with Quazar mirror optics (Mo-Kα radiation, λ = 0.71073 Å).
The data obtained were integrated with SAINT and a semi-empirical absorption correction from equivalents with SADABS was applied. The structures were solved and refined using the Bruker SHELX 2014 software package.[9] All non-hydrogen atoms were refined with anisotropic displacement parameters. All C-H hydrogen atoms were refined isotropically on calculated positions by using a riding model with their U_{iso} values constrained to 1.5 U_{eq} of their pivot atoms for terminal sp3 carbon atoms and 1.2 times for all other atoms.

X-ray Single-Crystal Structure Analysis of 4

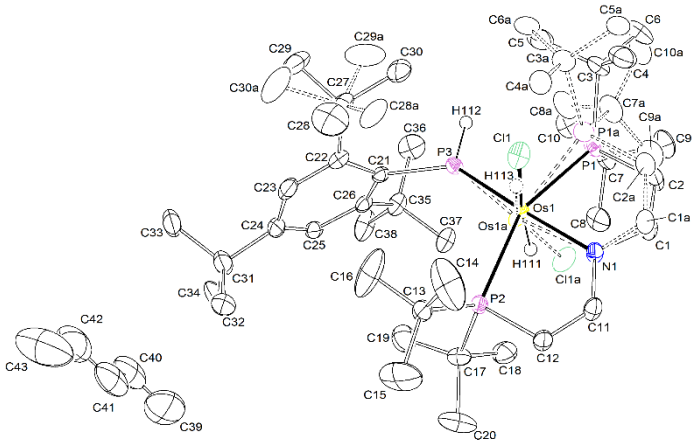

Figure S28. Thermal ellipsoid plot of **4** with the anisotropic displacement parameters drawn at the 50% probability level. The asymmetric unit contains one disordered complex molecule and one disordered pentane solvent molecule. The disordered Os(PNP)-part of the complex molecule was refined with population of 0.915(2) on the main domain using some restraints and constraints (SADI, RIGU, EADP). The disordered -$C(CH_3)_3$- part of the complex molecule was refined with population of 0.737(7) on the main domain using some restraints (SADI, RIGU,). The disordered solvent molecule was refined using PART-1 command and some restraints (SADI, RIGU) and constraints (EADP). The Os-H and P-H hydrogen atoms were found from the residual density map and isotropically refined.

Table S8. Crystal data and structure refinement for **4**.

Identification code	mo_CW_JA_060917_3_0m_a (JA-MN-45)	
Empirical formula	$C_{39}H_{71}ClNOsP_3 \times ½\ C_5H_{12}$	
Formula weight	896.59	
Temperature	100(2) K	
Wavelength	0.71073 Å	
Crystal system	Monoclinic	
Space group	C2/c	
Unit cell dimensions	a = 28.7206(11) Å	α= 90°
	b = 12.8908(5) Å	β= 99.050(2)°
	c = 23.8342(9) Å	γ = 90°
Volume	8714.3(6) $Å^3$	
Z	8	
Density (calculated)	1.367 Mg/m^3	
Absorption coefficient	3.125 mm^{-1}	
F(000)	3720	
Crystal size	0.163 x 0.105 x 0.054 mm^3	
Crystal shape and color	Plate,	clear intense blue-green
Theta range for data collection	2.370 to 28.352°	
Index ranges	-38<=h<=38, -17<=k<=17, -31<=l<=31	
Reflections collected	152470	
Independent reflections	10862 [R(int) = 0.0597]	
Completeness to theta = 25.242°	99.9 %	
Refinement method	Full-matrix least-squares on F^2	
Data / restraints / parameters	10862 / 619 / 612	

Goodness-of-fit on F^2	1.201	
Final R indices [I>2sigma(I)]	R1 = 0.0332,	wR2 = 0.0546
R indices (all data)	R1 = 0.0420,	wR2 = 0.0564
Largest diff. peak and hole	1.000 and -1.522 $eÅ^{-3}$	

Table S9. Bond lengths [Å] and angles [°] for **4**.

P(3)-C(21)	1.838(3)
P(3)-Os(1A)	2.109(9)
P(3)-Os(1)	2.1919(11)
P(3)-H(112)	1.35(3)
N(1)-C(1A)	1.357(19)
N(1)-C(11)	1.369(4)
N(1)-C(1)	1.376(4)
N(1)-Os(1)	2.078(3)
N(1)-Os(1A)	2.182(9)
P(2)-C(12)	1.785(3)
P(2)-C(13)	1.891(3)
P(2)-C(17)	1.900(4)
P(2)-Os(1A)	2.336(9)
P(2)-Os(1)	2.4475(10)
C(11)-C(12)	1.332(4)
C(13)-C(16)	1.505(5)
C(13)-C(14)	1.507(6)
C(13)-C(15)	1.515(5)
C(17)-C(19)	1.529(5)
C(17)-C(18)	1.537(5)
C(17)-C(20)	1.538(5)
C(21)-C(22)	1.423(4)
C(21)-C(26)	1.428(4)
C(22)-C(23)	1.385(5)
C(22)-C(27)	1.556(4)
C(23)-C(24)	1.385(5)
C(24)-C(25)	1.394(5)
C(24)-C(31)	1.527(5)
C(25)-C(26)	1.392(4)
C(26)-C(35)	1.553(4)
C(27)-C(28A)	1.378(15)
C(27)-C(29)	1.503(6)
C(27)-C(30)	1.542(6)
C(27)-C(28)	1.557(7)
C(27)-C(29A)	1.584(19)
C(27)-C(30A)	1.602(17)
C(31)-C(34)	1.531(6)
C(31)-C(32)	1.533(5)
C(31)-C(33)	1.542(5)
C(35)-C(36)	1.528(5)
C(35)-C(37)	1.528(4)
C(35)-C(38)	1.543(5)
C(40)-C(39)	1.332(13)
C(40)-C(41)	1.368(12)
C(42)-C(43)	1.329(13)
C(42)-C(41)	1.333(13)
P(1)-C(2)	1.789(3)
P(1)-C(3)	1.905(4)
P(1)-C(7)	1.913(4)
P(1)-Os(1)	2.4004(11)
Os(1)-Cl(1)	2.4912(11)
Os(1)-H(111)	1.54(2)
C(1)-C(2)	1.337(5)
C(3)-C(5)	1.511(6)
C(3)-C(4)	1.537(6)
C(3)-C(6)	1.547(5)
C(7)-C(8)	1.530(5)
C(7)-C(10)	1.533(5)
C(7)-C(9)	1.542(5)
Cl(1A)-Os(1A)	2.412(12)
Os(1A)-P(1A)	2.507(14)
Os(1A)-H(113)	1.54(2)
C(1A)-C(2A)	1.33(2)
C(2A)-P(1A)	1.80(4)
C(3A)-C(6A)	1.41(5)
C(3A)-C(4A)	1.43(5)
C(3A)-C(5A)	1.48(5)
C(3A)-P(1A)	1.99(4)
C(7A)-C(9A)	1.535(16)
C(7A)-C(8A)	1.538(16)
C(7A)-C(10A)	1.542(16)
C(7A)-P(1A)	1.88(4)
C(21)-P(3)-Os(1A)	134.9(2)
C(21)-P(3)-Os(1)	138.78(10)
C(21)-P(3)-H(112)	99.9(14)
Os(1A)-P(3)-H(112)	123.0(14)
Os(1)-P(3)-H(112)	121.0(14)
C(1A)-N(1)-C(11)	115.1(17)
C(11)-N(1)-C(1)	117.0(3)
C(11)-N(1)-Os(1)	122.1(2)
C(1)-N(1)-Os(1)	120.8(2)
C(1A)-N(1)-Os(1A)	125.8(17)
C(11)-N(1)-Os(1A)	118.4(3)
C(12)-P(2)-C(13)	103.31(15)
C(12)-P(2)-C(17)	102.49(16)
C(13)-P(2)-C(17)	108.42(15)
C(12)-P(2)-Os(1A)	102.3(2)
C(13)-P(2)-Os(1A)	126.7(2)
C(17)-P(2)-Os(1A)	110.45(19)
C(12)-P(2)-Os(1)	99.36(11)
C(13)-P(2)-Os(1)	122.09(11)
C(17)-P(2)-Os(1)	117.49(11)
C(12)-C(11)-N(1)	122.6(3)
C(11)-C(12)-P(2)	116.5(2)
C(16)-C(13)-C(14)	109.1(4)
C(16)-C(13)-C(15)	108.1(4)
C(14)-C(13)-C(15)	107.0(4)
C(16)-C(13)-P(2)	108.7(3)
C(14)-C(13)-P(2)	108.4(3)
C(15)-C(13)-P(2)	115.4(3)
C(19)-C(17)-C(18)	109.0(3)
C(19)-C(17)-C(20)	110.5(3)
C(18)-C(17)-C(20)	104.8(3)
C(19)-C(17)-P(2)	110.8(2)
C(18)-C(17)-P(2)	107.5(2)
C(20)-C(17)-P(2)	113.9(3)
C(22)-C(21)-C(26)	118.2(3)
C(22)-C(21)-P(3)	119.6(2)
C(26)-C(21)-P(3)	121.5(2)
C(23)-C(22)-C(21)	118.1(3)
C(23)-C(22)-C(27)	116.6(3)
C(21)-C(22)-C(27)	124.6(3)
C(24)-C(23)-C(22)	123.3(3)
C(23)-C(24)-C(25)	116.6(3)
C(23)-C(24)-C(31)	120.0(3)
C(25)-C(24)-C(31)	123.4(3)
C(26)-C(25)-C(24)	122.8(3)
C(25)-C(26)-C(21)	117.9(3)
C(25)-C(26)-C(35)	118.6(3)
C(21)-C(26)-C(35)	123.4(3)
C(29)-C(27)-C(30)	107.9(4)
C(28A)-C(27)-C(22)	113.9(7)

C(29)-C(27)-C(22)	106.0(3)
C(30)-C(27)-C(22)	115.4(3)
C(29)-C(27)-C(28)	109.1(5)
C(30)-C(27)-C(28)	104.6(4)
C(22)-C(27)-C(28)	113.6(3)
C(28A)-C(27)-C(29A)	115.0(11)
C(22)-C(27)-C(29A)	103.9(6)
C(28A)-C(27)-C(30A)	111.8(10)
C(22)-C(27)-C(30A)	107.2(7)
C(29A)-C(27)-C(30A)	104.2(12)
C(24)-C(31)-C(34)	112.0(3)
C(24)-C(31)-C(32)	108.5(3)
C(34)-C(31)-C(32)	108.1(3)
C(24)-C(31)-C(33)	110.3(3)
C(34)-C(31)-C(33)	109.7(4)
C(32)-C(31)-C(33)	108.2(3)
C(36)-C(35)-C(37)	110.4(3)
C(36)-C(35)-C(38)	105.1(3)
C(37)-C(35)-C(38)	106.7(3)
C(36)-C(35)-C(26)	110.0(3)
C(37)-C(35)-C(26)	113.0(2)
C(38)-C(35)-C(26)	111.3(3)
C(39)-C(40)-C(41)	114.7(10)
C(43)-C(42)-C(41)	123.3(16)
C(42)-C(41)-C(40)	114.2(13)
C(2)-P(1)-C(3)	104.38(17)
C(2)-P(1)-C(7)	101.81(17)
C(3)-P(1)-C(7)	108.42(16)
C(2)-P(1)-Os(1)	100.02(12)
C(3)-P(1)-Os(1)	122.24(13)
C(7)-P(1)-Os(1)	116.55(12)
N(1)-Os(1)-P(3)	171.59(8)
N(1)-Os(1)-P(1)	80.24(7)
P(3)-Os(1)-P(1)	93.81(4)
N(1)-Os(1)-P(2)	79.29(7)
P(3)-Os(1)-P(2)	105.12(4)
P(1)-Os(1)-P(2)	156.14(5)
N(1)-Os(1)-Cl(1)	85.23(8)
P(3)-Os(1)-Cl(1)	101.17(4)
P(1)-Os(1)-Cl(1)	93.62(5)
P(2)-Os(1)-Cl(1)	96.76(4)
N(1)-Os(1)-H(111)	85.1(11)
P(3)-Os(1)-H(111)	88.8(11)
P(1)-Os(1)-H(111)	87.8(8)
P(2)-Os(1)-H(111)	78.4(10)
Cl(1)-Os(1)-H(111)	169.8(12)
C(2)-C(1)-N(1)	122.8(3)
C(1)-C(2)-P(1)	115.8(3)
C(5)-C(3)-C(4)	109.5(4)
C(5)-C(3)-C(6)	109.3(4)
C(4)-C(3)-C(6)	104.9(3)
C(5)-C(3)-P(1)	109.4(3)
C(4)-C(3)-P(1)	107.5(3)
C(6)-C(3)-P(1)	115.9(3)
C(8)-C(7)-C(10)	107.8(3)
C(8)-C(7)-C(9)	105.5(3)
C(10)-C(7)-C(9)	109.8(3)
C(8)-C(7)-P(1)	108.4(2)
C(10)-C(7)-P(1)	112.3(3)
C(9)-C(7)-P(1)	112.6(3)
P(3)-Os(1A)-N(1)	165.7(4)
P(3)-Os(1A)-P(2)	112.0(4)
N(1)-Os(1A)-P(2)	79.8(3)
P(3)-Os(1A)-Cl(1A)	105.6(4)
N(1)-Os(1A)-Cl(1A)	79.3(4)
P(2)-Os(1A)-Cl(1A)	99.9(4)
P(3)-Os(1A)-P(1A)	90.0(4)
N(1)-Os(1A)-P(1A)	76.4(3)
P(2)-Os(1A)-P(1A)	151.6(4)
Cl(1A)-Os(1A)-P(1A)	90.7(5)
P(3)-Os(1A)-H(113)	95(3)
N(1)-Os(1A)-H(113)	77(3)
P(2)-Os(1A)-H(113)	90(2)
Cl(1A)-Os(1A)-H(113)	152(3)
P(1A)-Os(1A)-H(113)	70(2)
C(2A)-C(1A)-N(1)	118(3)
C(2A)-C(1A)-H(1A)	121.2
N(1)-C(1A)-H(1A)	121.2
C(1A)-C(2A)-P(1A)	121(3)
C(1A)-C(2A)-H(2A)	119.4
P(1A)-C(2A)-H(2A)	119.4
C(6A)-C(3A)-C(4A)	114(4)
C(6A)-C(3A)-C(5A)	109(3)
C(4A)-C(3A)-C(5A)	109(3)
C(6A)-C(3A)-P(1A)	108(3)
C(4A)-C(3A)-P(1A)	107(3)
C(5A)-C(3A)-P(1A)	109(3)
C(9A)-C(7A)-C(8A)	106(4)
C(9A)-C(7A)-C(10A)	108(4)
C(8A)-C(7A)-C(10A)	105(3)
C(9A)-C(7A)-P(1A)	109(3)
C(8A)-C(7A)-P(1A)	112(3)
C(10A)-C(7A)-P(1A)	116(3)
C(2A)-P(1A)-C(7A)	104.7(17)
C(2A)-P(1A)-C(3A)	102.9(18)
C(7A)-P(1A)-C(3A)	110.9(16)
C(2A)-P(1A)-Os(1A)	98.9(12)
C(7A)-P(1A)-Os(1A)	119.8(12)
C(3A)-P(1A)-Os(1A)	116.4(13)

Symmetry transformations used to generate equivalent atoms:

Table S10. Torsion angles [°] for **4**.

C(1A)-N(1)-C(11)-C(12)	165(2)
C(1)-N(1)-C(11)-C(12)	-173.7(3)
Os(1)-N(1)-C(11)-C(12)	2.6(5)
Os(1A)-N(1)-C(11)-C(12)	-5.6(5)
N(1)-C(11)-C(12)-P(2)	0.4(5)
C(13)-P(2)-C(12)-C(11)	-128.8(3)
C(17)-P(2)-C(12)-C(11)	118.6(3)
Os(1A)-P(2)-C(12)-C(11)	4.1(4)
Os(1)-P(2)-C(12)-C(11)	-2.5(3)
C(12)-P(2)-C(13)-C(16)	171.2(3)
C(17)-P(2)-C(13)-C(16)	-80.6(3)
Os(1A)-P(2)-C(13)-C(16)	54.5(4)
Os(1)-P(2)-C(13)-C(16)	61.0(4)
C(12)-P(2)-C(13)-C(14)	52.8(3)
C(17)-P(2)-C(13)-C(14)	161.0(3)
Os(1A)-P(2)-C(13)-C(14)	-63.9(4)
Os(1)-P(2)-C(13)-C(14)	-57.5(3)
C(12)-P(2)-C(13)-C(15)	-67.2(4)
C(17)-P(2)-C(13)-C(15)	41.1(4)
Os(1A)-P(2)-C(13)-C(15)	176.1(4)
Os(1)-P(2)-C(13)-C(15)	-177.4(3)
C(12)-P(2)-C(17)-C(19)	172.9(2)
C(13)-P(2)-C(17)-C(19)	64.1(3)
Os(1A)-P(2)-C(17)-C(19)	-78.7(3)
Os(1)-P(2)-C(17)-C(19)	-79.4(3)
C(12)-P(2)-C(17)-C(18)	-68.1(2)
C(13)-P(2)-C(17)-C(18)	-176.9(2)
Os(1A)-P(2)-C(17)-C(18)	40.3(3)
Os(1)-P(2)-C(17)-C(18)	39.6(3)
C(12)-P(2)-C(17)-C(20)	47.6(3)
C(13)-P(2)-C(17)-C(20)	-61.2(3)
Os(1A)-P(2)-C(17)-C(20)	155.9(4)
Os(1)-P(2)-C(17)-C(20)	155.2(3)
Os(1A)-P(3)-C(21)-C(22)	86.2(4)
Os(1)-P(3)-C(21)-C(22)	75.8(3)
Os(1A)-P(3)-C(21)-C(26)	-83.3(4)
Os(1)-P(3)-C(21)-C(26)	-93.7(3)
C(26)-C(21)-C(22)-C(23)	18.1(4)
P(3)-C(21)-C(22)-C(23)	-151.8(2)
C(26)-C(21)-C(22)-C(27)	-151.8(3)
P(3)-C(21)-C(22)-C(27)	38.3(4)
C(21)-C(22)-C(23)-C(24)	-4.8(5)
C(27)-C(22)-C(23)-C(24)	165.9(3)
C(22)-C(23)-C(24)-C(25)	-9.1(5)
C(22)-C(23)-C(24)-C(31)	172.5(3)
C(23)-C(24)-C(25)-C(26)	10.0(4)
C(31)-C(24)-C(25)-C(26)	-171.7(3)
C(24)-C(25)-C(26)-C(21)	3.2(4)
C(24)-C(25)-C(26)-C(35)	-173.5(3)
C(22)-C(21)-C(26)-C(25)	-17.3(4)
P(3)-C(21)-C(26)-C(25)	152.4(2)
C(22)-C(21)-C(26)-C(35)	159.1(3)
P(3)-C(21)-C(26)-C(35)	-31.2(4)
C(23)-C(22)-C(27)-C(28A)	106.9(10)
C(21)-C(22)-C(27)-C(28A)	-83.1(10)
C(23)-C(22)-C(27)-C(29)	-57.9(5)
C(21)-C(22)-C(27)-C(29)	112.2(5)
C(23)-C(22)-C(27)-C(30)	-177.3(3)
C(21)-C(22)-C(27)-C(30)	-7.2(5)
C(23)-C(22)-C(27)-C(28)	61.9(5)
C(21)-C(22)-C(27)-C(28)	-128.0(4)
C(23)-C(22)-C(27)-C(29A)	-127.3(9)
C(21)-C(22)-C(27)-C(29A)	42.8(9)
C(23)-C(22)-C(27)-C(30A)	-17.4(10)
C(21)-C(22)-C(27)-C(30A)	152.7(10)
C(23)-C(24)-C(31)-C(34)	177.1(3)
C(25)-C(24)-C(31)-C(34)	-1.2(5)
C(23)-C(24)-C(31)-C(32)	-63.7(4)
C(25)-C(24)-C(31)-C(32)	118.0(4)
C(23)-C(24)-C(31)-C(33)	54.6(4)
C(25)-C(24)-C(31)-C(33)	-123.7(4)
C(25)-C(26)-C(35)-C(36)	125.6(3)
C(21)-C(26)-C(35)-C(36)	-50.8(4)
C(25)-C(26)-C(35)-C(37)	-110.5(3)
C(21)-C(26)-C(35)-C(37)	73.1(4)
C(25)-C(26)-C(35)-C(38)	9.6(4)
C(21)-C(26)-C(35)-C(38)	-166.9(3)
C(43)-C(42)-C(41)-C(40)	173.0(16)
C(39)-C(40)-C(41)-C(42)	-178.8(14)
C(11)-N(1)-C(1)-C(2)	172.4(3)
Os(1)-N(1)-C(1)-C(2)	-4.0(5)
N(1)-C(1)-C(2)-P(1)	-1.3(5)
C(3)-P(1)-C(2)-C(1)	131.9(3)
C(7)-P(1)-C(2)-C(1)	-115.3(3)
Os(1)-P(1)-C(2)-C(1)	4.7(3)
C(11)-N(1)-C(1A)-C(2A)	-170(3)
Os(1A)-N(1)-C(1A)-C(2A)	1(6)
N(1)-C(1A)-C(2A)-P(1A)	-2(6)
C(1A)-C(2A)-P(1A)-C(7A)	-122(4)
C(1A)-C(2A)-P(1A)-C(3A)	122(4)
C(1A)-C(2A)-P(1A)-Os(1A)	2(4)
C(9A)-C(7A)-P(1A)-C(2A)	40(3)
C(8A)-C(7A)-P(1A)-C(2A)	157(3)
C(10A)-C(7A)-P(1A)-C(2A)	-83(3)
C(9A)-C(7A)-P(1A)-C(3A)	150(3)
C(8A)-C(7A)-P(1A)-C(3A)	-93(3)
C(10A)-C(7A)-P(1A)-C(3A)	28(3)
C(9A)-C(7A)-P(1A)-Os(1A)	-70(3)
C(8A)-C(7A)-P(1A)-Os(1A)	47(3)
C(10A)-C(7A)-P(1A)-Os(1A)	168(3)

Symmetry transformations used to generate equivalent atoms:

X-ray Single-Crystal Structure Analysis of 5

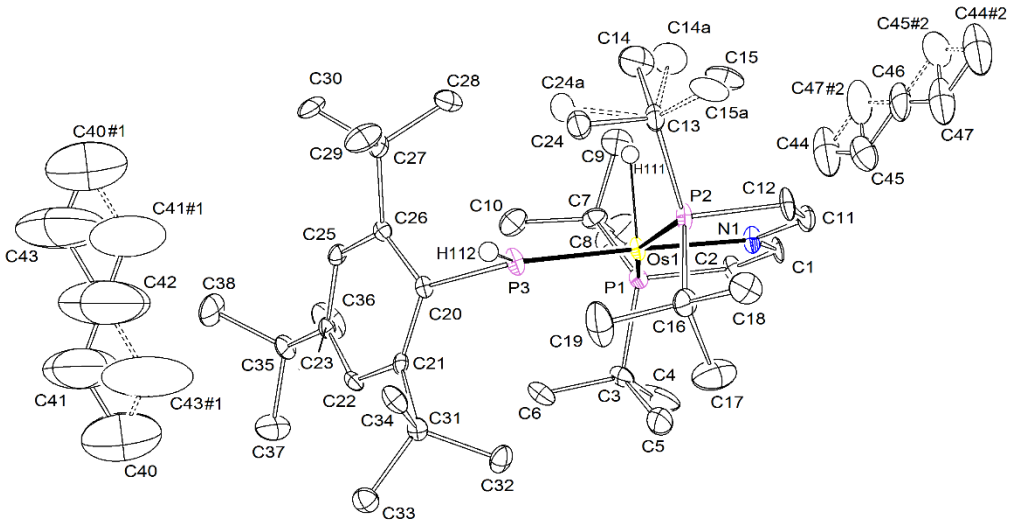

Figure S29. Thermal ellipsoid plot of **5** with the anisotropic displacement parameters drawn at the 50% probability level. The asymmetric unit contains one disordered complex molecule and two half pentane solvent molecules located at special positions. The disordered complex molecule was refined with population of 0.71(1) on the main domain using some restraints (SADI) and constraints (EADP). The Os-H and P-H hydrogen atoms were found from the residual density map and isotropically refined.

Table S11. Crystal data and structure refinement for **5**.

Identification code	mo_CW_JA_290517_0m (JA-MN-29)	
Empirical formula	$C_{43}H_{83}NOsP_3$	
Formula weight	897.21	
Temperature	100(2) K	
Wavelength	0.71073 Å	
Crystal system	Monoclinic	
Space group	$P2_1/n$	
Unit cell dimensions	a = 14.2026(6) Å	α = 90°
	b = 15.4095(7) Å	β = 97.2097(18)°
	c = 21.0809(10) Å	γ = 90°
Volume	4577.2(4) $Å^3$	
Z	4	
Density (calculated)	1.302 Mg/m^3	
Absorption coefficient	2.918 mm^{-1}	
F(000)	1876	
Crystal size	0.238 x 0.211 x 0.162 mm^3	
Crystal shape and color	Block,	dark green
Theta range for data collection	2.267 to 27.976°	
Index ranges	-18<=h<=18, -20<=k<=20, -27<=l<=27	
Reflections collected	124611	
Independent reflections	11010 [R(int) = 0.1202]	
Completeness to theta = 25.242°	99.9 %	
Refinement method	Full-matrix least-squares on F^2	

Data / restraints / parameters	11010 / 45 / 498	
Goodness-of-fit on F^2	1.053	
Final R indices [I>2sigma(I)]	R1 = 0.0416,	wR2 = 0.0531
R indices (all data)	R1 = 0.1021,	wR2 = 0.0636
Largest diff. peak and hole	0.695 and -0.830 $eÅ^{-3}$	

Table S12. Bond lengths [Å] and angles [°] for **5**.

N(1)-C(11)	1.373(6)
N(1)-C(1)	1.392(5)
N(1)-Os(1)	2.069(4)
Os(1)-P(3)	2.2301(13)
Os(1)-P(2)	2.3537(13)
Os(1)-P(1)	2.3723(12)
Os(1)-H(111)	1.69(6)
P(2)-C(12)	1.786(5)
P(2)-C(13)	1.890(5)
P(2)-C(16)	1.898(5)
P(1)-C(2)	1.788(4)
P(1)-C(7)	1.871(5)
P(1)-C(3)	1.885(5)
P(3)-C(20)	1.860(4)
P(3)-H(112)	1.33(5)
C(1)-C(2)	1.332(6)
C(3)-C(4)	1.516(6)
C(3)-C(6)	1.521(6)
C(3)-C(5)	1.541(7)
C(7)-C(9)	1.521(7)
C(7)-C(10)	1.529(7)
C(7)-C(8)	1.535(7)
C(11)-C(12)	1.338(6)
C(13)-C(14)	1.530(8)
C(13)-C(15A)	1.534(14)
C(13)-C(24)	1.540(7)
C(13)-C(24A)	1.544(12)
C(13)-C(15)	1.546(8)
C(13)-C(14A)	1.554(14)
C(16)-C(19)	1.522(7)
C(16)-C(18)	1.523(6)
C(16)-C(17)	1.533(7)
C(20)-C(21)	1.415(5)
C(20)-C(26)	1.433(6)
C(21)-C(22)	1.404(6)
C(21)-C(31)	1.564(6)
C(22)-C(23)	1.385(6)
C(23)-C(25)	1.387(6)
C(23)-C(35)	1.529(6)
C(25)-C(26)	1.389(6)
C(26)-C(27)	1.561(6)
C(27)-C(28)	1.538(6)
C(27)-C(29)	1.538(6)
C(27)-C(30)	1.540(6)
C(31)-C(32)	1.532(6)
C(31)-C(33)	1.541(6)
C(31)-C(34)	1.547(6)
C(35)-C(37)	1.527(6)
C(35)-C(38)	1.537(6)
C(35)-C(36)	1.539(7)
C(41)-C(42)	1.22(2)
C(41)-C(40)	1.40(2)
C(43)-C(40)#1	1.21(2)
C(43)-C(42)	1.47(2)
C(45)-C(44)	1.381(14)
C(45)-C(46)	1.499(12)
C(47)-C(46)	1.352(14)
C(47)-C(44)#2	1.470(16)
C(11)-N(1)-C(1)	116.7(4)
C(11)-N(1)-Os(1)	121.6(3)
C(1)-N(1)-Os(1)	121.6(3)
N(1)-Os(1)-P(3)	172.17(11)
N(1)-Os(1)-P(2)	80.18(10)
P(3)-Os(1)-P(2)	92.57(4)
N(1)-Os(1)-P(1)	80.09(10)
P(3)-Os(1)-P(1)	107.03(5)
P(2)-Os(1)-P(1)	160.20(4)
N(1)-Os(1)-H(111)	88(2)
P(3)-Os(1)-H(111)	95(2)
P(2)-Os(1)-H(111)	88(2)
P(1)-Os(1)-H(111)	93(2)
C(12)-P(2)-C(13)	103.0(2)
C(12)-P(2)-C(16)	102.2(2)
C(13)-P(2)-C(16)	110.7(2)
C(12)-P(2)-Os(1)	101.18(16)
C(13)-P(2)-Os(1)	120.19(15)
C(16)-P(2)-Os(1)	116.19(15)
C(2)-P(1)-C(7)	102.9(2)
C(2)-P(1)-C(3)	102.3(2)
C(7)-P(1)-C(3)	111.2(2)
C(2)-P(1)-Os(1)	101.04(14)
C(7)-P(1)-Os(1)	120.80(15)
C(3)-P(1)-Os(1)	115.22(15)
C(20)-P(3)-Os(1)	137.38(14)
C(20)-P(3)-H(112)	101(2)
Os(1)-P(3)-H(112)	122(2)
C(2)-C(1)-N(1)	121.5(4)
C(1)-C(2)-P(1)	115.7(3)
C(4)-C(3)-C(6)	111.0(4)
C(4)-C(3)-C(5)	107.5(5)
C(6)-C(3)-C(5)	109.0(4)
C(4)-C(3)-P(1)	114.0(3)
C(6)-C(3)-P(1)	110.9(3)
C(5)-C(3)-P(1)	104.0(3)
C(9)-C(7)-C(10)	107.8(4)
C(9)-C(7)-C(8)	108.2(4)
C(10)-C(7)-C(8)	108.8(4)
C(9)-C(7)-P(1)	106.1(4)
C(10)-C(7)-P(1)	110.9(3)
C(8)-C(7)-P(1)	114.7(3)
C(12)-C(11)-N(1)	121.6(4)
C(11)-C(12)-P(2)	115.3(4)
C(14)-C(13)-C(24)	109.7(6)
C(15A)-C(13)-C(24A)	115.1(15)
C(14)-C(13)-C(15)	107.4(5)
C(24)-C(13)-C(15)	107.0(5)
C(15A)-C(13)-C(14A)	107.1(14)
C(24A)-C(13)-C(14A)	100.6(13)
C(14)-C(13)-P(2)	107.7(5)
C(15A)-C(13)-P(2)	114.6(15)
C(24)-C(13)-P(2)	112.2(4)
C(24A)-C(13)-P(2)	114.0(7)
C(15)-C(13)-P(2)	112.8(5)
C(14A)-C(13)-P(2)	103.4(14)
C(19)-C(16)-C(18)	109.8(4)
C(19)-C(16)-C(17)	107.2(4)
C(18)-C(16)-C(17)	109.0(4)
C(19)-C(16)-P(2)	113.6(3)
C(18)-C(16)-P(2)	112.7(3)
C(17)-C(16)-P(2)	104.1(3)
C(21)-C(20)-C(26)	118.2(4)
C(21)-C(20)-P(3)	120.8(3)
C(26)-C(20)-P(3)	120.5(3)
C(22)-C(21)-C(20)	118.4(4)
C(22)-C(21)-C(31)	117.3(4)
C(20)-C(21)-C(31)	123.9(4)
C(23)-C(22)-C(21)	122.3(4)
C(22)-C(23)-C(25)	117.1(4)
C(22)-C(23)-C(35)	122.6(4)
C(25)-C(23)-C(35)	120.2(4)
C(23)-C(25)-C(26)	123.1(4)
C(25)-C(26)-C(20)	117.8(4)
C(25)-C(26)-C(27)	118.0(4)
C(20)-C(26)-C(27)	123.7(4)
C(28)-C(27)-C(29)	110.5(4)
C(28)-C(27)-C(30)	106.2(4)
C(29)-C(27)-C(30)	105.4(4)
C(28)-C(27)-C(26)	114.3(4)
C(29)-C(27)-C(26)	108.7(4)
C(30)-C(27)-C(26)	111.4(3)
C(32)-C(31)-C(33)	106.0(4)

C(32)-C(31)-C(34)	110.7(4)
C(33)-C(31)-C(34)	105.5(3)
C(32)-C(31)-C(21)	114.8(3)
C(33)-C(31)-C(21)	111.6(3)
C(34)-C(31)-C(21)	107.9(3)
C(37)-C(35)-C(23)	112.9(4)
C(37)-C(35)-C(38)	108.1(4)
C(23)-C(35)-C(38)	110.4(4)
C(37)-C(35)-C(36)	108.7(4)
C(23)-C(35)-C(36)	108.1(4)
C(38)-C(35)-C(36)	108.5(4)
C(42)-C(41)-C(40)	130(2)
C(40)#1-C(43)-C(42)	124(3)
C(44)-C(45)-C(46)	123.8(11)
C(46)-C(47)-C(44)#2	128.4(15)
C(41)-C(42)-C(43)	129.4(16)
C(47)-C(46)-C(45)	126.3(8)

Symmetry transformations used to generate equivalent atoms:
#1 -x+1,-y,-z+2 #2 -x,-y+1,-z

Table S13. Torsion angles [°] for **5**.

C(11)-N(1)-C(1)-C(2)	-179.2(4)
Os(1)-N(1)-C(1)-C(2)	-2.3(6)
N(1)-C(1)-C(2)-P(1)	0.2(6)
C(7)-P(1)-C(2)-C(1)	126.9(4)
C(3)-P(1)-C(2)-C(1)	-117.7(4)
Os(1)-P(1)-C(2)-C(1)	1.5(4)
C(2)-P(1)-C(3)-C(4)	-43.7(5)
C(7)-P(1)-C(3)-C(4)	65.5(5)
Os(1)-P(1)-C(3)-C(4)	-152.3(4)
C(2)-P(1)-C(3)-C(6)	-169.8(3)
C(7)-P(1)-C(3)-C(6)	-60.6(4)
Os(1)-P(1)-C(3)-C(6)	81.5(3)
C(2)-P(1)-C(3)-C(5)	73.1(3)
C(7)-P(1)-C(3)-C(5)	-177.7(3)
Os(1)-P(1)-C(3)-C(5)	-35.6(3)
C(2)-P(1)-C(7)-C(9)	-65.9(4)
C(3)-P(1)-C(7)-C(9)	-174.8(3)
Os(1)-P(1)-C(7)-C(9)	45.5(4)
C(2)-P(1)-C(7)-C(10)	177.2(3)
C(3)-P(1)-C(7)-C(10)	68.4(4)
Os(1)-P(1)-C(7)-C(10)	-71.4(4)
C(2)-P(1)-C(7)-C(8)	53.5(4)
C(3)-P(1)-C(7)-C(8)	-55.4(4)
Os(1)-P(1)-C(7)-C(8)	164.8(3)
C(1)-N(1)-C(11)-C(12)	178.4(4)
Os(1)-N(1)-C(11)-C(12)	1.5(6)
N(1)-C(11)-C(12)-P(2)	1.1(6)
C(13)-P(2)-C(12)-C(11)	-127.5(4)
C(16)-P(2)-C(12)-C(11)	117.6(4)
Os(1)-P(2)-C(12)-C(11)	-2.6(4)
C(12)-P(2)-C(13)-C(14)	85.0(5)
C(16)-P(2)-C(13)-C(14)	-166.4(5)
Os(1)-P(2)-C(13)-C(14)	-26.3(5)
C(12)-P(2)-C(13)-C(15A)	-52.5(11)
C(16)-P(2)-C(13)-C(15A)	56.1(11)
Os(1)-P(2)-C(13)-C(15A)	-163.9(10)
C(12)-P(2)-C(13)-C(24)	-154.2(4)
C(16)-P(2)-C(13)-C(24)	-45.6(5)
Os(1)-P(2)-C(13)-C(24)	94.4(4)
C(12)-P(2)-C(13)-C(24A)	171.9(10)
C(16)-P(2)-C(13)-C(24A)	-79.5(10)
Os(1)-P(2)-C(13)-C(24A)	60.6(10)
C(12)-P(2)-C(13)-C(15)	-33.3(5)
C(16)-P(2)-C(13)-C(15)	75.3(5)
Os(1)-P(2)-C(13)-C(15)	-144.7(4)
C(12)-P(2)-C(13)-C(14A)	63.7(10)
C(16)-P(2)-C(13)-C(14A)	172.3(10)
Os(1)-P(2)-C(13)-C(14A)	-47.7(10)
C(12)-P(2)-C(16)-C(19)	175.9(4)
C(13)-P(2)-C(16)-C(19)	66.8(4)
Os(1)-P(2)-C(16)-C(19)	-75.0(4)
C(12)-P(2)-C(16)-C(18)	50.2(4)
C(13)-P(2)-C(16)-C(18)	-58.9(4)
Os(1)-P(2)-C(16)-C(18)	159.3(3)
C(12)-P(2)-C(16)-C(17)	-67.8(4)
C(13)-P(2)-C(16)-C(17)	-176.9(3)
Os(1)-P(2)-C(16)-C(17)	41.4(4)
Os(1)-P(3)-C(20)-C(21)	88.5(4)
Os(1)-P(3)-C(20)-C(26)	-83.3(4)
C(26)-C(20)-C(21)-C(22)	17.8(6)
P(3)-C(20)-C(21)-C(22)	-154.2(3)
C(26)-C(20)-C(21)-C(31)	-155.3(4)
P(3)-C(20)-C(21)-C(31)	32.7(5)
C(20)-C(21)-C(22)-C(23)	-4.5(6)
C(31)-C(21)-C(22)-C(23)	169.0(4)
C(21)-C(22)-C(23)-C(25)	-9.1(6)
C(21)-C(22)-C(23)-C(35)	174.4(4)
C(22)-C(23)-C(25)-C(26)	9.6(6)
C(35)-C(23)-C(25)-C(26)	-173.9(4)
C(23)-C(25)-C(26)-C(20)	3.6(6)
C(23)-C(25)-C(26)-C(27)	-168.8(4)
C(21)-C(20)-C(26)-C(25)	-17.3(6)
P(3)-C(20)-C(26)-C(25)	154.7(3)
C(21)-C(20)-C(26)-C(27)	154.6(4)
P(3)-C(20)-C(26)-C(27)	-33.4(5)
C(25)-C(26)-C(27)-C(28)	-109.2(5)
C(20)-C(26)-C(27)-C(28)	78.8(5)
C(25)-C(26)-C(27)-C(29)	126.8(4)
C(20)-C(26)-C(27)-C(29)	-45.1(5)
C(25)-C(26)-C(27)-C(30)	11.1(5)
C(20)-C(26)-C(27)-C(30)	-160.8(4)
C(22)-C(21)-C(31)-C(32)	111.2(4)
C(20)-C(21)-C(31)-C(32)	-75.6(5)
C(22)-C(21)-C(31)-C(33)	-9.4(5)
C(20)-C(21)-C(31)-C(33)	163.8(4)
C(22)-C(21)-C(31)-C(34)	-124.8(4)
C(20)-C(21)-C(31)-C(34)	48.3(5)
C(22)-C(23)-C(35)-C(37)	2.6(6)
C(25)-C(23)-C(35)-C(37)	-173.8(4)
C(22)-C(23)-C(35)-C(38)	123.7(5)
C(25)-C(23)-C(35)-C(38)	-52.7(6)
C(22)-C(23)-C(35)-C(36)	-117.7(5)
C(25)-C(23)-C(35)-C(36)	65.9(5)
C(40)-C(41)-C(42)-C(43)	168.9(18)
C(40)#1-C(43)-C(42)-C(41)	168(2)
C(44)#2-C(47)-C(46)-C(45)	-175.7(10)
C(44)-C(45)-C(46)-C(47)	-175.7(10)

Symmetry transformations used to generate equivalent atoms:
#1 -x+1,-y,-z+2 #2 -x,-y+1,-z

X-ray Single-Crystal Structure Analysis of 8

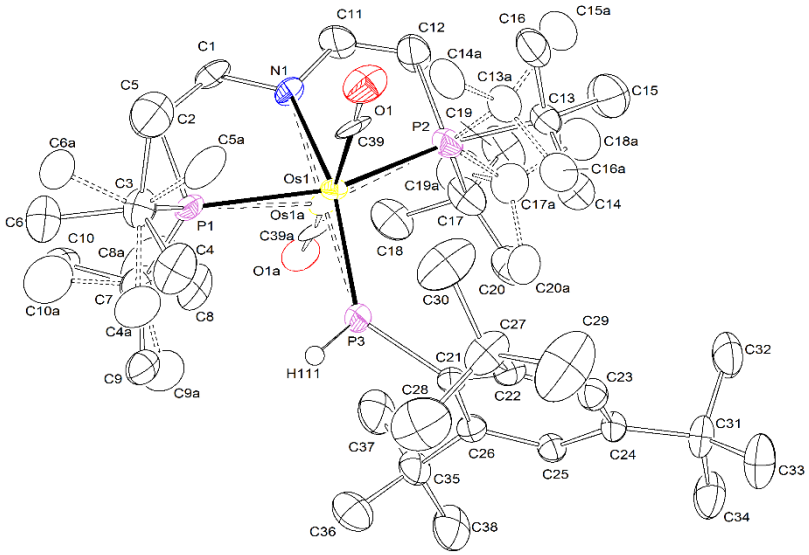

Figure S30. Thermal ellipsoid plot of **8** with the anisotropic displacement parameters drawn at the 50% probability level. The asymmetric unit contains one disordered complex molecule. The disordered complex molecule was refined with population of 0.682(7) on the main domain using some restraints and constraints (RIGU, SADI, EADP). The P-H hydrogen atom was found from the residual density map and isotropically refined. The structure was refined as an inversion twin using the twin law -100 0-10 00-1 (BASF: 0.061(16)). The reflections -2 2 4, 1 4 4, 0 1 9 and -2 1 10 are removed from the refinement using OMIT commands.

Table S14. Crystal data and structure refinement for **8**.

Identification code	CW_JA_041217_a (JA-vi-16)	
Empirical formula	$C_{39}H_{70}NOOsP_3$	
Formula weight	852.07	
Temperature	100(2) K	
Wavelength	0.71073 Å	
Crystal system	Orthorhombic	
Space group	$P2_12_12_1$	
Unit cell dimensions	a = 20.1894(14) Å	α = 90°
	b = 11.4930(8) Å	β = 90°
	c = 17.4542(14) Å	γ = 90°
Volume	4050.0(5) $Å^3$	
Z	4	
Density (calculated)	1.397 Mg/m^3	
Absorption coefficient	3.296 mm^{-1}	
F(000)	1760	
Crystal size	0.265 x 0.178 x 0.120 mm^3	
Crystal shape and color	Block,	clear intense red
Theta range for data collection	2.331 to 28.424°	
Index ranges	-26<=h<=26, -15<=k<=15, -23<=l<=23	
Reflections collected	79045	
Independent reflections	10098 [R(int) = 0.1626]	
Completeness to theta = 25.242°	99.9 %	
Refinement method	Full-matrix least-squares on F^2	

Data / restraints / parameters	10098 / 396 / 559	
Goodness-of-fit on F^2	1.155	
Final R indices [I>2sigma(I)]	R1 = 0.0588,	wR2 = 0.1161
R indices (all data)	R1 = 0.0762,	wR2 = 0.1245
Absolute structure parameter	0.061(16)	
Largest diff. peak and hole	1.550 and -2.048 $eÅ^{-3}$	

Table S15. Bond lengths [Å] and angles [°] for **8**.

C(1)-C(2)	1.34(2)
C(1)-N(1)	1.348(15)
C(2)-P(1)	1.750(12)
C(3)-C(6A)	1.44(4)
C(3)-C(4)	1.44(2)
C(3)-C(5A)	1.48(5)
C(3)-C(6)	1.53(2)
C(3)-C(5)	1.59(2)
C(3)-C(4A)	1.65(4)
C(3)-P(1)	1.874(12)
C(7)-C(10)	1.494(16)
C(7)-C(9)	1.527(17)
C(7)-C(9A)	1.53(2)
C(7)-C(8A)	1.54(2)
C(7)-C(8)	1.556(17)
C(7)-C(10A)	1.58(2)
C(7)-P(1)	1.885(15)
C(11)-N(1)	1.328(16)
C(11)-C(12)	1.35(2)
C(12)-P(2)	1.776(13)
C(21)-C(22)	1.417(15)
C(21)-C(26)	1.426(13)
C(21)-P(3)	1.853(11)
C(22)-C(23)	1.408(15)
C(22)-C(27)	1.553(15)
C(23)-C(24)	1.390(15)
C(24)-C(25)	1.374(15)
C(24)-C(31)	1.519(15)
C(25)-C(26)	1.405(14)
C(26)-C(35)	1.506(15)
C(27)-C(29)	1.49(2)
C(27)-C(30)	1.513(19)
C(27)-C(28)	1.53(2)
C(31)-C(33)	1.517(17)
C(31)-C(34)	1.53(2)
C(31)-C(32)	1.54(2)
C(35)-C(36)	1.503(17)
C(35)-C(38)	1.551(15)
C(35)-C(37)	1.56(2)
N(1)-Os(1A)	2.120(9)
N(1)-Os(1)	2.141(9)
P(1)-Os(1A)	2.342(4)
P(1)-Os(1)	2.443(3)
P(2)-C(17A)	1.85(2)
P(2)-C(13)	1.883(14)
P(2)-C(13A)	1.91(2)
P(2)-C(17)	1.923(14)
P(2)-Os(1)	2.372(3)
P(2)-Os(1A)	2.462(4)
P(3)-Os(1A)	2.245(4)
P(3)-Os(1)	2.264(3)
P(3)-H(111)	1.31(12)
C(13)-C(14)	1.511(18)
C(13)-C(15)	1.520(17)
C(13)-C(16)	1.526(17)
C(17)-C(20)	1.508(19)
C(17)-C(19)	1.515(18)
C(17)-C(18)	1.522(19)
C(39)-O(1)	1.24(2)
C(39)-Os(1)	1.761(16)
C(13A)-C(16A)	1.52(2)
C(13A)-C(15A)	1.53(2)
C(13A)-C(14A)	1.54(2)
C(17A)-C(20A)	1.49(2)
C(17A)-C(18A)	1.49(2)
C(17A)-C(19A)	1.49(2)
C(39A)-O(1A)	1.29(5)
C(39A)-Os(1A)	1.72(4)
C(2)-C(1)-N(1)	124.1(10)
C(1)-C(2)-P(1)	116.7(10)
C(6A)-C(3)-C(5A)	111(2)
C(4)-C(3)-C(6)	108.6(14)
C(4)-C(3)-C(5)	107.4(15)
C(6)-C(3)-C(5)	103.6(13)
C(6A)-C(3)-C(4A)	110(2)
C(5A)-C(3)-C(4A)	102(3)
C(6A)-C(3)-P(1)	119.6(18)
C(4)-C(3)-P(1)	115.4(9)
C(5A)-C(3)-P(1)	103(2)
C(6)-C(3)-P(1)	114.0(11)
C(5)-C(3)-P(1)	107.0(11)
C(4A)-C(3)-P(1)	109.0(16)
C(10)-C(7)-C(9)	111.8(13)
C(9A)-C(7)-C(8A)	108.0(19)
C(10)-C(7)-C(8)	108.4(12)
C(9)-C(7)-C(8)	106.4(11)
C(9A)-C(7)-C(10A)	105.6(18)
C(8A)-C(7)-C(10A)	104.3(18)
C(10)-C(7)-P(1)	114.2(10)
C(9)-C(7)-P(1)	111.5(12)
C(9A)-C(7)-P(1)	118(2)
C(8A)-C(7)-P(1)	113(3)
C(8)-C(7)-P(1)	104.0(11)
C(10A)-C(7)-P(1)	107(2)
N(1)-C(11)-C(12)	122.6(11)
C(11)-C(12)-P(2)	115.4(9)
C(22)-C(21)-C(26)	118.8(9)
C(22)-C(21)-P(3)	122.2(7)
C(26)-C(21)-P(3)	118.5(8)
C(23)-C(22)-C(21)	118.0(10)
C(23)-C(22)-C(27)	116.9(11)
C(21)-C(22)-C(27)	124.3(10)
C(24)-C(23)-C(22)	122.5(10)
C(25)-C(24)-C(23)	116.5(10)
C(25)-C(24)-C(31)	123.1(10)
C(23)-C(24)-C(31)	120.4(10)
C(24)-C(25)-C(26)	124.0(9)
C(25)-C(26)-C(21)	117.0(10)
C(25)-C(26)-C(35)	116.7(9)
C(21)-C(26)-C(35)	125.6(10)
C(29)-C(27)-C(30)	108.7(14)
C(29)-C(27)-C(28)	103.8(16)
C(30)-C(27)-C(28)	108.0(13)
C(29)-C(27)-C(22)	111.8(12)
C(30)-C(27)-C(22)	117.2(11)
C(28)-C(27)-C(22)	106.5(11)
C(33)-C(31)-C(24)	112.4(10)
C(33)-C(31)-C(34)	109.8(13)
C(24)-C(31)-C(34)	112.1(11)
C(33)-C(31)-C(32)	107.8(12)
C(24)-C(31)-C(32)	106.5(10)
C(34)-C(31)-C(32)	108.1(12)
C(36)-C(35)-C(26)	110.0(11)
C(36)-C(35)-C(38)	105.9(10)
C(26)-C(35)-C(38)	114.6(10)
C(36)-C(35)-C(37)	109.8(12)
C(26)-C(35)-C(37)	113.3(9)
C(38)-C(35)-C(37)	102.8(12)
C(11)-N(1)-C(1)	119.3(10)
C(11)-N(1)-Os(1A)	123.8(9)
C(1)-N(1)-Os(1A)	116.8(8)
C(11)-N(1)-Os(1)	120.1(9)
C(1)-N(1)-Os(1)	119.4(8)
C(2)-P(1)-C(3)	104.8(6)
C(2)-P(1)-C(7)	102.7(6)
C(3)-P(1)-C(7)	109.3(6)
C(2)-P(1)-Os(1A)	100.1(5)
C(3)-P(1)-Os(1A)	128.6(5)
C(7)-P(1)-Os(1A)	108.0(4)
C(2)-P(1)-Os(1)	100.2(5)
C(3)-P(1)-Os(1)	117.6(4)

C(7)-P(1)-Os(1)	119.4(4)
C(12)-P(2)-C(17A)	108.1(12)
C(12)-P(2)-C(13)	104.2(7)
C(12)-P(2)-C(13A)	97.4(11)
C(17A)-P(2)-C(13A)	113.2(16)
C(12)-P(2)-C(17)	102.4(7)
C(13)-P(2)-C(17)	107.7(7)
C(12)-P(2)-Os(1)	100.8(5)
C(13)-P(2)-Os(1)	124.5(4)
C(17)-P(2)-Os(1)	114.1(5)
C(12)-P(2)-Os(1A)	100.9(5)
C(17A)-P(2)-Os(1A)	124.9(11)
C(13A)-P(2)-Os(1A)	108.0(9)
C(21)-P(3)-Os(1A)	137.2(3)
C(21)-P(3)-Os(1)	134.2(3)
C(21)-P(3)-H(111)	97(6)
Os(1A)-P(3)-H(111)	124(5)
Os(1)-P(3)-H(111)	121(5)
C(14)-C(13)-C(15)	108.6(13)
C(14)-C(13)-C(16)	108.6(13)
C(15)-C(13)-C(16)	107.4(12)
C(14)-C(13)-P(2)	109.2(12)
C(15)-C(13)-P(2)	116.6(14)
C(16)-C(13)-P(2)	106.3(12)
C(20)-C(17)-C(19)	109.1(14)
C(20)-C(17)-C(18)	107.8(13)
C(19)-C(17)-C(18)	108.1(13)
C(20)-C(17)-P(2)	110.8(16)
C(19)-C(17)-P(2)	114.6(13)
C(18)-C(17)-P(2)	106.1(12)
O(1)-C(39)-Os(1)	176.5(15)
C(39)-Os(1)-N(1)	91.4(6)
C(39)-Os(1)-P(3)	105.7(5)
N(1)-Os(1)-P(3)	161.4(3)
C(39)-Os(1)-P(2)	91.6(6)
N(1)-Os(1)-P(2)	78.7(3)
P(3)-Os(1)-P(2)	107.49(11)
C(39)-Os(1)-P(1)	98.7(6)
N(1)-Os(1)-P(1)	78.7(3)
P(3)-Os(1)-P(1)	91.24(10)
P(2)-Os(1)-P(1)	155.39(13)
C(16A)-C(13A)-C(15A)	107.4(18)
C(16A)-C(13A)-C(14A)	107.1(18)
C(15A)-C(13A)-C(14A)	106.2(17)
C(16A)-C(13A)-P(2)	107(3)
C(15A)-C(13A)-P(2)	116(3)
C(14A)-C(13A)-P(2)	112(2)
C(20A)-C(17A)-C(18A)	112.8(19)
C(20A)-C(17A)-C(19A)	112(2)
C(18A)-C(17A)-C(19A)	111.4(19)
C(20A)-C(17A)-P(2)	110(3)
C(18A)-C(17A)-P(2)	111(3)
C(19A)-C(17A)-P(2)	98(4)
O(1A)-C(39A)-Os(1A)	173(3)
C(39A)-Os(1A)-N(1)	86.2(11)
C(39A)-Os(1A)-P(3)	103.9(10)
N(1)-Os(1A)-P(3)	169.7(4)
C(39A)-Os(1A)-P(1)	100.7(13)
N(1)-Os(1A)-P(1)	81.5(3)
P(3)-Os(1A)-P(1)	94.40(14)
C(39A)-Os(1A)-P(2)	87.2(14)
N(1)-Os(1A)-P(2)	77.1(3)
P(3)-Os(1A)-P(2)	105.09(17)
P(1)-Os(1A)-P(2)	156.60(18)

Symmetry transformations used to generate equivalent atoms:

Table S16. Torsion angles [°] for **8**.

N(1)-C(1)-C(2)-P(1)	1(2)
N(1)-C(11)-C(12)-P(2)	4(2)
C(26)-C(21)-C(22)-C(23)	17.6(14)
P(3)-C(21)-C(22)-C(23)	-154.3(8)
C(26)-C(21)-C(22)-C(27)	-152.3(10)
P(3)-C(21)-C(22)-C(27)	35.9(14)
C(21)-C(22)-C(23)-C(24)	-4.1(16)
C(27)-C(22)-C(23)-C(24)	166.6(10)
C(22)-C(23)-C(24)-C(25)	-10.1(16)
C(22)-C(23)-C(24)-C(31)	170.5(10)
C(23)-C(24)-C(25)-C(26)	11.1(16)
C(31)-C(24)-C(25)-C(26)	-169.4(11)
C(24)-C(25)-C(26)-C(21)	2.0(16)
C(24)-C(25)-C(26)-C(35)	-168.7(10)
C(22)-C(21)-C(26)-C(25)	-16.6(14)
P(3)-C(21)-C(26)-C(25)	155.6(8)
C(22)-C(21)-C(26)-C(35)	153.2(10)
P(3)-C(21)-C(26)-C(35)	-34.6(14)
C(23)-C(22)-C(27)-C(29)	-2.2(18)
C(21)-C(22)-C(27)-C(29)	167.8(14)
C(23)-C(22)-C(27)-C(30)	124.1(14)
C(21)-C(22)-C(27)-C(30)	-65.9(17)
C(23)-C(22)-C(27)-C(28)	-115.0(13)
C(21)-C(22)-C(27)-C(28)	55.0(15)
C(25)-C(24)-C(31)-C(33)	-143.9(13)
C(23)-C(24)-C(31)-C(33)	35.5(17)
C(25)-C(24)-C(31)-C(34)	-19.7(17)
C(23)-C(24)-C(31)-C(34)	159.7(12)
C(25)-C(24)-C(31)-C(32)	98.2(14)
C(23)-C(24)-C(31)-C(32)	-82.4(14)
C(25)-C(26)-C(35)-C(36)	123.5(11)
C(21)-C(26)-C(35)-C(36)	-46.4(15)
C(25)-C(26)-C(35)-C(38)	4.3(16)
C(21)-C(26)-C(35)-C(38)	-165.5(12)
C(25)-C(26)-C(35)-C(37)	-113.2(12)
C(21)-C(26)-C(35)-C(37)	76.9(14)
C(12)-C(11)-N(1)-C(1)	176.7(15)
C(12)-C(11)-N(1)-Os(1A)	-7(2)
C(12)-C(11)-N(1)-Os(1)	9(2)
C(2)-C(1)-N(1)-C(11)	-176.3(15)
C(2)-C(1)-N(1)-Os(1A)	7.0(19)
C(2)-C(1)-N(1)-Os(1)	-8.5(19)
C(1)-C(2)-P(1)-C(3)	128.1(12)
C(1)-C(2)-P(1)-C(7)	-117.7(12)
C(1)-C(2)-P(1)-Os(1A)	-6.5(13)
C(1)-C(2)-P(1)-Os(1)	5.8(13)
C(6A)-C(3)-P(1)-C(2)	32(2)
C(4)-C(3)-P(1)-C(2)	-164.4(14)
C(5A)-C(3)-P(1)-C(2)	-92.0(19)
C(6)-C(3)-P(1)-C(2)	68.9(13)
C(5)-C(3)-P(1)-C(2)	-45.0(13)
C(4A)-C(3)-P(1)-C(2)	159.7(17)
C(6A)-C(3)-P(1)-C(7)	-77(2)
C(4)-C(3)-P(1)-C(7)	86.2(14)
C(5A)-C(3)-P(1)-C(7)	158.5(18)
C(6)-C(3)-P(1)-C(7)	-40.5(13)
C(5)-C(3)-P(1)-C(7)	-154.4(11)
C(4A)-C(3)-P(1)-C(7)	50.3(18)
C(6A)-C(3)-P(1)-Os(1A)	149(2)
C(5A)-C(3)-P(1)-Os(1A)	24.2(19)
C(4A)-C(3)-P(1)-Os(1A)	-84.0(17)
C(4)-C(3)-P(1)-Os(1)	-54.2(14)
C(6)-C(3)-P(1)-Os(1)	179.1(11)
C(5)-C(3)-P(1)-Os(1)	65.2(12)
C(10)-C(7)-P(1)-C(2)	-37.4(12)
C(9)-C(7)-P(1)-C(2)	-165.3(10)
C(9A)-C(7)-P(1)-C(2)	173(2)
C(8A)-C(7)-P(1)-C(2)	46(2)
C(8)-C(7)-P(1)-C(2)	80.5(10)
C(10A)-C(7)-P(1)-C(2)	-68(2)
C(10)-C(7)-P(1)-C(3)	73.5(11)
C(9)-C(7)-P(1)-C(3)	-54.4(11)
C(9A)-C(7)-P(1)-C(3)	-76(2)

C(8A)-C(7)-P(1)-C(3)	157(2)
C(8)-C(7)-P(1)-C(3)	-168.7(9)
C(10A)-C(7)-P(1)-C(3)	43(2)
C(9A)-C(7)-P(1)-Os(1A)	68(2)
C(8A)-C(7)-P(1)-Os(1A)	-59(2)
C(10A)-C(7)-P(1)-Os(1A)	-173.1(19)
C(10)-C(7)-P(1)-Os(1)	-147.0(9)
C(9)-C(7)-P(1)-Os(1)	85.1(10)
C(8)-C(7)-P(1)-Os(1)	-29.1(10)
C(11)-C(12)-P(2)-C(17A)	131.9(18)
C(11)-C(12)-P(2)-C(13)	-142.9(13)
C(11)-C(12)-P(2)-C(13A)	-110.7(16)
C(11)-C(12)-P(2)-C(17)	105.0(14)
C(11)-C(12)-P(2)-Os(1)	-12.9(14)
C(11)-C(12)-P(2)-Os(1A)	-0.6(14)
C(22)-C(21)-P(3)-Os(1A)	90.6(9)
C(26)-C(21)-P(3)-Os(1A)	-81.2(9)
C(22)-C(21)-P(3)-Os(1)	72.3(10)
C(26)-C(21)-P(3)-Os(1)	-99.5(8)
C(12)-P(2)-C(13)-C(14)	167.5(11)
C(17)-P(2)-C(13)-C(14)	-84.2(11)
Os(1)-P(2)-C(13)-C(14)	53.5(12)
C(12)-P(2)-C(13)-C(15)	-69.0(13)
C(17)-P(2)-C(13)-C(15)	39.2(13)
Os(1)-P(2)-C(13)-C(15)	176.9(10)
C(12)-P(2)-C(13)-C(16)	50.5(12)
C(17)-P(2)-C(13)-C(16)	158.8(11)
Os(1)-P(2)-C(13)-C(16)	-63.5(11)
C(12)-P(2)-C(17A)-C(20A)	-166(2)
C(13A)-P(2)-C(17A)-C(20A)	87(2)
Os(1A)-P(2)-C(17A)-C(20A)	-48(3)
C(12)-P(2)-C(17A)-C(18A)	68(2)
C(13A)-P(2)-C(17A)-C(18A)	-38(3)
Os(1A)-P(2)-C(17A)-C(18A)	-173.7(19)
C(12)-P(2)-C(17A)-C(19A)	-49(2)
C(13A)-P(2)-C(17A)-C(19A)	-155(2)
Os(1A)-P(2)-C(17A)-C(19A)	69(2)

Symmetry transformations used to generate equivalent atoms:

X-ray Single-Crystal Structure Analysis of 9

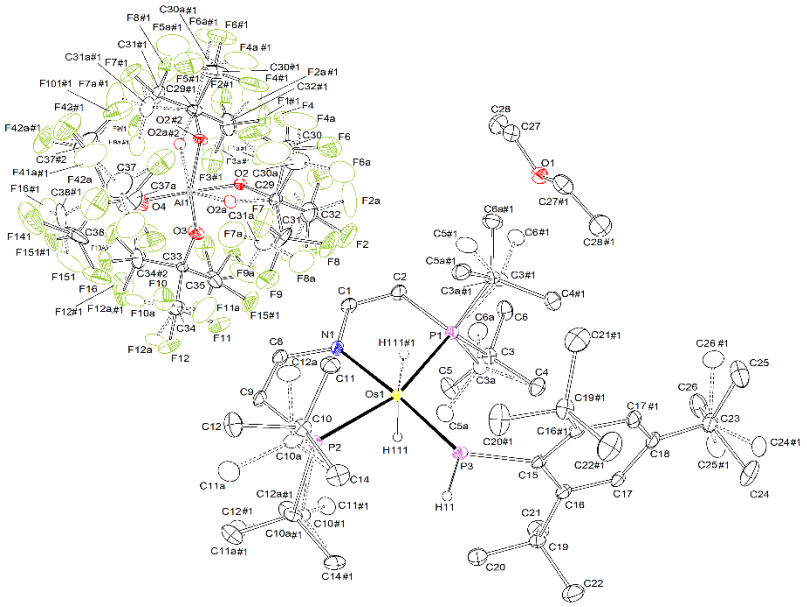

Figure S31. Thermal ellipsoid plot of **9** with the anisotropic displacement parameters drawn at the 50% probability level. The asymmetric unit contains a half disordered complex molecule, a half disordered $[Al\{OC(CF_3)_3\}_4]^-$ anion and a half diethyl ether solvent molecule. The disorder was refined with site occupation factors of 0.5 for both sites using PART commands and some restraints and constraints (SADI, RIGU, EADP). The Os-H hydrogen atom was found from the residual density map and isotropically refined using DFIX.

Table S17. Crystal data and structure refinement for **9**.

Identification code	mo_CW_JA_180917_2_0m_a (JA-v-75	
Empirical formula	$C_{58}H_{81}AlF_{36}NO_5OsP_3$	
Formula weight	1866.32	
Temperature	100(2) K	
Wavelength	0.71073 Å	
Crystal system	Monoclinic	
Space group	$P2_1/m$	
Unit cell dimensions	a = 14.9152(8) Å	α = 90°
	b = 15.4377(8) Å	β = 107.823(2)°
	c = 16.7109(9) Å	γ = 90°
Volume	3663.1(3) $Å^3$	
Z	2	
Density (calculated)	1.692 Mg/m^3	
Absorption coefficient	1.955 mm^{-1}	
F(000)	1868	
Crystal size	0.513 x 0.242 x 0.128 mm^3	
Theta range for data collection	2.195 to 28.443°.	
Index ranges	-19<=h<=19, -20<=k<=20, -22<=l<=22	
Reflections collected	99819	
Independent reflections	9531 [R(int) = 0.0648]	
Completeness to theta = 25.242°	99.9 %	
Refinement method	Full-matrix least-squares on F^2	

Data / restraints / parameters	9531 / 301 / 741
Goodness-of-fit on F^2	1.086
Final R indices [I>2sigma(I)]	R1 = 0.0508, wR2 = 0.1312
R indices (all data)	R1 = 0.0573, wR2 = 0.1378
Extinction coefficient	n/a
Largest diff. peak and hole	1.562 and -1.653 $eÅ^{-3}$

Table S18. Bond lengths [Å] and angles [°] for **9.**

N(1)-C(1)	1.391(8)
N(1)-C(8)	1.407(8)
N(1)-Os(1)	2.004(5)
C(1)-C(2)	1.317(10)
C(2)-P(1)	1.802(6)
C(4)-C(3)	1.46(3)
C(4)-C(3A)	1.56(3)
C(8)-C(9)	1.327(9)
C(9)-P(2)	1.798(6)
C(14)-C(10)	1.52(2)
C(14)-C(10A)	1.52(2)
C(15)-C(16)	1.425(5)
C(15)-C(16)#1	1.425(5)
C(15)-P(3)	1.837(6)
C(17)-C(18)	1.386(6)
C(17)-C(16)	1.394(7)
C(18)-C(17)#1	1.386(6)
C(18)-C(23)	1.540(10)
C(19)-C(20)	1.528(8)
C(19)-C(21)	1.533(9)
C(19)-C(22)	1.542(8)
C(19)-C(16)	1.551(6)
C(23)-C(24)	1.512(13)
C(23)-C(26)	1.521(13)
C(23)-C(25)	1.529(14)
C(27)-O(1)	1.419(7)
C(27)-C(28)	1.488(11)
C(29)-O(2)	1.294(9)
C(29)-O(2A)	1.365(9)
C(29)-C(31)	1.502(14)
C(29)-C(30A)	1.508(17)
C(29)-C(32)	1.543(10)
C(29)-C(31A)	1.562(15)
C(29)-C(30)	1.578(17)
C(32)-F(1)	1.216(13)
C(32)-F(2A)	1.247(14)
C(32)-F(3A)	1.31(5)
C(32)-F(3)	1.34(5)
C(32)-F(2)	1.386(14)
C(32)-F(1A)	1.477(13)
C(33)-O(3)	1.306(7)
C(33)-C(35)	1.533(9)
C(33)-C(34)	1.555(8)
C(33)-C(34)#2	1.555(8)
C(34)-F(11A)	1.271(10)
C(34)-F(10)	1.271(9)
C(34)-F(12)	1.275(11)
C(34)-F(12A)	1.340(10)
C(34)-F(11)	1.402(10)
C(34)-F(10A)	1.433(9)
C(35)-F(14)	1.199(10)
C(35)-F(13)	1.299(9)
C(35)-F(15)	1.502(11)
C(36)-O(4)	1.316(9)
C(36)-C(37A)	1.454(18)
C(36)-C(37A)#2	1.454(18)
C(36)-C(37)	1.504(17)
C(36)-C(37)#2	1.504(17)
C(36)-C(38)	1.554(13)
P(1)-C(3)	1.85(3)
P(1)-C(3)#1	1.85(3)
P(1)-C(3A)#1	1.90(3)
P(1)-C(3A)	1.90(3)
P(1)-Os(1)	2.4011(15)
P(2)-C(10A)	1.85(2)
P(2)-C(10A)#1	1.85(2)
P(2)-C(10)#1	1.91(2)
P(2)-C(10)	1.91(2)
P(2)-Os(1)	2.3927(15)
P(3)-Os(1)	2.1943(15)
P(3)-H(11)	1.27(7)
Os(1)-H(111)	1.59(2)
Al(1)-O(2A)#2	1.690(7)
Al(1)-O(2A)	1.690(7)
Al(1)-O(4)	1.709(6)
Al(1)-O(3)	1.727(5)
Al(1)-O(2)	1.740(7)
Al(1)-O(2)#2	1.740(7)
O(1)-C(27)#1	1.419(7)
C(3)-C(5)	1.553(19)
C(3)-C(6)	1.56(2)
C(10)-C(11)	1.515(18)
C(10)-C(12)	1.54(2)
C(3A)-C(6A)	1.52(2)
C(3A)-C(5A)	1.524(18)
C(10A)-C(12A)	1.531(19)
C(10A)-C(11A)	1.55(2)
F(141)-C(38)	1.445(17)
F(101)-C(37)	1.328(14)
F(101)-C(37A)	1.402(13)
F(151)-C(38)	0.893(14)
F(151)-F(151)#2	1.07(3)
F(151)-F(16)	1.140(17)
F(14)-F(15)	1.005(12)
F(16)-C(38)	1.32(2)
F(11)-F(12)	1.762(17)
C(37)-F(42)	1.331(12)
C(37)-F(41)	1.352(13)
F(42)-F(42)#2	1.45(2)
F(42A)-C(37A)	1.355(12)
C(37A)-F(41A)	1.333(13)
F(7)-C(31)	1.306(11)
F(8)-C(31)	1.327(11)
F(9)-C(31)	1.309(12)
F(7A)-C(31A)	1.318(12)
F(8A)-C(31A)	1.302(12)
F(9A)-C(31A)	1.305(13)
C(30)-F(5)	1.284(13)
C(30)-F(6)	1.299(12)
C(30)-F(4)	1.330(13)
C(30A)-F(4A)	1.293(13)
C(30A)-F(5A)	1.320(13)
C(30A)-F(6A)	1.350(13)
C(1)-N(1)-C(8)	115.1(5)
C(1)-N(1)-Os(1)	123.3(4)
C(8)-N(1)-Os(1)	121.6(4)
C(2)-C(1)-N(1)	122.1(6)
C(1)-C(2)-P(1)	114.7(5)
C(9)-C(8)-N(1)	123.0(6)
C(8)-C(9)-P(2)	114.3(5)
C(16)-C(15)-C(16)#1	118.4(6)
C(16)-C(15)-P(3)	120.4(3)
C(16)#1-C(15)-P(3)	120.4(3)
C(18)-C(17)-C(16)	123.3(5)
C(17)-C(18)-C(17)#1	116.4(6)
C(17)-C(18)-C(23)	121.7(3)
C(17)#1-C(18)-C(23)	121.7(3)
C(20)-C(19)-C(21)	105.5(5)
C(20)-C(19)-C(22)	106.0(5)
C(21)-C(19)-C(22)	108.8(5)
C(20)-C(19)-C(16)	116.9(4)
C(21)-C(19)-C(16)	112.5(4)
C(22)-C(19)-C(16)	106.8(4)
C(24)-C(23)-C(26)	109.6(8)
C(24)-C(23)-C(25)	108.2(10)
C(26)-C(23)-C(25)	109.7(11)
C(24)-C(23)-C(18)	108.5(7)
C(26)-C(23)-C(18)	108.6(6)
C(25)-C(23)-C(18)	112.3(6)
O(1)-C(27)-C(28)	108.5(6)
O(2)-C(29)-C(32)	102.2(6)

O(2A)-C(29)-C(32)	113.5(6)	Os(1)-P(3)-H(11)	124(3)
C(31)-C(29)-C(32)	104.3(6)	N(1)-Os(1)-P(3)	175.14(15)
C(30A)-C(29)-C(32)	110.9(8)	N(1)-Os(1)-P(2)	81.03(15)
C(32)-C(29)-C(31A)	114.2(7)	P(3)-Os(1)-P(2)	94.11(6)
C(32)-C(29)-C(30)	111.1(7)	N(1)-Os(1)-P(1)	80.00(15)
F(2A)-C(32)-F(3A)	111.5(17)	P(3)-Os(1)-P(1)	104.86(6)
F(1)-C(32)-F(3)	125(2)	P(2)-Os(1)-P(1)	161.03(5)
F(1)-C(32)-F(2)	110.9(12)	N(1)-Os(1)-H(111)	93(4)
F(3)-C(32)-F(2)	93.9(14)	P(3)-Os(1)-H(111)	87(4)
F(2A)-C(32)-F(1A)	101.9(11)	P(2)-Os(1)-H(111)	91(4)
F(3A)-C(32)-F(1A)	97(2)	P(1)-Os(1)-H(111)	90(4)
F(1)-C(32)-C(29)	109.6(9)	O(2A)#2-Al(1)-O(2A)	128.3(6)
F(2A)-C(32)-C(29)	118.3(11)	O(2A)#2-Al(1)-O(4)	102.3(3)
F(3A)-C(32)-C(29)	115.8(18)	O(2A)-Al(1)-O(4)	102.3(3)
F(3)-C(32)-C(29)	106.4(15)	O(2A)#2-Al(1)-O(3)	107.1(3)
F(2)-C(32)-C(29)	109.8(9)	O(2A)-Al(1)-O(3)	107.1(3)
F(1A)-C(32)-C(29)	109.3(8)	O(4)-Al(1)-O(3)	108.4(3)
O(3)-C(33)-C(35)	110.9(6)	O(4)-Al(1)-O(2)	118.7(3)
O(3)-C(33)-C(34)	111.2(4)	O(3)-Al(1)-O(2)	111.6(3)
C(35)-C(33)-C(34)	108.3(4)	O(4)-Al(1)-O(2)#2	118.7(3)
O(3)-C(33)-C(34)#2	111.2(4)	O(3)-Al(1)-O(2)#2	111.6(3)
C(35)-C(33)-C(34)#2	108.3(4)	O(2)-Al(1)-O(2)#2	86.5(6)
C(34)-C(33)-C(34)#2	106.8(6)	C(27)-O(1)-C(27)#1	112.8(7)
F(10)-C(34)-F(12)	119.6(11)	C(33)-O(3)-Al(1)	151.5(5)
F(11A)-C(34)-F(12A)	130.7(9)	C(36)-O(4)-Al(1)	154.0(6)
F(10)-C(34)-F(11)	104.6(9)	C(4)-C(3)-C(5)	109.9(16)
F(12)-C(34)-F(11)	82.2(8)	C(4)-C(3)-C(6)	106.6(14)
F(11A)-C(34)-F(10A)	101.7(8)	C(5)-C(3)-C(6)	105.4(15)
F(12A)-C(34)-F(10A)	86.2(7)	C(4)-C(3)-P(1)	115.8(14)
F(11A)-C(34)-C(33)	113.8(7)	C(5)-C(3)-P(1)	106.2(13)
F(10)-C(34)-C(33)	114.8(6)	C(6)-C(3)-P(1)	112.5(15)
F(12)-C(34)-C(33)	121.5(9)	C(11)-C(10)-C(14)	108.2(14)
F(12A)-C(34)-C(33)	110.5(7)	C(11)-C(10)-C(12)	107.8(14)
F(11)-C(34)-C(33)	103.9(6)	C(14)-C(10)-C(12)	111.7(14)
F(10A)-C(34)-C(33)	105.2(6)	C(11)-C(10)-P(2)	105.4(12)
F(14)-C(35)-F(13)	117.7(7)	C(14)-C(10)-P(2)	110.1(11)
F(14)-C(35)-F(15)	41.8(5)	C(12)-C(10)-P(2)	113.3(13)
F(13)-C(35)-F(15)	96.2(6)	C(6A)-C(3A)-C(5A)	109.3(14)
F(14)-C(35)-C(33)	117.4(7)	C(6A)-C(3A)-C(4)	113.4(15)
F(13)-C(35)-C(33)	115.1(7)	C(5A)-C(3A)-C(4)	107.5(16)
F(15)-C(35)-C(33)	102.7(5)	C(6A)-C(3A)-P(1)	113.8(16)
O(4)-C(36)-C(37A)	103.7(6)	C(5A)-C(3A)-P(1)	104.1(13)
O(4)-C(36)-C(37A)#2	103.7(6)	C(4)-C(3A)-P(1)	108.2(12)
C(37A)-C(36)-C(37A)#2	127.9(11)	C(14)-C(10A)-C(12A)	110.2(14)
O(4)-C(36)-C(37)	119.5(6)	C(14)-C(10A)-C(11A)	105.3(13)
O(4)-C(36)-C(37)#2	119.5(6)	C(12A)-C(10A)-C(11A)	108.2(14)
C(37)-C(36)-C(37)#2	89.3(10)	C(14)-C(10A)-P(2)	113.6(12)
O(4)-C(36)-C(38)	109.5(7)	C(12A)-C(10A)-P(2)	106.8(12)
C(2)-P(1)-C(3)	103.4(8)	C(11A)-C(10A)-P(2)	112.5(13)
C(2)-P(1)-C(3)#1	103.4(8)	C(38)-F(151)-F(151)#2	85.8(17)
C(3)-P(1)-C(3)#1	101.9(9)	C(38)-F(151)-F(16)	80.2(17)
C(2)-P(1)-C(3A)#1	101.4(8)	F(151)#2-F(151)-F(16)	159.9(8)
C(2)-P(1)-C(3A)	101.4(8)	F(15)-F(14)-C(35)	85.5(9)
C(3A)#1-P(1)-C(3A)	122.6(10)	F(14)-F(15)-C(35)	52.7(8)
C(2)-P(1)-Os(1)	99.9(2)	C(17)-C(16)-C(15)	118.0(4)
C(3)-P(1)-Os(1)	122.5(6)	C(17)-C(16)-C(19)	114.7(4)
C(3)#1-P(1)-Os(1)	122.5(6)	C(15)-C(16)-C(19)	126.9(4)
C(3A)#1-P(1)-Os(1)	113.4(5)	F(151)-F(16)-C(38)	41.7(10)
C(3A)-P(1)-Os(1)	113.4(5)	F(151)-C(38)-F(16)	58.1(13)
C(9)-P(2)-C(10A)	101.8(7)	F(151)-C(38)-F(141)	106.6(16)
C(9)-P(2)-C(10A)#1	101.8(7)	F(16)-C(38)-F(141)	126.6(11)
C(10A)-P(2)-C(10A)#1	102.8(10)	F(151)-C(38)-C(36)	138.7(14)
C(9)-P(2)-C(10)#1	101.9(7)	F(16)-C(38)-C(36)	118.1(14)
C(9)-P(2)-C(10)	101.9(7)	F(141)-C(38)-C(36)	105.3(10)
C(10)#1-P(2)-C(10)	123.6(10)	C(29)-O(2)-Al(1)	152.4(6)
C(9)-P(2)-Os(1)	100.1(2)	C(34)-F(11)-F(12)	45.8(5)
C(10A)-P(2)-Os(1)	123.0(5)	C(34)-F(12)-F(11)	52.0(6)
C(10A)#1-P(2)-Os(1)	123.0(5)	C(29)-O(2A)-Al(1)	149.6(6)
C(10)#1-P(2)-Os(1)	112.5(5)	F(101)-C(37)-F(42)	99.9(11)
C(10)-P(2)-Os(1)	112.5(5)	F(101)-C(37)-F(41)	98.0(11)
C(15)-P(3)-Os(1)	137.4(2)	F(42)-C(37)-F(41)	110.2(12)
C(15)-P(3)-H(11)	99(3)	F(101)-C(37)-C(36)	110.9(10)

F(42)-C(37)-C(36)	116.4(11)
F(41)-C(37)-C(36)	118.3(11)
C(37)-F(42)-F(42)#2	104.5(8)
F(41A)-C(37A)-F(42A)	106.6(11)
F(41A)-C(37A)-F(101)	111.2(11)
F(42A)-C(37A)-F(101)	110.2(11)
F(41A)-C(37A)-C(36)	109.1(11)
F(42A)-C(37A)-C(36)	110.1(12)
F(101)-C(37A)-C(36)	109.7(10)
F(7)-C(31)-F(9)	111.8(11)
F(7)-C(31)-F(8)	105.1(10)
F(9)-C(31)-F(8)	104.3(10)
F(7)-C(31)-C(29)	106.9(9)
F(9)-C(31)-C(29)	116.2(9)
F(8)-C(31)-C(29)	112.1(10)
F(8A)-C(31A)-F(9A)	106.4(12)
F(8A)-C(31A)-F(7A)	106.6(11)
F(9A)-C(31A)-F(7A)	101.4(11)
F(8A)-C(31A)-C(29)	116.3(11)
F(9A)-C(31A)-C(29)	106.0(10)
F(7A)-C(31A)-C(29)	118.5(11)
F(5)-C(30)-F(6)	112.4(12)
F(5)-C(30)-F(4)	105.7(12)
F(6)-C(30)-F(4)	106.4(12)
F(5)-C(30)-C(29)	111.6(12)
F(6)-C(30)-C(29)	111.3(11)
F(4)-C(30)-C(29)	109.1(11)
F(4A)-C(30A)-F(5A)	105.7(12)
F(4A)-C(30A)-F(6A)	104.8(12)
F(5A)-C(30A)-F(6A)	105.0(12)
F(4A)-C(30A)-C(29)	114.6(12)
F(5A)-C(30A)-C(29)	114.1(12)
F(6A)-C(30A)-C(29)	111.8(11)

Symmetry transformations used to generate equivalent atoms:
#1 x,-y+3/2,z #2 x,-y+1/2,z

Table S19. Torsion angles [°] for **9**.

C(8)-N(1)-C(1)-C(2)	180.000(1)
Os(1)-N(1)-C(1)-C(2)	0.000(1)
N(1)-C(1)-C(2)-P(1)	0.000(1)
C(1)-N(1)-C(8)-C(9)	180.000(1)
Os(1)-N(1)-C(8)-C(9)	0.000(2)
N(1)-C(8)-C(9)-P(2)	0.000(2)
C(16)-C(17)-C(18)-C(17)#1	10.0(9)
C(16)-C(17)-C(18)-C(23)	-173.2(6)
C(17)-C(18)-C(23)-C(24)	-66.3(9)
C(17)#1-C(18)-C(23)-C(24)	110.3(8)
C(17)-C(18)-C(23)-C(26)	52.8(10)
C(17)#1-C(18)-C(23)-C(26)	-130.7(8)
C(17)-C(18)-C(23)-C(25)	174.2(9)
C(17)#1-C(18)-C(23)-C(25)	-9.2(12)
O(2)-C(29)-C(32)-F(1)	65.8(14)
O(2A)-C(29)-C(32)-F(2A)	159.1(14)
O(2A)-C(29)-C(32)-F(3A)	-65(2)
O(2)-C(29)-C(32)-F(3)	-71.7(18)
O(2)-C(29)-C(32)-F(2)	-172.1(9)
O(2A)-C(29)-C(32)-F(1A)	43.2(10)
O(3)-C(33)-C(34)-F(11A)	-33.3(9)
C(35)-C(33)-C(34)-F(11A)	88.8(8)
C(34)#2-C(33)-C(34)-F(11A)	-154.8(6)
O(3)-C(33)-C(34)-F(10)	32.8(9)
C(35)-C(33)-C(34)-F(10)	154.9(7)
C(34)#2-C(33)-C(34)-F(10)	-88.8(8)
O(3)-C(33)-C(34)-F(12)	-170.1(9)
C(35)-C(33)-C(34)-F(12)	-48.0(10)
C(34)#2-C(33)-C(34)-F(12)	68.4(10)
O(3)-C(33)-C(34)-F(12A)	168.9(6)
C(35)-C(33)-C(34)-F(12A)	-69.1(7)
C(34)#2-C(33)-C(34)-F(12A)	47.3(9)
O(3)-C(33)-C(34)-F(11)	-80.8(8)
C(35)-C(33)-C(34)-F(11)	41.2(8)
C(34)#2-C(33)-C(34)-F(11)	157.6(6)
O(3)-C(33)-C(34)-F(10A)	77.2(7)
C(35)-C(33)-C(34)-F(10A)	-160.7(6)
C(34)#2-C(33)-C(34)-F(10A)	-44.3(8)
O(3)-C(33)-C(35)-F(14)	-34.9(6)
C(34)-C(33)-C(35)-F(14)	-157.2(7)
C(34)#2-C(33)-C(35)-F(14)	87.4(8)
O(3)-C(33)-C(35)-F(13)	180.000(1)
C(34)-C(33)-C(35)-F(13)	57.7(4)
C(34)#2-C(33)-C(35)-F(13)	-57.7(4)
O(3)-C(33)-C(35)-F(15)	-76.8(6)
C(34)-C(33)-C(35)-F(15)	160.9(7)
C(34)#2-C(33)-C(35)-F(15)	45.5(8)
C(1)-C(2)-P(1)-C(3)	127.0(5)
C(1)-C(2)-P(1)-C(3)#1	-127.0(5)
C(1)-C(2)-P(1)-C(3A)#1	-116.5(5)
C(1)-C(2)-P(1)-C(3A)	116.5(5)
C(1)-C(2)-P(1)-Os(1)	0.000(1)
C(8)-C(9)-P(2)-C(10A)	127.0(5)
C(8)-C(9)-P(2)-C(10A)#1	-127.0(5)
C(8)-C(9)-P(2)-C(10)#1	-115.7(5)
C(8)-C(9)-P(2)-C(10)	115.7(5)
C(8)-C(9)-P(2)-Os(1)	0.000(1)
C(16)-C(15)-P(3)-Os(1)	-84.7(4)
C(16)#1-C(15)-P(3)-Os(1)	84.7(4)
C(28)-C(27)-O(1)-C(27)#1	169.6(5)
C(35)-C(33)-O(3)-Al(1)	180.000(1)
C(34)-C(33)-O(3)-Al(1)	-59.5(4)
C(34)#2-C(33)-O(3)-Al(1)	59.5(4)
O(2A)#2-Al(1)-O(3)-C(33)	-109.7(3)
O(2A)-Al(1)-O(3)-C(33)	109.7(3)
O(4)-Al(1)-O(3)-C(33)	0.000(2)
O(2)-Al(1)-O(3)-C(33)	132.5(3)
O(2)#2-Al(1)-O(3)-C(33)	-132.5(3)
C(37A)-C(36)-O(4)-Al(1)	-67.6(6)
C(37A)#2-C(36)-O(4)-Al(1)	67.6(6)
C(37)-C(36)-O(4)-Al(1)	-53.8(7)
C(37)#2-C(36)-O(4)-Al(1)	53.8(7)
C(38)-C(36)-O(4)-Al(1)	-161.3(8)
O(2A)#2-Al(1)-O(4)-C(36)	-67.1(3)
O(2A)-Al(1)-O(4)-C(36)	67.1(3)
O(3)-Al(1)-O(4)-C(36)	180.000(3)
O(2)-Al(1)-O(4)-C(36)	51.4(3)
O(2)#2-Al(1)-O(4)-C(36)	-51.4(3)
C(2)-P(1)-C(3)-C(4)	176.3(9)
C(3)#1-P(1)-C(3)-C(4)	69.3(16)
Os(1)-P(1)-C(3)-C(4)	-72.5(10)
C(2)-P(1)-C(3)-C(5)	-61.4(14)
C(3)#1-P(1)-C(3)-C(5)	-168.5(6)
Os(1)-P(1)-C(3)-C(5)	49.7(17)
C(2)-P(1)-C(3)-C(6)	53.5(12)
C(3)#1-P(1)-C(3)-C(6)	-54(2)
Os(1)-P(1)-C(3)-C(6)	164.6(8)
C(9)-P(2)-C(10A)-C(14)	-177.1(8)
C(10A)#1-P(2)-C(10A)-C(14)	77.8(13)
Os(1)-P(2)-C(10A)-C(14)	-66.7(11)
C(9)-P(2)-C(10A)-C(12A)	-55.3(12)
C(10A)#1-P(2)-C(10A)-C(12A)	-160.5(6)
Os(1)-P(2)-C(10A)-C(12A)	55.1(15)
C(9)-P(2)-C(10A)-C(11A)	63.3(12)
C(10A)#1-P(2)-C(10A)-C(11A)	-41.8(19)
Os(1)-P(2)-C(10A)-C(11A)	173.7(8)
F(13)-C(35)-F(14)-F(15)	66.3(10)
C(33)-C(35)-F(14)-F(15)	-78.0(9)
F(13)-C(35)-F(15)-F(14)	-125.4(10)
C(33)-C(35)-F(15)-F(14)	117.1(10)
C(18)-C(17)-C(16)-C(15)	2.3(7)
C(18)-C(17)-C(16)-C(19)	-171.4(5)
C(16)#1-C(15)-C(16)-C(17)	-14.9(8)

P(3)-C(15)-C(16)-C(17)	154.8(4)
C(16)#1-C(15)-C(16)-C(19)	157.9(4)
P(3)-C(15)-C(16)-C(19)	-32.4(7)
C(20)-C(19)-C(16)-C(17)	-179.9(5)
C(21)-C(19)-C(16)-C(17)	-57.6(6)
C(22)-C(19)-C(16)-C(17)	61.6(6)
C(20)-C(19)-C(16)-C(15)	7.0(8)
C(21)-C(19)-C(16)-C(15)	129.4(5)
C(22)-C(19)-C(16)-C(15)	-111.4(6)
F(151)#2-F(151)-F(16)-C(38)	47(2)
F(151)#2-F(151)-C(38)-F(16)	-165.5(8)
F(151)#2-F(151)-C(38)-F(141)	71.4(12)
F(16)-F(151)-C(38)-F(141)	-123.1(15)
F(151)#2-F(151)-C(38)-C(36)	-68(3)
F(16)-F(151)-C(38)-C(36)	98(3)
F(151)-F(16)-C(38)-F(141)	87.6(18)
F(151)-F(16)-C(38)-C(36)	-132.2(17)
O(4)-C(36)-C(38)-F(151)	-21(4)
O(4)-C(36)-C(38)-F(16)	51.9(15)
O(4)-C(36)-C(38)-F(141)	-160.3(8)
C(32)-C(29)-O(2)-Al(1)	85.8(16)
O(4)-Al(1)-O(2)-C(29)	77.3(16)
O(3)-Al(1)-O(2)-C(29)	-49.8(16)
O(2)#2-Al(1)-O(2)-C(29)	-161.7(13)
F(10)-C(34)-F(11)-F(12)	118.6(11)
C(33)-C(34)-F(11)-F(12)	-120.6(10)
F(10)-C(34)-F(12)-F(11)	-102.4(11)
C(33)-C(34)-F(12)-F(11)	101.5(9)
C(32)-C(29)-O(2A)-Al(1)	-41.9(15)
O(2A)#2-Al(1)-O(2A)-C(29)	-51.8(17)
O(4)-Al(1)-O(2A)-C(29)	-168.4(12)
O(3)-Al(1)-O(2A)-C(29)	77.7(13)
O(4)-C(36)-C(37)-F(101)	38.7(12)
C(37)#2-C(36)-C(37)-F(101)	-85.2(10)
O(4)-C(36)-C(37)-F(42)	152.0(9)
C(37)#2-C(36)-C(37)-F(42)	28.1(15)
O(4)-C(36)-C(37)-F(41)	-73.2(13)
C(37)#2-C(36)-C(37)-F(41)	162.8(7)
F(101)-C(37)-F(42)-F(42)#2	99.2(9)
F(41)-C(37)-F(42)-F(42)#2	-158.5(9)
C(36)-C(37)-F(42)-F(42)#2	-20.2(11)
O(4)-C(36)-C(37A)-F(41A)	-46.7(10)
C(37A)#2-C(36)-C(37A)-F(41A)	-166.6(7)
O(4)-C(36)-C(37A)-F(42A)	-163.3(9)
C(37A)#2-C(36)-C(37A)-F(42A)	76.8(16)
O(4)-C(36)-C(37A)-F(101)	75.3(9)
C(37A)#2-C(36)-C(37A)-F(101)	-44.5(17)
C(32)-C(29)-C(31)-F(7)	164.9(8)
C(32)-C(29)-C(31)-F(9)	-69.6(10)
C(32)-C(29)-C(31)-F(8)	50.2(10)
C(32)-C(29)-C(31A)-F(8A)	55.8(13)
C(32)-C(29)-C(31A)-F(9A)	-62.1(11)
C(32)-C(29)-C(31A)-F(7A)	-175.0(10)
C(32)-C(29)-C(30)-F(5)	169.5(9)
C(32)-C(29)-C(30)-F(6)	-64.0(12)
C(32)-C(29)-C(30)-F(4)	53.1(11)
C(32)-C(29)-C(30A)-F(4A)	69.4(13)
C(32)-C(29)-C(30A)-F(5A)	-168.6(10)
C(32)-C(29)-C(30A)-F(6A)	-49.7(13)

Symmetry transformations used to generate equivalent atoms:
#1 x,-y+3/2,z #2 x,-y+1/2,z

Computational Details

DFT calculations were carried out with the ORCA 4.0.1.2[10] program package using the PBE[11] and PBE0[12]functionals, respectively. Ahlrichs' basis sets def2-SVP (for geometry optimization and frequency calculation) and def2-TZVP (for single-point energies) were used with a full basis for all elements but Os and Ni for which the Stuttgart-Dresden 60 electron core potential was chosen to replace the inner shell 1s-4f orbitals.[13,14] The RI-J[15] (PBE) approximation in combination with the corresponding auxiliary basis sets of Alrichs' was utilized to reduce computational costs in the geometry optimization and frequency calculations. Grimme's model (D3) with Becke-Johnson damping[16] was used to account for dispersion with the PBE or PBE0 functionals. No symmetry restrains were imposed and the optimized structures were defined as minima (no negative eigenvalues) by vibrational analyses. Geometries were analyzed and visualized with Avogadro[17], QRO-molecular orbitals were visualized with Chimera[18].

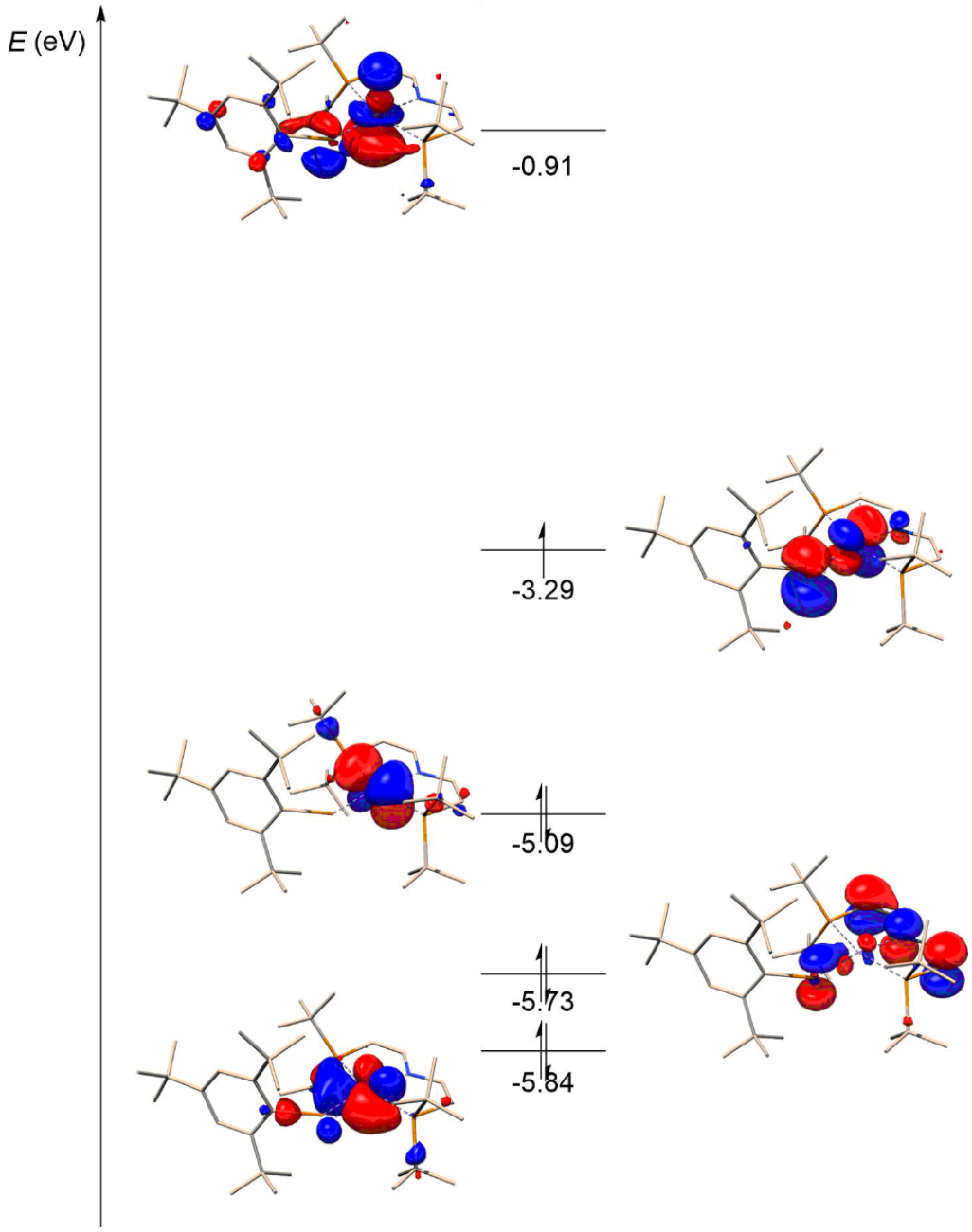

Figure S32. Frontier molecular orbital scheme (quasi-restricted orbitals) of **5** (D3BJ-PBE0-RIJCOSX/def2-TZVP//D3BJ-PBE-RI/def2-SVP).

BDE calculations

Geometry optimizations were carried out with the Turbomole program package[19] coupled to the PQS Baker optimizer[20] via the BOpt package,[21] at the spin unrestricted ri-DFT level using the BP86 functional[22] and the resolution-of-identity (ri) method.[23] We used the def2-TZVP basis set[24] (small-core pseudopotentials on Os[25]) and Grimme's version 3 dispersion corrections (disp3, "zero damping")[26] for all geometry optimizations. Scalar relativistic effects were included implicitly through the use of the Os ECPs. All minima (no imaginary frequencies) were characterized by calculating the Hessian matrix. ZPE and gas-phase thermal corrections (entropy and enthalpy, 298 K, 1 bar) from these analyses were calculated. Spectroscopic properties and BDEs were evaluated using the full atom model of the complexes. The optimized geometries of all species are supplied as separate files in .pdb and .xyz format. The calculated BDEs were calibrated (taking advantage of internal error cancelation) against the know experimental BDE of propene, using the following Hess cycle:

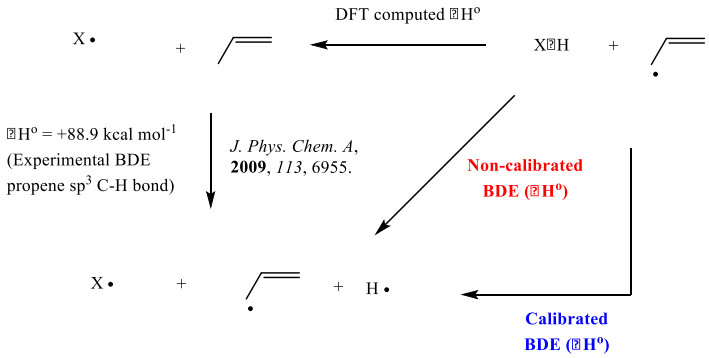

This resulted in the DFT calculated BDEs for the P–H and Os–H bonds of complex **5** shown in Table S20.

Table S20. Calibrated and uncalibrated DFT calculated BDEs (ΔH° in kcal mol^{-1}) of the P–H and Os–H bonds of complex **5**.

Bond type	*Uncalibrated BDEs*	*Calibrated BDEs*
P–H	***+64.0***	***+67.5***
Os–H	***+70.1***	***+73.6***

EPR Property calculations

EPR parameters[27] of **5** were calculated with the ADF[28] program system at the B3LYP/ZORA/QZ4P level, using the coordinates from the structure optimized in Turbomole as input. Unrestricted SPINORBIT ZORA COLLINEAR calculations were used to compute the SOC corrected HFI-tensors and Zeeman corrected g-tensors.

[1] a) J. Abbenseth, M. Diefenbach, S. C. Bete, C. Würtele, C. Volkmann, S. Demeshko, M. C. Holthausen, S. Schneider *Chem. Commun.* **2017**, *29*, 867; b) V. W. Manner, T. F: Markle, J. H. Freudenthal, J. P. Roth, J. J. Mayer *Chem Commun.* **2008**, 256.
[2] S. K. Sur, *J. Magn. Reson.* **1989**, *82*, 169.
[3] W95EPR; An EPR simulation program for windows. F. Neese, Diploma thesis, University of Konstanz (Konstanz, Germany), **1993**.
[4] J. J. Warren, T. A. Tronic, J. A. Mayer, *Chem. Rev.* **2010**, 6961-7001.
[5] a) Measurment by ITCRun Version 3.4.6.0, TA Instruments, **2017**. b) Evaluation by NanoAnalyze Version 3.7.5 TA Instruments, **2015**.
[6] E. P. Cappellani, S. D. Drouin, G. Jia, P. A. Maltby, R. H. Morris and C. T Schweitzer, *J. Am. Chem. Soc.*, 1994, 116, 3375-3388.
[7] F. G. Bordwell and J. Cheng, *J. Am. Chem. Soc.*, **1991**, 113, 1736-1743.
[8] F. Ding, J. M. Smith, H. Wang, *J. Org. Chem.* **2009**, *74*, 2679-2691.
[9] (a) APEX3 v2016.9-0 (SAINT/SADABS/SHELXT/SHELXL), Bruker AXS Inc., Madison, WI, USA, **2016**. (b) George M. Sheldrick, *Acta Cryst.* **2015**, A71, 3. (c) George M. Sheldrick, *Acta Cryst.* **2015**, C71, 3. (d) George M. Sheldrick, *Acta Cryst.* **2008**, A64, 112.
[10] F. Neese, *WIREs Comput. Mol. Sci.* **2012**, *2*, 73.
[11] J. P. Perdew, K. Burke, M. Ernzerhof, *Phys. Rev. Lett.* **1996**, *77*, 3865.
[12] J. P. Perdew, K. Burke, M. Ernzerhof, *J. Chem. Phys.* **1996**, *105*, 9982.
[13] F. Weigend, R. Ahlrichs, *Phys. Chem. Chem. Phys* **2005**, *7*, 3297.
[14] D. Andrae, U. Häussermann, M. Dolg, H. Stoll, H. Preuss, *Theor. Chim. Acta* **1990**, *77*, 123.
[15] (a) O. Treutler, R. Ahlrichs, *J. Chem. Phys.* **1995**, *102*, 346; (b) *Chem. Phys. Lett.* **1995**, *240*, 283; (c) *Chem. Phys. Lett.* **1995**, *242*, 652; (d) K. Eichkorn, F. Weigend, O. Treutler, R. Ahlrichs *Theo. Chem. Acc.* **1997**, *97*, 119.
[16] (a) S. Grimme, S. Ehrlich, L. Goerigk, *J. Comput. Chem.* **2011**, *32*, 1456; (b) S. Grimme, J. Antony, S. Ehrlich, H. Krieg, H. *J. Chem. Phys.* **2010**, *132*, 154104.
[17] M. D. Hanwell, D. E. Curtis, D. C. Lonie, T. Vandermeersch, E. Zurek, G. R. Hutchison, *J. Cheminform.* **2012**, *4*, 17.
[18] Pettersen, E. F.; Goddard, T. D.; Huang, C. C.; Couch, G. S.; Greenblatt, D. M.; Meng, E. C.; Ferrin, T. E. *J. Comput. Chem.* **2004**, *25*, 1605.
[19] R. Ahlrichs, Turbomole Version 7.3.1, 2018, Theoretical Chemistry Group, University of Karlsruhe.
[20] PQS version 2.4, 2001, Parallel Quantum Solutions, Fayettevile, Arkansas (USA); the Baker optimizer is available separately from PQS upon request: I. Baker, *J. Comput. Chem.* **1986**, *7*, 385-395.
[21] P. H. M. Budzelaar, *J. Comput. Chem.* **2007**, *28*, 2226-2236.
[22] (a) A. D. Becke, *Phys. Rev. A*, **1988,** *38*, 3098–3100. (b) J. P. Perdew, *Phys. Rev. B*, **1986**, *33*, 8822-8824.
[23] M. Sierka, A. Hogekamp, R. Ahlrichs, *J. Chem. Phys.* **2003**, *118*, 9136-9148.
[24] (a) F. Weigend, R. Ahlrichs, *Phys. Chem. Chem. Phys.* **2005**, *7*, 3297-3305. (b) F.Weigend, M. Häser, H. Patzelt, R. Ahlrichs, *Chem. Phys. Lett.* **1998**, *294*, 143-152.
[25] (a) Turbomole basisset library, Turbomole Version 6.5. (b) D. Andrae, U. Haeussermann, M. Dolg, H. Stoll, H. Preuss, *Theor. Chim. Acta* **1990**, *77*, 123–141.
[26] S. Grimme, J. Antony, S. Ehrlich, H. Krieg, *J. Chem. Phys.* **2010**, *132*, 154104.

[27] Lead reference for calculation of g-tensor (Zeeman interactions) parameters: E. van Lenthe, A. van der Avoird, P. E. S Wormer, *J. Chem. Phys.* **1997**, *107*, 2488. Lead reference for calculation of A-tensor (Nuclear magnetic dipole hyperfine interactions) parameters: E. van Lenthe, A. van der Avoird, P. E. S. Wormer, *J. Chem. Phys.* **1998**, *108*, 4783.

[28] ADF2018: (a) E.J. Baerends, D. E. Ellis, P. Ros, *Chem. Phys.* **1973**, *2*, 41. (b) L. Versluis, T. Ziegler, J. Chem. Phys., **1988**, *88*, 322. (c) G. te Velde, E. J. Baerends, *J. Comput. Phys.* **1992**, *99*, 84. (d) C. Fonseca Guerra, J. G. Snijders, G. te Velde, E. J. Baerends, *Theor. Chem. Acc.* **1998**, *99*, 391.